Chapter 4
Results and Discussion

"Get the habit of analysis - analysis will in time enable synthesis to become your habit of mind."
-Frank Lloyd Wright

4.1. Collection of germplasm

Clerodendrum species were collected from different locations of two districts of North Bengal (Darjeeling and Jalpaiguri) and Assam (Kamrup). The collection sites were noted from Taxonomists and visited for the collection of the germplasm. The collected germplasm were planted in the experimental garden of Molecular Genetics Laboratory, Department of Botany, North Bengal University, for further study after authentication by the plant taxonomists (Fig. 4.1).

4.2. *In-vitro* antioxidant activities

Plants are rich source of antioxidant and their demand as nutrition and health supplement is immense. Clinical trials have revealed that there is an inverse correlation between the intake of fruits and vegetables and the occurrence of free-radical induced disorders such as inflammation, cardiovascular disease, cancer and aging etc. (Durackova, 2010). Phenolic and flavonoid content in plants are the chief determinants in neutralizing ROS mediated oxidative damage causing most of the life's hazardous diseases such as diabetes, cancer and various neurological disorders. Hence, the present study was intended to investigate the free radical scavenging and reducing capabilities of selected plant species. The plants were chosen on the basis of preliminary screening of DPPH scavenging activity of all the

Fig. 4.1. Flowers and foliages of selected species of *Clerodendrum* used in the present study.

Table 4.1. Percentage of inhibition of all four plant species.

Parameters	CIL (%)	VIL (%)	CSL (%)	CCL (%)	Standard (%)
DPPH (200µg/ml)	43.6±0.3	63.1±4.8	60.5±0.8	65.7±1.0	58.5±0.02
Hydroxyl Radical (200µg/ml)	31.2±1.2	33.1±0.6	34.3±2.1	35.3±2.3	31.3±0.8
Hydrogen Peroxide (200 µg/ml)	33.3±1.5	30.1±0.8	43.1±1.3	45.8±3.2	7.6±0.6
Nitric Oxide (200 µg/ml)	49.4±2.1	46.3±0.6	58.5±0.02	44.3±1.1	100±0.0
Superoxide Anion (50 µg/ml)	37.4±1.4	33.2±0.2	28.2±0.8	29.3±1.0	39.4±1.4
Hypochlorous Acid (200 µg/ml)	47.7±2.2	42.6±0.3	36.7±1.5	42.7±2.1	62.3±0.3
Total Antioxidant (200 µg/ml)	91.1±0.6	76.8±0.2	74.4±1.0	74.1±0.5	69.2±0.0
Peroxynitrite (200 µg/ml)	22.0±0.9	23.4±0.9	21.7±0.3	26.2±0.9	17.6±0.2
Singlet Oxygen (200 µg/ml)	52.0±0.3	54.5±0.2	45.3±0.07	54.05±0.2	77.9±1.3
Lipid Peroxidation (25 µg/ml)	34.3±0.6	43.8±1.4	31.06±0.6	36.6±1.7	77.8±0.9
Iron chelation (200 µg/ml)	77.8±2.4	36.3±0.7	76.6±0.5	77.2±0.6	0.4±0.1

Table 4.2. IC_{50} values of each extract with their respective standard used in the present study.

Parameters	IC_{50} values (µg/ml)				
	CIL	VIL	CSL	CCL	Standard
DPPH	$287.8\pm11.9^{\beta}$	$160.4\pm16.6^{\alpha}$	$90.5\pm0.5^{\gamma}$	$67.7\pm2.5^{\gamma}$	203.2 ± 1.9
Hydroxyl Radical	$484.6\pm28.1^{\alpha}$	$452.1\pm29.0^{\alpha}$	$437.9\pm42.3^{\alpha}$	$438.3\pm39.9^{\alpha}$	597.1 ± 11.9
Hydrogen Peroxide	$396.4\pm24.4^{\beta}$	$433.5\pm16.8^{\beta}$	$371.1\pm26.2^{\gamma}$	$348.7\pm26.7^{\beta}$	2185.2 ± 187.4
Nitric Oxide	$155.0\pm8.0^{\beta}$	$211.3\pm6.3^{\gamma}$	$108.2\pm1.3^{\gamma}$	$188.7\pm21.0^{\beta}$	61.17 ± 0.41
Superoxide Anion	$373.4\pm25.2^{\beta}$	$395.1\pm9.3^{\gamma}$	$105.1\pm4.0^{\gamma}$	$366.7\pm20.3^{\beta}$	94.5 ± 3.7
Hypochlorous Acid	$308.3\pm33.3^{\alpha}$	$293.6\pm7.6^{\beta}$	$322.9\pm32.9^{\beta}$	$299.9\pm17.9^{\beta}$	130.0 ± 5.1
Total Anti-oxidant	$18.0\pm0.3^{\beta}$	$58.9\pm1.8^{\beta}$	$57.3\pm2.5^{\beta}$	$55.7\pm2.7^{\beta}$	116.4 ± 5.9
Peroxynitrite	$724.0\pm40.2^{\gamma}$	$637.8\pm25.9^{\alpha}$	$570.1\pm23.9^{\beta}$	$525.9\pm22.0^{\beta}$	799.3 ± 36.9
Singlet Oxy-gen	$240.4\pm3.8^{\Psi}$	$202.2\pm4.5^{\gamma}$	$276.0\pm3.6^{\gamma}$	$205.9\pm4.8^{\gamma}$	48.4 ± 3.6
Lipid Peroxi-dation	$316.6\pm13.8^{\beta}$	$226.3\pm7.5^{\alpha}$	$71.7\pm0.1^{\gamma}$	$270.3\pm20.3^{\beta}$	11.1 ± 0.2
Iron chelation	676.2 ± 45.2	116.4 ± 3.5	482.4 ± 2.9	576.2 ± 57.4	1.4 ± 0.02

Units in µg/ml. Data expressed as mean ± S.D (n=6). $^{\alpha}p<0.05$; $^{\beta}p<0.01$; $^{\gamma}p<0.001$; $^{\Psi}$Non significant when compared with standard.

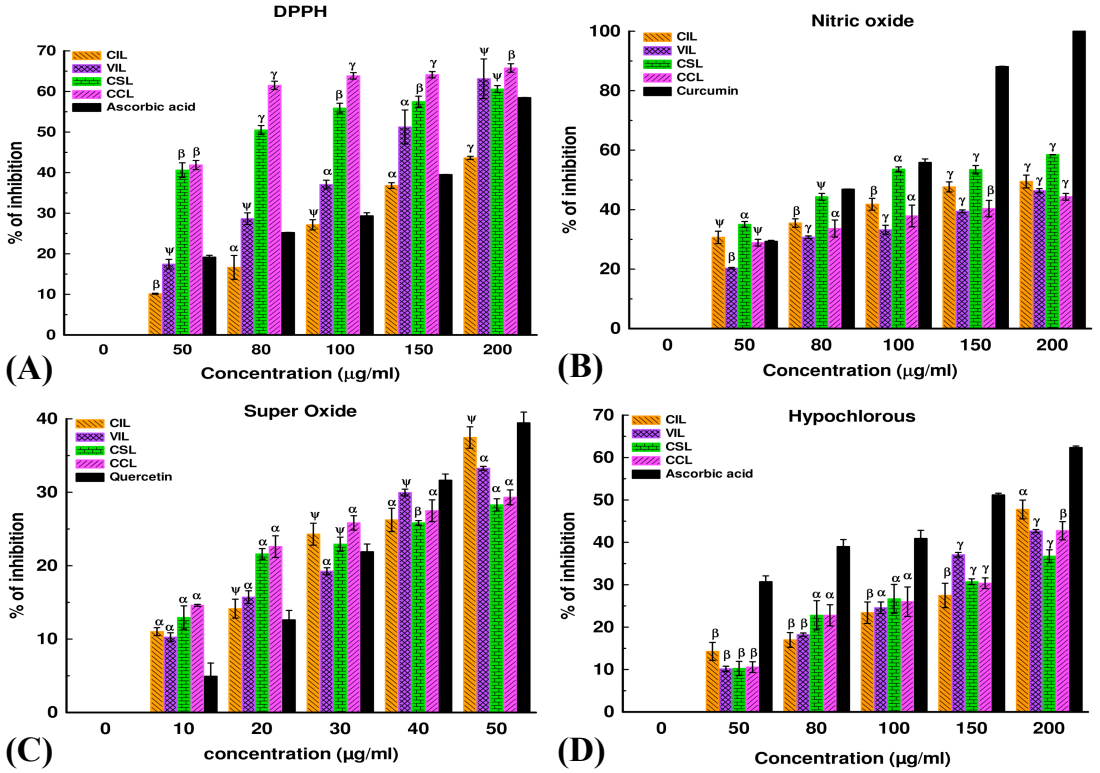

Fig. 4.2. Antioxidant activity of *Clerodendrum indicum*, *Volkameria inermis, C. serratum* and *C. colebrookianum*. (**A**) DPPH activity; (**B**) Nitric oxide scavenging activity; (**C**) Super oxide radical scavenging activity; (**D**) Hypochlorous acid scavenging assay. Data expressed as mean ± S.D (n=6). $^{\alpha}p<0.05$; $^{\beta}p<0.01$; $^{\gamma}p<0.001$; ^{NS}-Non significant when compared with standard.

extracts. Herein, four plant species, namely *Clerodendrum indicum* (CIL), *Volkameria inermis* (VIL), *Clerodendrum serratum* (CSL) and *Clerodendrum colebrookianum* (CCL) were chosen for further analysis of the test and rest were discarded.

In the present antioxidant profiling, all the *Clerodendrum* species (CIL, VIL, CSL and CCL) exhibited higher free radical scavenging activity (Table 4.1.) than the respective standard (ascorbic acid) as per DPPH assay (Fig. 4.2.A). Among the four extracts, the CCL (65.78±1.04% at 200µg/ml) extract showed higher percent of inhibition when compared to standard (58.5±0.02% at 200µg/ml). This was evident from the discoloration of DPPH and low IC_{50} (Table 4.2.) values in case of CCL extract (67.77±2.54µg/ml). Free radical DPPH accept an electron or hydrogen radical to become stable which reacts with a reducing agent to form a new bond, thus, changing the colour of the solution. The colored solution loses its color due to increased amount of natural antioxidant (Huang *et al.*, 2005). The elevated DPPH radical scavenging activity by CCL extract was due to the presence of significant antioxidant properties.

In nitric oxide (Fig. 4.2.B) scavenging activity, all the extracts (CIL, VIL, CSL and CCL) showed moderate scavenging activities (CIL 49.47±2.16%, VIL 46.36±0.69%, CSL 58.5±0.02%, CCL 44.31±1.12% at 200µg/ml) compared to the standard used (curcumin). Nitric oxide is a potent mediator of pro-inflammatory cellular activation and produced from the amino acid L- arginine by the activation of nitric oxide synthase (NOS). Due to chronic inflammation, calcium dependent NOS produces more NO which can initiate tumor development. iNOS (calcium independent isoform of NOS) produce larger amount of NO and is reported to express only during inflammation (Gimenez-Garzó *et al.*, 2015). iNOS is activated by LPS (lipopolysachharide) and induced by the translocation of NF -κβ and leads to the formation of cancer (Gimenez-Garzó *et al.*, 2015). Thus, the inhibitory affect of *Clerodendrum* extracts indicate their role in scavenging nitric oxide.

All the extracts of *Clerodendrum* species (CIL, VIL, CSL and CCL) were found to exhibit moderate scavenging activity in case of superoxide anion (CIL 37.46±1.45%, VIL 33.26±0.26%, CSL 28.28±0.83%,

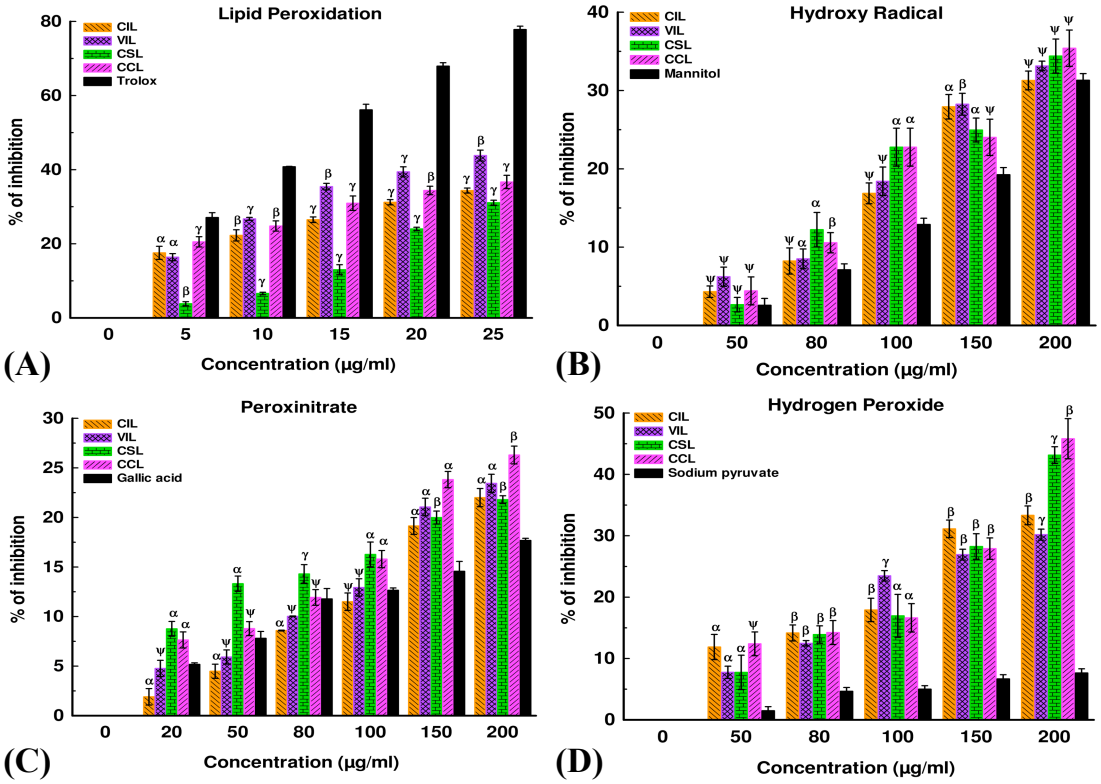

Fig. 4.3. Antioxidant activity of *Clerodendrum indicum*, *Volkameria inermis, C. serratum* and *C. colebrookianum*. (**A**) Lipid peroxidation activity; (**B**) Hydroxyl radical scavenging assay; (**C**) Peroxynitrate scavenging assay; (**D**) Hydrogen peroxide scavenging activity. Data expressed as mean ± S.D (n=6). $^{\alpha}p<0.05$; $^{\beta}p<0.01$; $^{\gamma}p<0.001$; ^{NS}- Non significant when compared with standard.

CCL 29.30±1.02% at 200 µg/ml) (Fig. 4.2.C), hypochlorous acid (CIL 47.74±2.21%, VIL 42.67±0.37%, CSL 36.73±1.52%, CCL 42.73±2.14% at 200 µg/ml) (Fig. 4.2.D) and lipid peroxidation (Fig. 4.3.A) scavenging assay in a dose dependent manner and highly significant scavenging activity in case of hydroxyl radical (CIL 31.28±1.20%, VIL 33.13±0.60%, CSL 34.39±2.17%, CCL 35.39±2.31% at 200 µg/ml) (Fig. 4.3.B), peroxinitrate (CIL 22.00±0.92%, VIL 23.43±0.91%, CSL 21.79±0.39%, CCL 26.29±0.90% at 200 µg/ml) (Fig. 4.3.C) and hydrogen peroxide scavenging assay (CIL 33.32±1.52%, VIL 30.18±0.89%, CSL 43.14±1.37%, CCL 45.81±3.27% at 200 µg/ml) (Fig. 4.3.D). Hydroxyl radical, the short-lived free radical is most harmful among ROS and has the potential to damage the bio-molecules (Huang *et al.*, 2005). Hydroxyl radical ($OH^{\cdot}$) are generally formed through the Fenton reaction between Fe^{+2} and H_2O_2 (Wanasundara and Shahidi, 2005). On the contrary, metal chelator may also contribute to the reduction of $OH^{\cdot}$ by the conversion of Fe^{+2} to Fe^{+3} and thus, hindering the Fenton reaction.

Hydrogen peroxide (H_2O_2), another potential ROS, is formed due to the mutation from superoxide anion or might be produced from superoxide in the presence of superoxide dismutase in the peroxisomes (Matés and Sánchez -Jiménez, 2000; Ray and Husain, 2002; Valko *et al.*, 2004).

Despite being capable of defusing through the mitochondria and cell membrane and producing various types of cellular injury, it is seen that this free radical is comparatively less reactive than other potential ROS candidates (Ray *et al.*, 2006). However, hydroxyl radical, produced from H_2O_2 by elimination of water mediates an injury to mammalian cell (Valko *et al.*, 2004). In *in-vivo* condition hydroxyl radical ($OH^{\cdot}$) produced in the presence of reduced transition metals like Fe, Cu, Co or Ni damages the cellular DNA and generates 8-hydroxy guanosine, which is the hydrolysis product of 8-hydroxydeoxyguanosine (8-OHdG). 8-OHdG is the most widely used fingerprint of radical attack on DNA and has been strongly implicated with carcinogenesis progression, especially breast carcinoma (Malins and Haimanot, 1991; Matsui *et al.*, 2000; Musarrat *et al.*, 1996). Thus, increase in the scavenging activity of H_2O_2 and $OH^{\cdot}$ by *Clerodendrum* sp. might facilitate chemoprevention. The highly toxic superoxide anion ($O_2^{\cdot -}$)

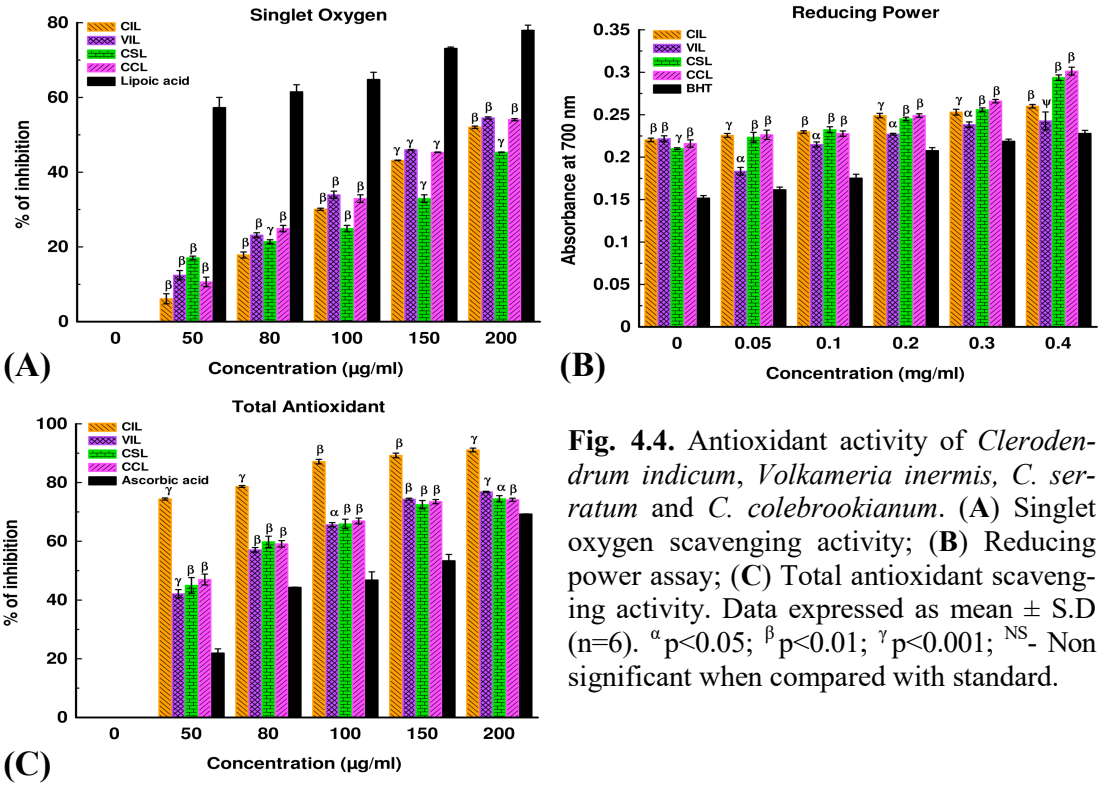

Fig. 4.4. Antioxidant activity of *Clerodendrum indicum*, *Volkameria inermis, C. serratum* and *C. colebrookianum*. (**A**) Singlet oxygen scavenging activity; (**B**) Reducing power assay; (**C**) Total antioxidant scavenging activity. Data expressed as mean ± S.D (n=6). $^{\alpha}p<0.05$; $^{\beta}p<0.01$; $^{\gamma}p<0.001$; ^{NS}- Non significant when compared with standard.

originating in mitochondria undergoes spontaneous dismutation and generates singlet oxygen. The presence of inhibition of singlet oxygen by *Clerodendrum* sp. (CIL 52.02±0.03%, VIL 54.53±0.28%, CSL 45.32±0.07%, CCL 54.05±0.29% and lipoic acid 77.96±1.37 at 200µg/ml) showed moderate scavenging activity (Fig. 4.4.A) when compared to standard Lipoic acid. Thus, generation of singlet oxygen from superoxide anion is one of the primary causative agents of lipid peroxidation. Reactive mediators generated from lipid peroxidation such as 4-hydroxy nonenal (4-HNE) are biomarkers of oxidative stress and are important players in a number of cancer signaling pathways (Zhong and Yin, 2015). The present study demonstrated the significant singlet oxygen, superoxide anion and lipid peroxidation scavenging capacity by all the extracts of *Clerodendrum* sp., thus suggesting a probable protective role against oxidative stress by the prevention of peroxidase formation. Nitric oxide (NO) together with super oxide generates an extremely reactive species called peroxynitrite ($ONOO^-$), one of the major cytotoxic molecules during inflammation, sepsis and ischemia-reperfusion injury (Beckman and Koppenol, 1996). Peroxynitrite causes the damage of protein, nucleic acid which leads to cellular apoptosis and necrosis (Zhuang and Simon, 2000). 3-nitrotyrosin (3-NT) is prevalent in hepatocytes adjacent to human metastatic colorectal carcinoma, which is the byproduct of peroxynitrite reaction. Myeloperoxidase, the neutrophilic enzyme, resulting from the oxidation of Cl^- ions at the site of inflammation produces hypochlorous acid (HOCl) and induce target cell

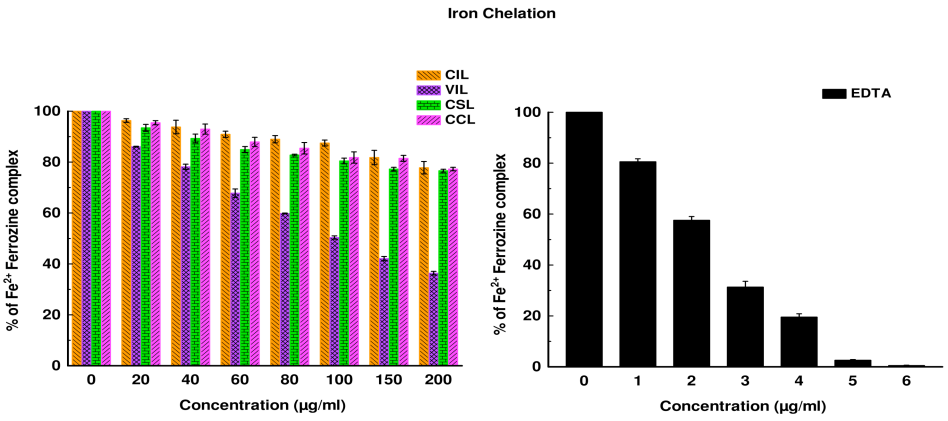

Fig. 4.5. Antioxidant activity of *Clerodendrum indicum*, *Volkameria inermis, C. serratum* and *C. colebrookianum*. (**A**) Iron chelation assay.

lyses (Aruoma *et al.*, 1989). The scavenging activity of peroxynitrite and hypochlorous acid by all concerned species of *Clerodendrum* appears quite promising and therefore, might be utility in combating inflammation related oxidative damages.

Iron is a potential enhancer of ROS formation as it leads to reduction of H_2O_2 and generation of reactive hydroxyl radical. In the present experiment, CIL (77.81±2.45% at 200µg/ml) and CCL (77.28±0.68% at 200µg/ml) extracts were found to fade the color of ferrozine-complex, indicating its iron chelating capacity (Fig. 4.5.Aa and Ab) and the presence of active component. Extracts of *Clerodendrum* sp. exhibited higher reducing power activity (Fig. 4.4.B) than the standard EDTA. The CCL extract inhibited 0.30±0.004% where the standard showed 0.22±0.003% at 400 mg/ml concentration. The total antioxidant activity (Fig. 4.4.C) was significantly high in case of all the extracts compared to the standard ascorbic acid. Among the four species of *Clerodendrum*, CCL contained highest phenolic and flavonoid compounds (67.29±3.15 mg/ml gallic acid equivalent per 100 mg plant extract and 48.71±1.69 mg/ml quercetin equivalent per 100 mg plant extract). These contents exert crucial antioxidant scavenging activities in all the plants which clearly display potent medicinal activity.

4.3. Evaluation of cytotoxicity

4.3.1. Assessment of haemolytic activity

The haemolytic activity of plant extracts is an indication towards the cytotoxicity of normal healthy cells (Da Silva *et al.*, 2004). The hemolysis process is actually related to the concentration and potency of extract. Plant derived metabolites showed haemolytic activity by altering changes in the erythrocyte membrane by means of destruction of red blood cells. Hence, *in-vitro* haemolytic assay by spectroscopic method represents a simple and effectual method for the quantitative measurement of hemolysis. In the mentioned experiment VIL extract showed higher percent of inhibition (24.51±1.12%) than the other three extracts (Fig. 4.6.A) at 200µg/ml of each concentration which is virtually a negligible one. Therefore, these data suggested the non-toxic effect of the extracts making it suitable for the

preparation of drugs involved in the treatment of various diseases.

4.3.2. Erythrocyte membrane stabilizing activity (EMSA)

Erythrocyte Membrane Stabilizing Activity (EMSA) (Fig. 4.6.B) is another crucial experiment which indirectly evaluates the antioxidant capacity against the superoxide radical mediated damage of the erythrocyte membrane. CCL extract displayed excellent membrane stabilizing activity (30.68±0.77%) by the inhibition of superoxide radical. Thus, membrane stabilizing activity by CCL extract might aid to improve the immune system (Dey *et al.*, 2013).

4.3.3. Measurement of cell viability (MTT) assay

Besides, antioxidant capacity, the leaf extract from CIL, VIL, CSL and CCL were analyzed *in-vitro* for immunomodulatory activity. MTT colorimetric assay was performed to determine the proliferation of mice splenocytes (Fig. 4.6.C). Spleen contains a relatively homogeneous fraction of B and T lymphocyte (Andersson *et al.*, 1972). Thus, immune-proliferation of spleen provides an understanding of the influence of the plant extracts on B and T cell lymphocyte. The B and T cell secrete several types of cytokines like IFN-γ, TNF-α, IL-4, IL-6, and IL-12.

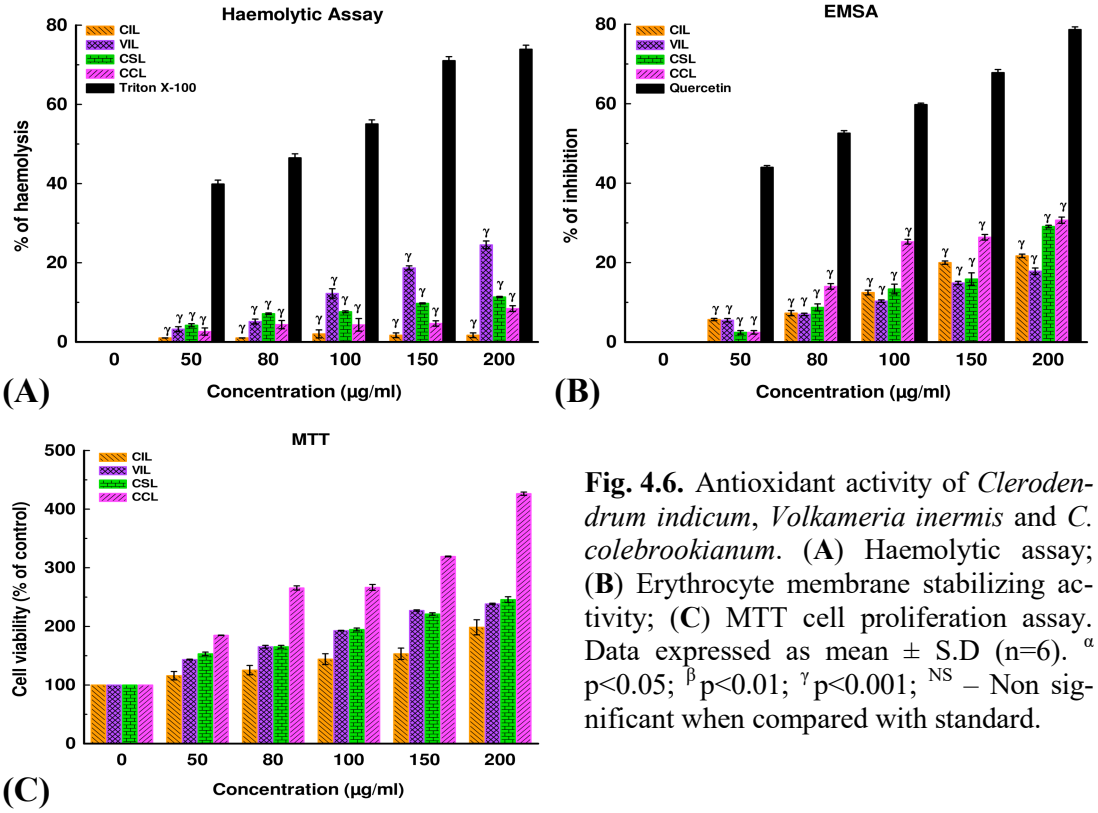

Fig. 4.6. Antioxidant activity of *Clerodendrum indicum*, *Volkameria inermis* and *C. colebrookianum*. (**A**) Haemolytic assay; (**B**) Erythrocyte membrane stabilizing activity; (**C**) MTT cell proliferation assay. Data expressed as mean ± S.D (n=6). $^{\alpha}$ $p<0.05$; $^{\beta}$ $p<0.01$; $^{\gamma}$ $p<0.001$; ^{NS} – Non significant when compared with standard.

CCL. Extract of the present study was observed to stimulate the proliferation of mice splenocyte by four fold in a dose dependent manner. Thus, the ability of CCL extract to modulate innate immune function suggests inhibition of tumor growth through the modulation of lymphocytes.

Hence, from the above experiments it could be inferred that all the extracts revealed negligible cytotoxic activity up to certain consumable doses, and therefore, can be safely used as bio-safety nutrient supplement for future purposes.

4.4. Detection of intracellular ROS generation

4.4.1. Measurement of ROS

Human hepatic cell line (WRL-68) and human liver cancer cell line (Hep-G2) were used to examine the effects of CIL, VIL and CCL under oxidative stress. CCl_4 increases oxidative stress levels in the liver tissue and based on that study, it is speculated that CCl_4 may induce the oxidative stress in WRL-68 and Hep-G2 cells. Therefore, WRL-68 and Hep-G2 cells were treated with CCl_4 for 0–24 h and intracellular oxidative levels were

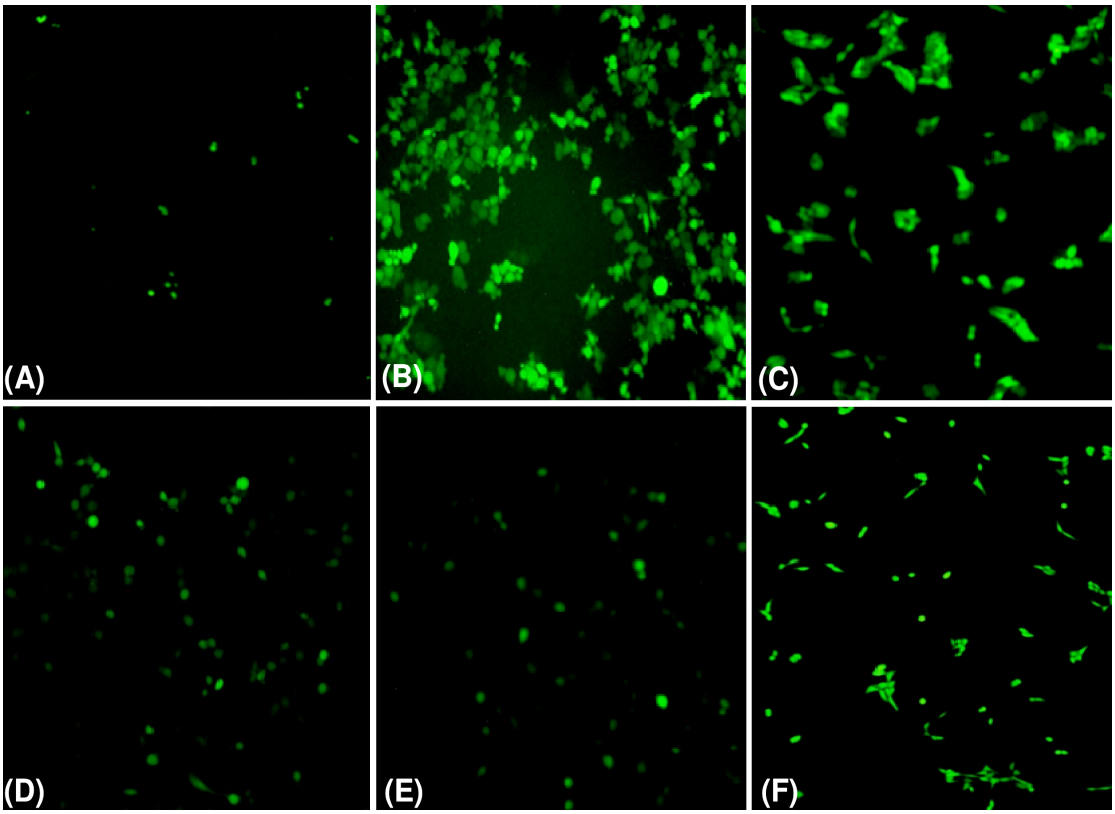

Fig. 4.7. Effects of *Clerodendrum* species (CIL, VIL and CCL) on oxidative stress in the Human Hepatic Cell Line (WRL-68). (**A**) Control cell culture; (**B**) Cells exposed to 200 µg/ml concentration of H_2O_2; (**C**) Cells exposed to 200 µg/ml concentration of CCl_4; (**D-F**) Cells exposed to 200 µg/ml concentration of CIL, VIL and CCL for 24 h.

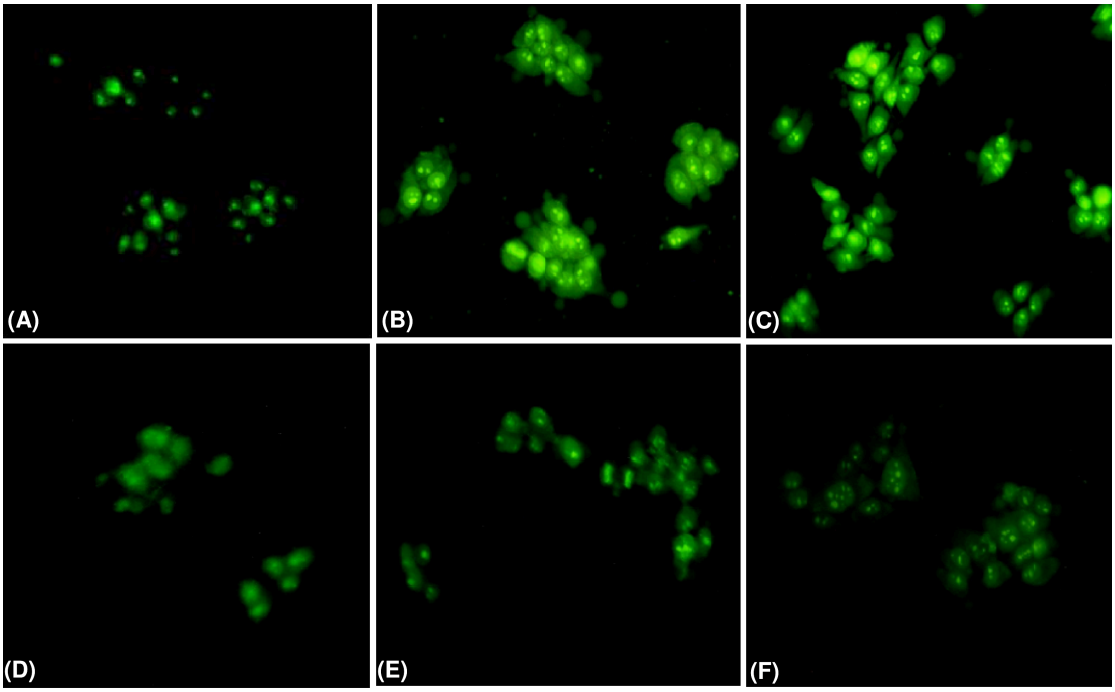

Fig. 4.8. Effects of *Clerodendrum* species (CIL, VIL and CCL) on oxidative stress in the human liver cancer cell line (Hep G2). (**A**) Control cell culture; (**B**) Cells exposed to 200 µg/ml concentration of H_2O_2; (**C**) Cells exposed to 200 µg/ml concentration of CCl_4; (**D-F**) Cells exposed to 200 µg/ml concentration of CIL, VIL and CCL for 24 h.

measured using the dichlorofluorescein assay. Figure 4.7 and 4.8 demonstrated that cells exposed to CCl_4 exhibited significantly increase in ROS levels. Tremendous decrease in fluorescence was detected at higher doses of CIL, VIL and CCL (200µg/ml) at 24h post exposure compared to the CCl_4 (Fig. 4.7.C and 4.8.C). The resulting change in fluorescence intensity gives strength to the hypothesis that CIL, VIL and CCL affects in the production of intracellular ROS. Cellular response in case of ROS is generally characterized by up regulation of antioxidants such as superoxide dismutase (SOD). Production of ROS was measured through H_2DCFDA and was found to get normalized in presence of CCL (Fig. 4.7.F and 4.8.F) when compared to CIL and VIL in case of WRL-68 and Hep-G2 cell lines. ROS generation was truly high in case of H_2O_2 and CCl_4 group but gradually diminished in the presence of *Clerodendrum* extract. The results were in complete accordance with our hypothesis pertaining to scavenging activity of CIL, VIL and CCL extracts and there was no harmful effect on viability of cells. It can be concluded that increasing production of hydrogen peroxide due to oxidative damage generates an excess amount of ROS and causes hepatic damage. Thus, it has been evident that *Clerodendrum* extracts possesses both *in-vivo* and *in-*

vitro antioxidant capacity and might have potential to prevent different types of oxidative stress related disorders.

4.4.2. Measurement of ROS in kidney cell line (HEK-293)

Hydrogen peroxide (H_2O_2) is a stable free radical having important role in signaling pathways (Ohno and Gallin, 1985). Increased levels of ROS productions are associated with oxidative stress in cell. H_2DCFDA was used to detect the production of intracellular ROS generation. ROS play a key role in apoptosis and the production of ROS in cells was determined after 24 hours of incubation. The control group of HEK-293 (Fig. 4.9.A) showed light and scattered green fluorescence, indicating that ROS formation was at a basal level. Whereas, H_2O_2 and gentamicin groups of HEK-293 (Fig. 4.9.B and 4.9.C) showed a large amount of ROS generation due to the formation of reactive oxygen species. A substantial reduction of fluorescence intensity was seen in highest concentration of CSL extract (200µg/ml) (Fig. 4.9.D). This suggests that under the influence of CSL, gentamicin induced ROS was diminished proportionately. It can be inferred that CSL plays an important

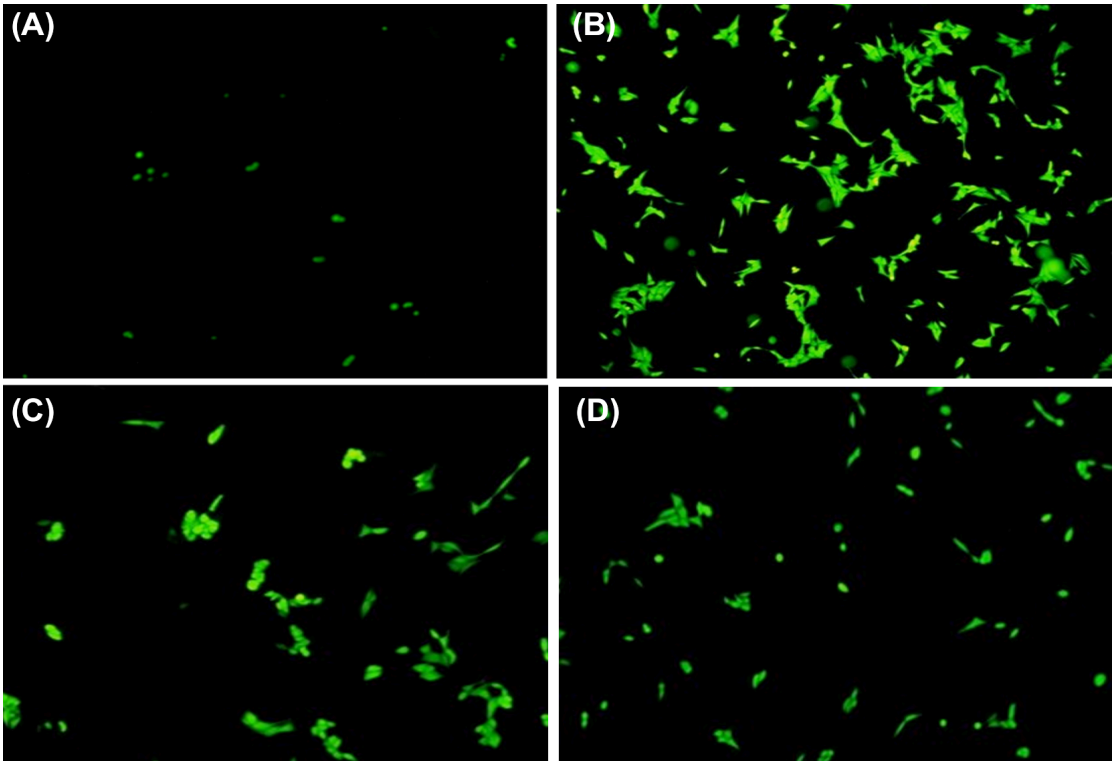

Fig. 4.9. Effects of *Clerodendrum serratum* (CSL) on oxidative stress in the human embryonic kidney cell line (HEK-293). (**A**) Control cell culture; (**B**) Cells exposed to 200 µg/ml concentration of H_2O_2; (**C**) Cells exposed to 200 µg/ml concentration of gentamicin; (**D**) Cells exposed to 200 µg/ml concentration of CSL for 24 h.

role in reducing the impact of gentamicin on normal intracellular function.

4.5. Antimicrobial activity

The methanolic extract of four *Clerodendrum* species namely *C. indicum*, *C. inerme* (syn: *Volkameria inermis*), *C. serratum* and *C. colebrookianum* showed antibacterial activity (zone of inhibition, mm) against two pathogenic gram positive bacteria *Bacillus subtilis* (Fig. 4.10), *Staphylococcus aureus* (Fig. 4.11) and two pathogenic gram negative bacteria *Escherichia coli* (Fig. 4.12) and *Enterobacter aerogenes* (Fig. 4.13) at a concentration of 0.1, 0.25, 0.5 and 1.0 mg/ml (Table 4.3.). Earlier it has also been reported by George and Pandalai (1949) that alcoholic extracts of leaves and flowers of *C. inerme* exhibited

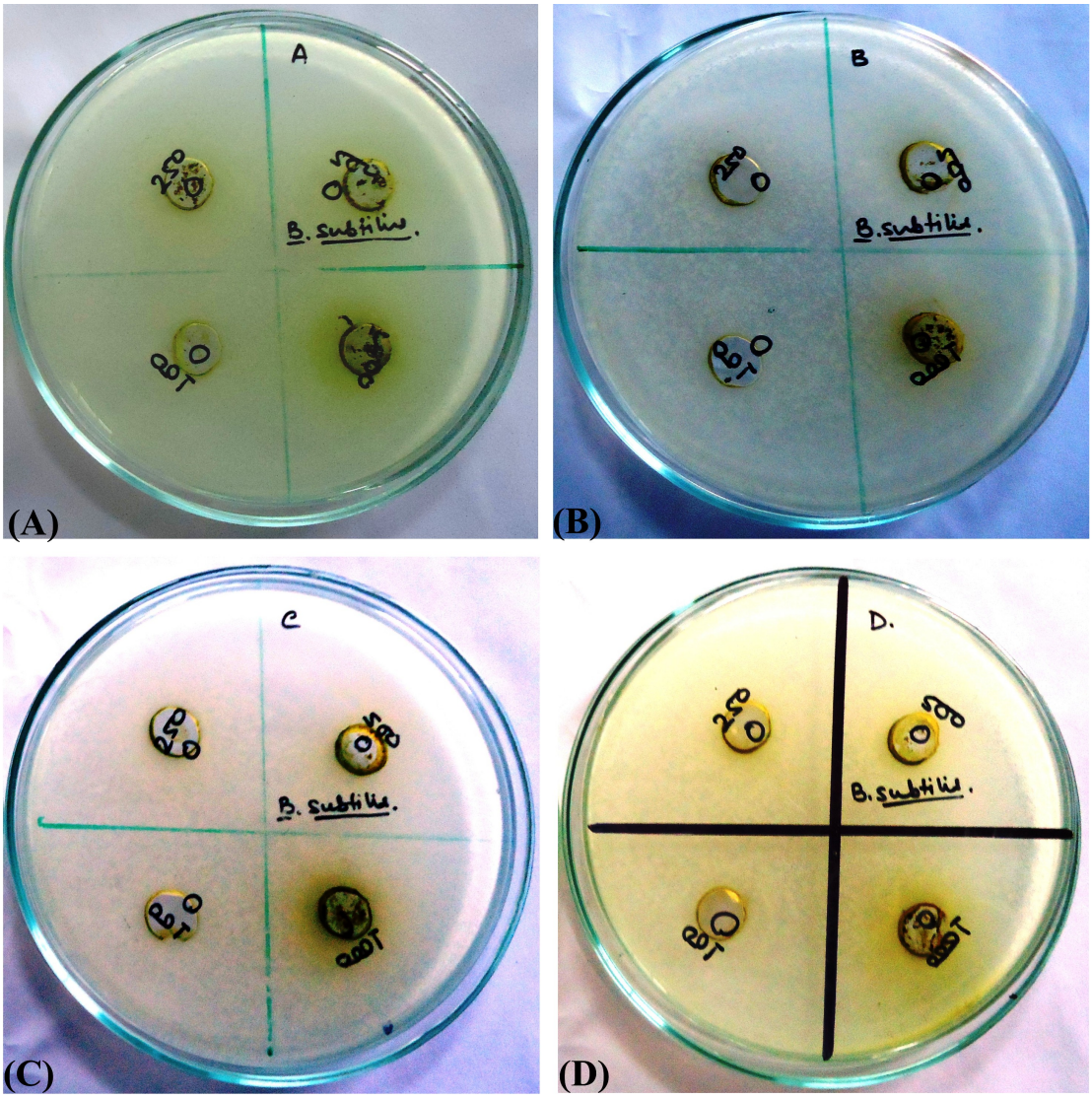

Fig. 4.10. Antimicrobial activity of four *Clerodendrum* species namely **(A)** *C. indicum*; **(B)** *C. inerme*; **(C)** *C. serratum* and **(D)** *C. colebrookianum* against pathogenic bacteria *B. subtilis.*

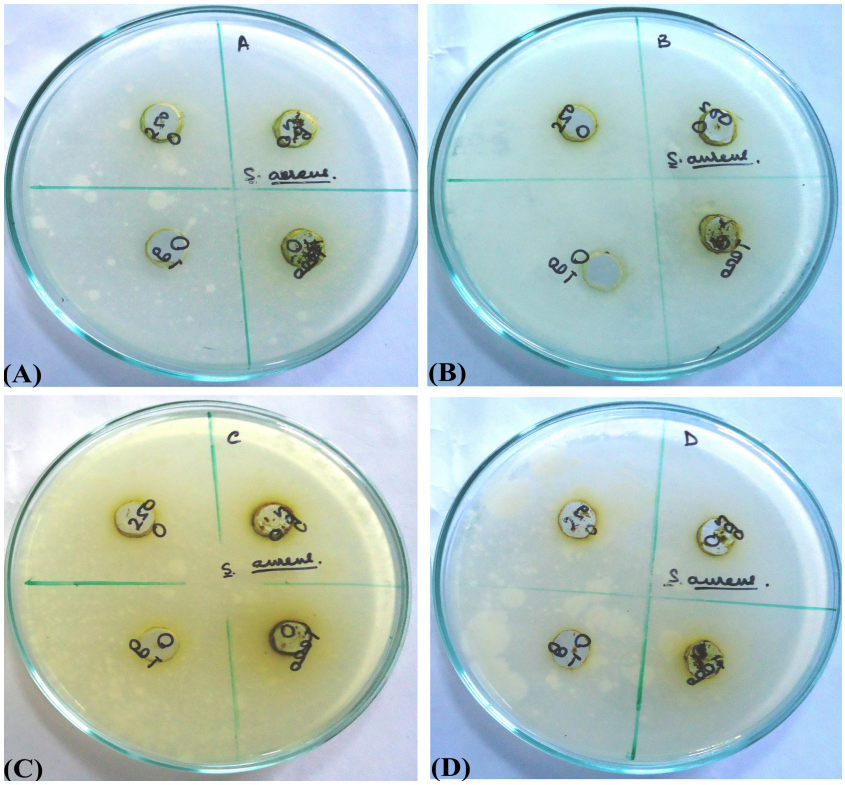

Fig. 4.11. Antimicrobial activity of four *Clerodendrum* species namely **(A)** *C. indicum*; **(B)** *C. inerme*; **(C)** *C. serratum* and **(D)** *C. colebrookianum* against pathogenic bacteria *S. aureus.*

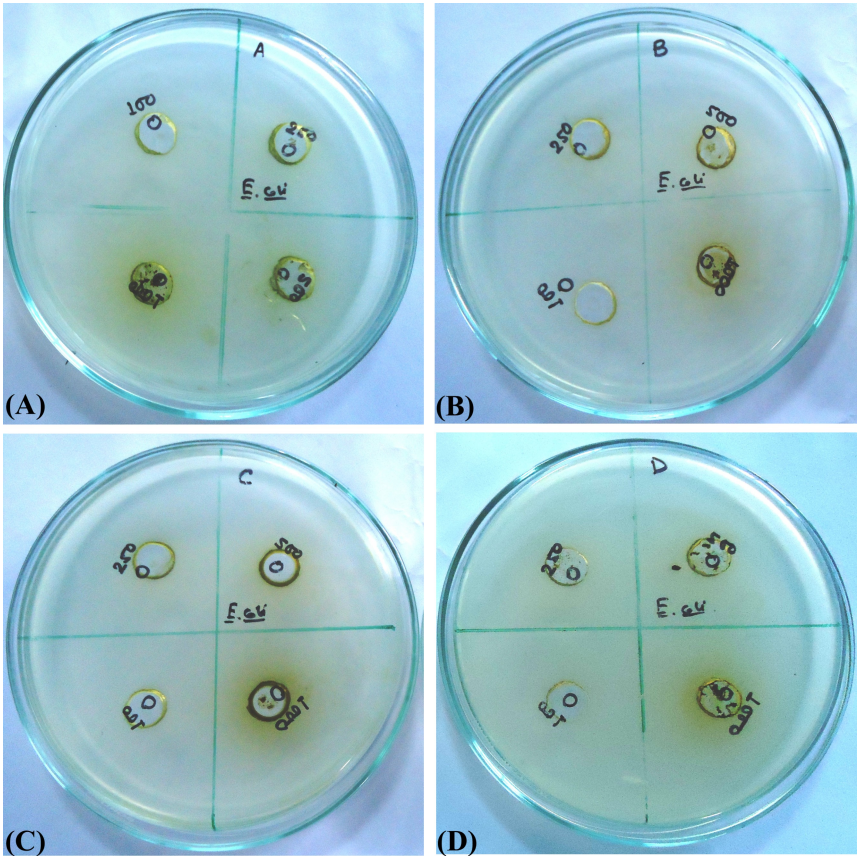

Fig. 4.12. Antimicrobial activity of four *Clerodendrum* species namely **(A)** *C. indicum*; **(B)** *C. inerme*; **(C)** *C. serratum* and **(D)** *C. colebrookianum* against pathogenic bacteria *E. coli.*

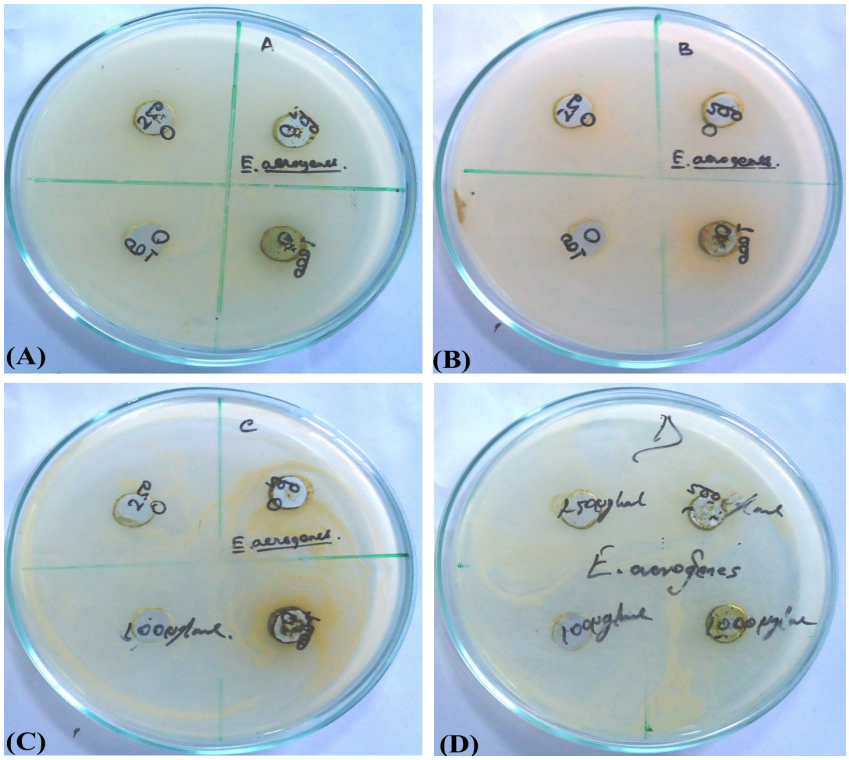

Fig. 4.13. Antimicrobial activity of four *Clerodendrum* species namely **(A)** *C. indicum*; **(B)** *C. inerme*; **(C)** *C. serratum* and **(D)** *C. colebrookianum* against pathogenic bacteria *E. aerogenes.*

Table 4.3. Antimicrobial activity of four *Clerodendrum* species (CIL, VIL, CSL and CCL).

Sample	Concentration (µg/ml)	Diameter of zone of inhibition (mm.)			
		B. subtilis	***S. aureus***	***E. coli***	***E. aerogenes***
C. indicum	100	10.33±0.57	10.33±0.47	10.33±0.57	10.33±0.57
	250	11.0±1.0	10.66±0.67	10.66±0.67	10.66±0.47
	500	13.0±1.0	13.33±1.15	12.66±1.15	12.66±1.15
	1000	18.0±1.0	18.33±0.57	13.66±1.15	15.33±0.57
C. inerme	100	10.3±0.57	10.43±0.67	9.3±0.57	10.33±0.57
	250	12.6±1.15	12.76±1.15	11.6±1.25	12.6±1.09
	500	14.0±1.73	14.0±1.73	13.0±1.53	13.53±0.77
	1000	15.3±0.57	15.23±0.47	14.3±0.47	15.13±0.57
C. serratum	100	10.33±0.57	10.23±0.57	11.27±0.15	9.23±1.11
	250	11.6±1.09	12.61±1.09	12.44±1.5	10.31±1.0
	500	12.53±0.78	14.43±0.77	14.20±.11	11.23±0.53
	1000	15.13±0.57	15.73±0.57	15.57±0.47	12.39±0.33
C. colebrookianum	100	12.44±0.85	10.23±0.47	12.6±1.09	9.23±1.11
	250	13.21±0.55	10.56±0.67	13.53±0.77	10.31±1.0
	500	16.0±0.21	12.66±1.15	15.57±0.47	11.6±1.09
	1000	19.54±1.1	13.66±1.15	16.06±0.33	13.21±0.55
Tetracycline	100	21.11±0.25	25.43±1.1	23.45±0.55	20.58±0.41

antibacterial activity against *Escherichia coli* and *Staphylococcus aureus*. Vidya et al. (2010) reported that the different bacterial strains tested root extract of *C. serratum* produced maximum zone of growth inhibition against *Enterobacter aerogenes*. Similarly, Misra et al. (1995) found that hexane extracts of *C. colebrookianum* showed strong antibacterial activities against various Gram positive and Gram negative pathogens such as *Staphylococcus haemolyticus*, *S. aureus*, *E. coli* and *Pseudomonas aeruginosa*. The findings in the present study offer a scientific support to the use of leaves of four *Clerodendrum* species as a new antibacterial drug against bacterial infection in future.

4.6. *In-vivo* hepatoprotective activity

4.6.1. Acute toxicity study

CIL, VIL and CCL extracts were administered orally and no mortality was observed in the experimental animals at 2000 mg/kg dose. Therefore, $1/40^{th}$ (50 mg/kg) and $1/10^{th}$ (200 mg/kg) of the maximum dose were considered safe for the *in-vivo* studies.

4.6.2. Body weight changes

Changes in mouse body weight after the treatment of CCl_4, silymarin, CIL, VIL and CCL have been shown in Table 4.4. No significant weight gain was noticed in the treated mice when final body weight was compared with the initial body weight of the corresponding group.

Table 4.4. Effects of three *Clerodendrum* species (CIL, VIL and CCL) on the body weight of the treated mice.

Group	Initial weight	Final Weight	% body weight change
Control	33.98±1.65	35.99±0.71 ^{NS}	5.61±3.06▲
CCl_4	36.95±1.34	32.71±1.86**	13.05±2.28▼
Silymarin	35.57±1.26	36.93±1.63 ^{NS}	3.64±1.99▲
CIL 50 mg/kg	33.01±1.97	35.32±0.82 ^{NS}	6.59±3.44▲
CIL 200 mg/kg	33.08±1.93	35.36±0.88 ^{NS}	6.49±3.15▲
VIL 50 mg/kg	33.05±1.95	35.34±0.8 ^{NS}	6.53±3.41▲
VIL 200 mg/kg	33.01±1.92	35.42±0.98*	6.86±2.80▲
CCL 50 mg/kg	32.05±1.04	35.51±1.1**	9.73±1.29▲
CCL 200 mg/kg	31.34±0.86	35.09±0.47*	10.67±2.50▲

Weight (mean ± SD) in gram, * P<=0.05, ** P<=0.01, ^{NS} = Non significant. Final body weight was compared with initial body weight of corresponding group. ▲ Increase weight; ▼ Decrease weight.

4.6.3. In-vivo antioxidant assays

In the present study, we tried to further investigate how free radicals are linked to hepatic damage or disorder and the potential therapeutic role of *Clerodendrum* extracts in this regard. In this study, CCl_4 (Haloalkane) was chosen to induce hepatic damage in murine model and the antioxidant and anti-inflammatory activities were investigated. The toxicity profile of CCl_4 is well established worldwide (Ruprah *et al.*, 1985). Extensive usage of CCl_4 in industrial sectors has a history of environmental toxicity and occupational hazards. Carbon tetrachloride (CCl_4) induced hepato-toxicity is caused to some extent by the partial pressure of reactive oxygen in tissues. The low partial pressure of oxygen results in the formation of CCl_3^* and $CHCl_2^*$ radicals (De Groot *et al.*, 1988). Metabolism of lipid is hampered by CCl_4 and cause steatosis or fatty liver. In CCl_4 induced liver injury model, oxidative stress can provoke and promote lipid peroxidation that damage the hepatocellular membrane (De Groot *et al.*, 1988). CCl_4 is generally required for the synthesis of chlorofluorocarbons (CFCs) which are used as heat transfer agents in refrigerating equipment and as aerosol propellants. In the studied animal model, significant ($P<0.001$) loss of body weight have occurred after CCl_4 toxicity. CCl_4 is bio-transformed by CYP2E1, is a member of cytochrome P_{450} mixed function oxidase system, involved in the metabolism of xenobiotics in the body to produce $CCl_3^{\cdot}$ and $CCl_3OO^{\cdot}$, and as a result of that tremendous hepatocellular necrosis is caused. Zonal hemorrhagic necrosis around the portal veins in the CCl_4 group demonstrated the hepatocellular injury.

Significant inhibition of enzymatic catalase and SOD (superoxide dismutase) and non-enzymatic reduced glutathione (GSH) by *Clerodendrum* (CIL, VIL and CCL) extract occurred in CCl_4 intoxicated mice when compared with the control (Fig. 4.14.A, 4.14.D and 4.14.C). CCL treatment enabled a significant increase in the percent of inhibition of catalase and reduced glutathione when compared with CCl_4 intoxicated groups and other *Clerodendrum* species (CIL and VIL). On the other hand silymarin treatment significantly increase the percent of inhibition compared with the CCl_4 treated mice. CCl_4 treatment significantly lowers the peroxidase

enzyme activity in hepatic tissue (Fig. 4.14.B). The peroxidase activity in the control group was 17.12 ± 1.15 unit/mg tissues which were lowered 6.09 ± 0.54 unit/mg tissues due to CCl_4 administration. The lowered peroxidase activity was significantly elevated by CCLH (15.37 ± 0.45 unit/mg tissue) when compared with the standard silymarin treated group (12.73 ± 0.93 unit/mg tissue). Lipid peroxidation or MDA level in the treated groups are illustrated in Fig. 4.14.E. The MDA content was elevated from 8.98 ± 1.56 mM/litre in control to 19.27 ± 1.31 mM/litre in CCl_4 group. Significant results found when the elevated MDA level was lowered to 5.64 ± 0.86 mM/litre after CCLH administration. CCl_4 toxicity resulted increases in NO release when compared to the control (Fig. 4.14.F). However, significant ($p < 0.001$) lowering of NO level was observed in the treated groups. The NO level in silymarin and CCLH groups were 142.37 ± 11.70 and 175.33 ± 12.50% respectively when NO release of control was considered as 100 %.

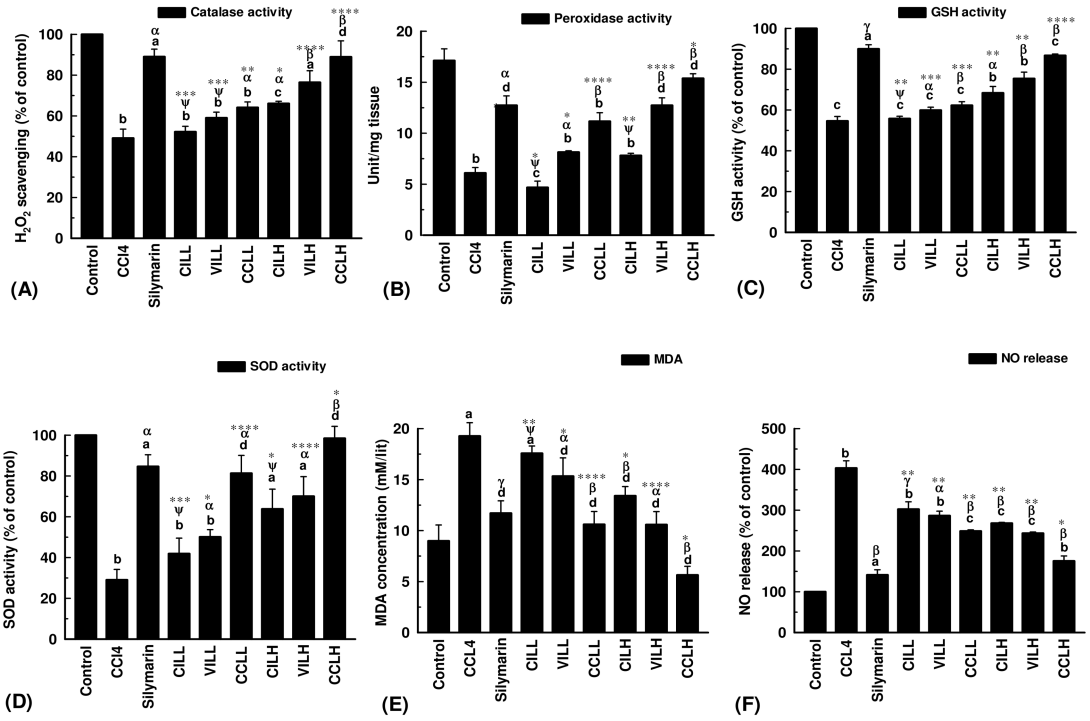

Fig. 4.14. The effect of *Clerodendrum* extracts (CIL, VIL and CCL) on (**A**) Catalase activity; (**B**) Peroxidase activity; (**C**) Reduced Glutathione (GSH) activity; (**D**) Superoxide Dismutase (SOD) activity; (**E**) Lipid Peroxidation (LPO) activity; (**F**) NO release. CILL: *C. indicum* Low Dose; VILL: *V. inermis* Low Dose; CCLL: *C. colebrookianum* Low Dose; CILH: *C. indicum* High Dose; VILH: *V. inermis* High Dose; CCLH: *C. colebrookianum* High Dose. Data expressed as mean ± S.D (n=6). $^{a}p<0.05$; $^{b}p<0.01$; ^{c} $p<0.001$; $^{d}p=$ non significant vs control group; $^{\alpha}p<0.05$; $^{\beta}p<0.01$; $^{\gamma}p<0.001$; $^{\Psi}p=$non significant vs CCl_4 group; $^{*}p<0.05$; $^{**}p<0.01$; *** $p<0.001$; $^{****}p=$non significant vs silymarin group.

Peroxidase, catalase and superoxide dismutase are the major anti-oxidative enzymes responsible for the neutralization of free radicals. Hydrogen peroxide and lipid peroxides convert into nonreactive species by the action of peroxidase enzyme. On the other hand, catalase prevents the formation of highly reactive $OH^{\cdot}$ by scavenging H_2O_2, the key molecule of fenton reaction. SOD (super oxide dismutase) alternatively catalyzes the dismutation of superoxide radicals into ordinary molecular oxygen or hydrogen peroxide. Glutathione is a major anti-oxidant enzyme that can also serve as a redox or cell signaling regulator and guard the cells against oxidative injury by reducing H_2O_2 and scavenging reactive oxygen and nitrogen radicals. CCl_4 derived trichloromethyl peroxy radicals ($CCl_3OO^{\cdot}$) accepts the proton from polyunsaturated fatty acid in the biological membrane and cause lipid peroxidation and inhibition of oxidative enzymes. By the inhibition of anti-oxidative enzymes, there is an accumulation of $O_2^{\cdot-}$ and H_2O_2, these free radical formation causes hepatic damage (Malins and Haimanot, 1991). Nitric oxide (NO) plays a major role as pro-inflammatory mediators during oxidative stress which in turn leads to apoptotic cell death. In the present study, oxidative stress increased the NO levels, which was subsequently lowered by the CIL, VIL and CCL extract. This exhibited potent anti-inflammatory activities of plant extract through suppression of pro-inflammatory mediators of oxidative stress. In this study, it is established that the diminished catalase, peroxidase and superoxide dismutase levels and elevated MDA levels were subsequently normalized by *Clerodendrum* administration.

4.6.4. Histopathological examination

The hepatoprotective potentialities of leaf extract of *Clerodendrum* species (CIL, VIL and CCL) were further established by the detailed histopathological study. There are several histological parameters showed the injury level of experimental groups (Fig. 4.15 and 4.16). The haematoxylin -eosin staining of hepatocytes displayed clearly the well maintained hepatocellular integrity, healthy cellular architecture and clear cytoplasm with prominent nucleus in the control group. But in the CCl_4 group, several damages have been observed such as hepatocellular necrosis, sinusoidal dilation, bile duct

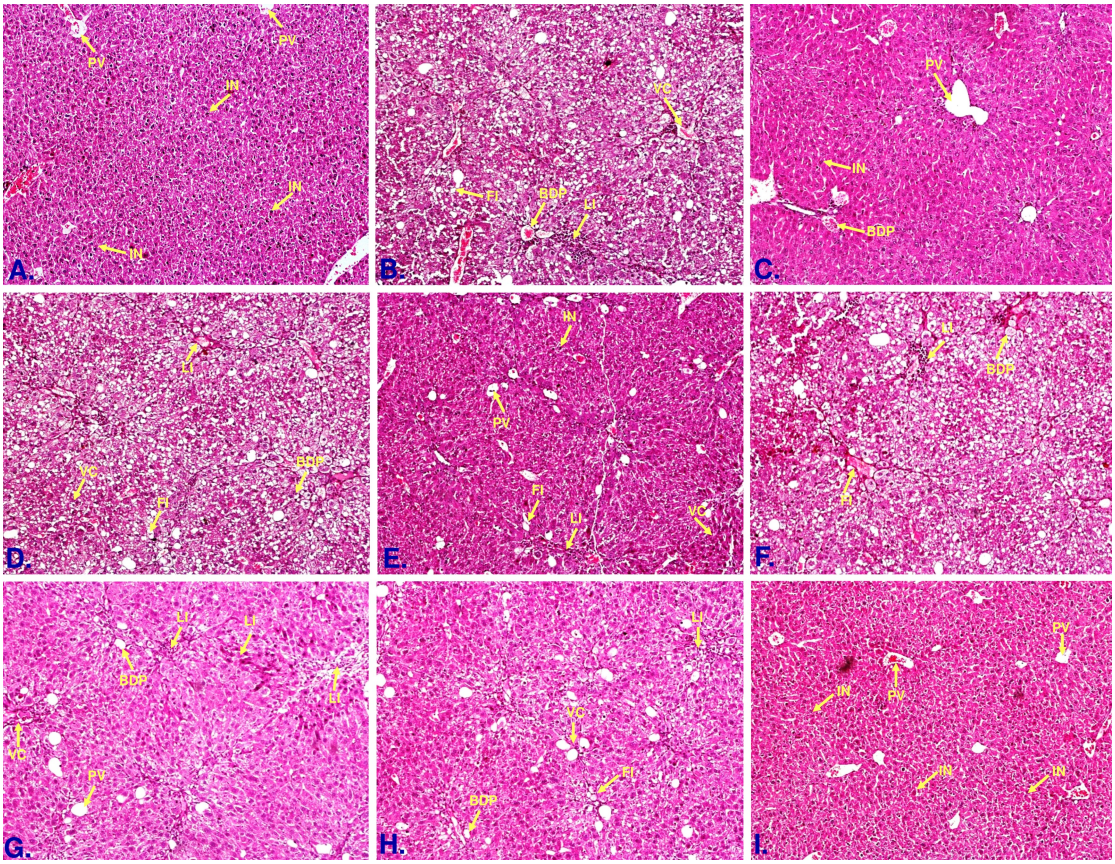

Fig. 4.15. Photomicrographs (100×) of the histopathological examinations of the liver samples of different groups.

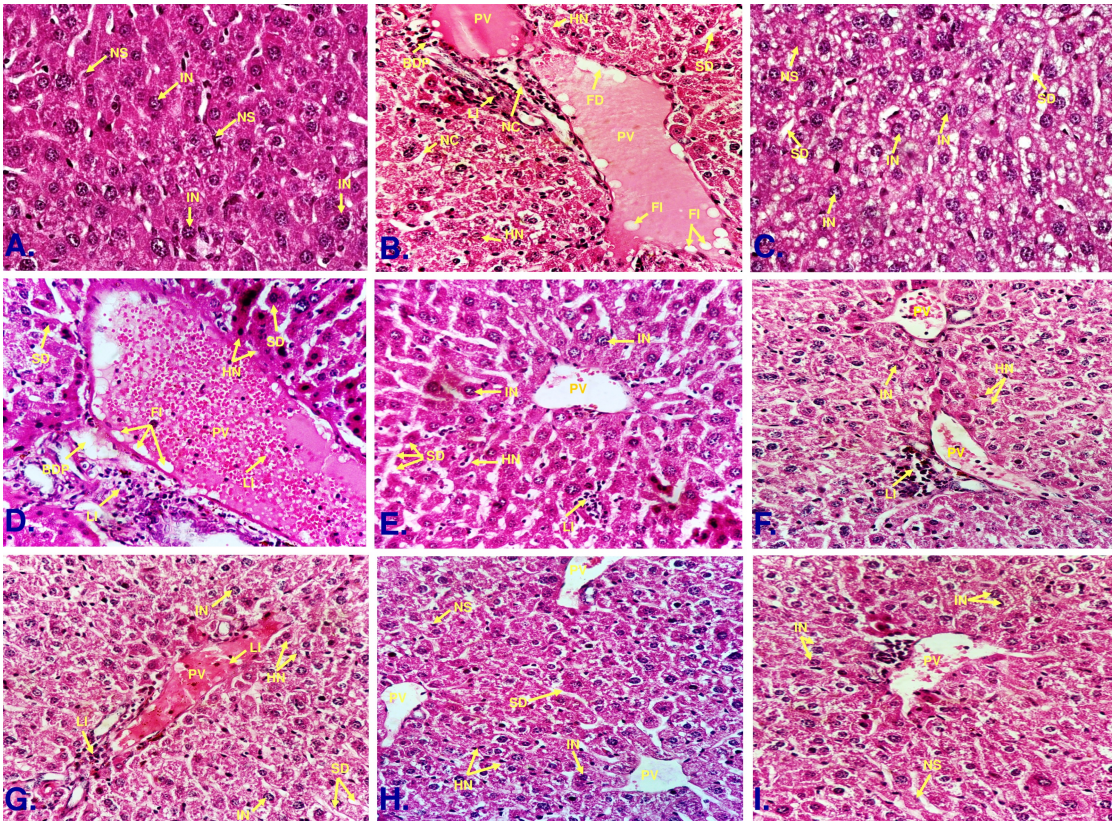

Fig. 4.16. Photomicrographs (400×) of the histopathological examinations of the liver samples of different groups.

proliferation, inflammation (leukocyte infiltration), vascular congestion, loss of structure of hepatic nodules, fatty infiltration, vascular degeneration and calcification. The thickening and scoring of connective tissue, as a result of injury were notified in the CCl_4 group (Fig. 4.15.B and 4.16.B). The injury level found in the CCl_4 group was down regulated by the administration of standard drug silymarin (Fig. 4.15.C and 4.16.C). Interestingly, in the present study it was observed that high dose of plant extract (CCLH) (Fig. 4.15.I and 4.16.I) down regulates the injury better or similar compared to the standard silymarin.

4.7. Neurotherapeutic effects

4.7.1. Acute toxicity study

CSL extract was administered orally and no mortality was observed in the experimental animals at 2000 mg/kg dose. Therefore, $1/20^{th}$ (100 mg/kg) and $1/5^{th}$ (400 mg/kg) of the maximum dose were considered safe for the *in-vivo* studies.

4.7.2. Body weight changes

Changes of mouse body weight after the treatment of Scopolamine, donepezil, CSL low and CSL high have been shown in Table 4.5. No significant weight gain was noticed in the treated mice when final body weight was compared with initial body weight of the corresponding group.

4.7.3. Step through passive avoidance test

The present study accounted an inclusive report of neurotherapeutic effect of CSL on memory deficits in a mouse model of amnesia (passive avoidance test) induced by scopolamine. Step through passive avoidance test, a fear-motivated avoidance test, was employed to describe the way in which the animal learns to avoid an aversive stimulus (electric footshock) as a part of long-term memory. Table 4.6. revealed that

Table 4.5. Effects of *Clerodendrum serratum* on the body weight of the treated mice.

	Control	Scopolamine	Donepezil	CSL Low	CSL High
Initial Weight	34.35±1.07	36.95±1.34	35.57±1.26	32.78±1.47	33.68±1.96
Final Weight	36.45±2.03 ^{NS}	32.71±1.86**	36.93±1.63^{NS}	35.41±0.90^{NS}	35.43±1.67*
% body weight change	5.67±2.37▲	11.51±1.79▼	3.63±1.99▲	7.43±3.03▲	4.98±1.16▲

Weight (mean ± SD) in gram, * P<=0.05, ** P<=0.01, ^{NS} = Non significant. Final body weight was compared with initial body weight of corresponding group. ▲ Increase weight; ▼ Decrease weight.

Table 4.6. Effect of CSL extract on scopolamine induced memory impairment in the passive avoidance test.

Groups	IL (Sec.)	STL (Sec.)
Group I (Control)	18.13±1.99	132.41±8.29
Group II (SCP)	107.23±4.83	80.14±1.33
Group III (SCP + Donepezil)	27.12±2.19	176.79±2.19
Group IV (SCP + CSL low)	57.78±4.34	130.24±0.83
Group V (SCP + CSL high)	35.66±2.39	165.23±1.45

IL- Initial latency; STL- Step Through Latency; SCP- Scopolamine; CSL- *Clerodendrum serratum*, [Data represented as mean ± SD].

the initial latency time to enter the dark chamber was significantly longer in the mice given only scopolamine as compared to the control group suggesting amnesic effect of mice. The treatment with CSL extract significantly attenuated the scopolamine induced memory deficit in mice to a great extent and also associated with the short-term memory (STL) improvement (Table 4.6.) suggesting anti-amnesic effect of extracts in the scopolamine induced rodent model. While considering brain AChE inhibitory activity, CSL was also recorded to be reversed the scopolamine induced memory impairment in mice by increasing cholinergic activity through the inhibition of AChE (Fig. 4.17.A). Hence, it can be inferred that CSL could be a potent AChE-inhibitors by hindering the destruction of Ach (McGleenon *et al.*, 1999). This result also supports the ideas which might be due to a decrease in gene transcription, translation and enhance cholinergic activity thereby improving cognitive function (Shahidi *et al.*, 2008).

4.7.4. In-vivo antioxidant assays

In the present study, scopolamine treatment significantly reduced antioxidant capacity of DPPH, enzymatic catalase and SOD (superoxide dismutase) (Fig. 4.17.B, 4.17.D, 4.17.F) and non-enzymatic reduced glutathione (GSH) system in brain tissues (Fig. 4.17.E). At the same time, CSL treatment significantly increased the percent of inhibition of DPPH, catalase, SOD and reduced glutathione when compared with scopolamine groups. Lipid peroxidation or MDA level in the treated groups are illustrated in Fig. 4.17.C. The MDA content was elevated from 28.26 ± 2.89 mM/litre in control to 51.89 ± 5.17 mM/litre in scopolamine group. Significant results found when the elevated MDA level

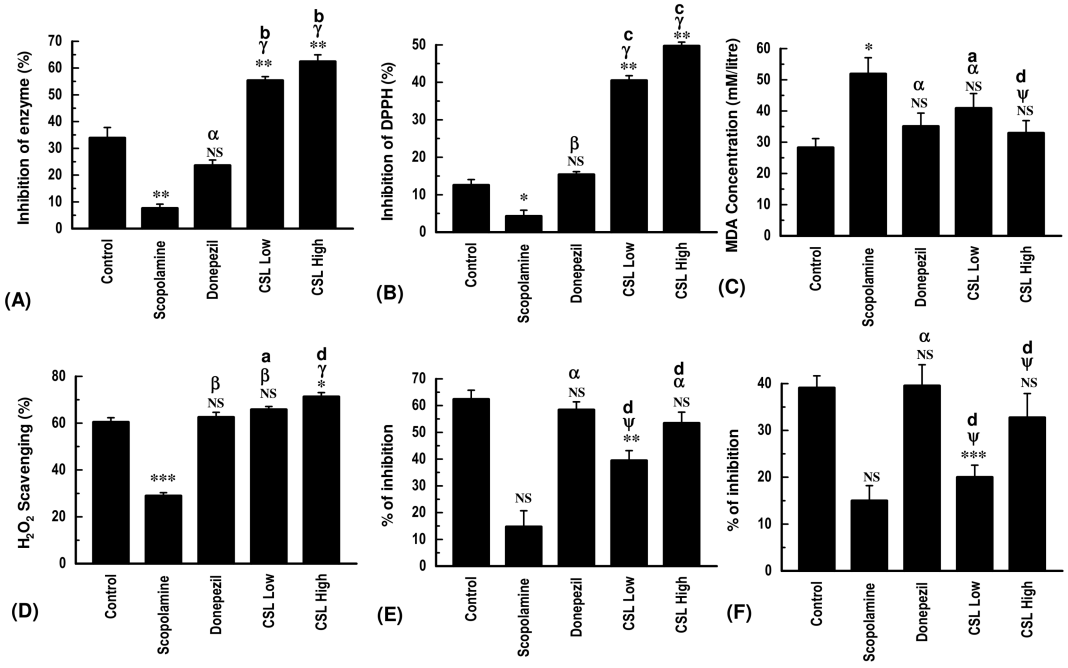

Fig. 4.17. Effect of CSL extract on scopolamine-induced memory impairment in the passive avoidance test. **(A)** AChE **(B)** DPPH **(C)** Lipid peroxidation **(D)** Catalase **(E)** GSH and **(F)** SOD activity of CSL extract. *p<0.05; **p<0.01; *** p<0.001; ^{NS}p=non significant vs control group; $^{\alpha}$p<0.05; $^{\beta}$p<0.01; $^{\gamma}$p<0.001; $^{\Psi}$p=non significant vs Scopolamine group; ^{a}p<0.05; ^{b}p<0.01; ^{c}p<0.001; ^{d}p= non significant vs donepezil group. [Data represented as mean ± SD].

was lowered to 32.93 ± 3.98 mM/litre after high dose of CSL administration. Hence, the results suggest anti-oxidative potential of CSL that contributed to effective neuronal plasticity and memory function. Thus, most importantly, we provide first evidence for a potent neurotherapeutic role of CSL in the protection from ROS mediated neuronal damage as well as we identified some of the responsible target phytocompounds that could be treated as future CNS drug. It has been well speculated that every cellular organism sustains its own antioxidant stability to protect tissues from oxidative damage at a certain stage. SOD, catalase, GSH etc. are the fundamental antioxidant enzymes that protect tissues from highly reactive hydroxyl radicals and superoxide anions, linked with NDs (Flora *et al.*, 2012; Gilgun-Sherki *et al.*, 2001).

4.7.5. Histopathological examination

The neuroprotective potentialities of CSL extract was further established by detailed histopathological study. Histopathological examination of brain sections of control mice showed the normal structure of the cerebral cortex and hippocampus (Fig. 4.18.A and 4.19.A). Mice with scopolamine

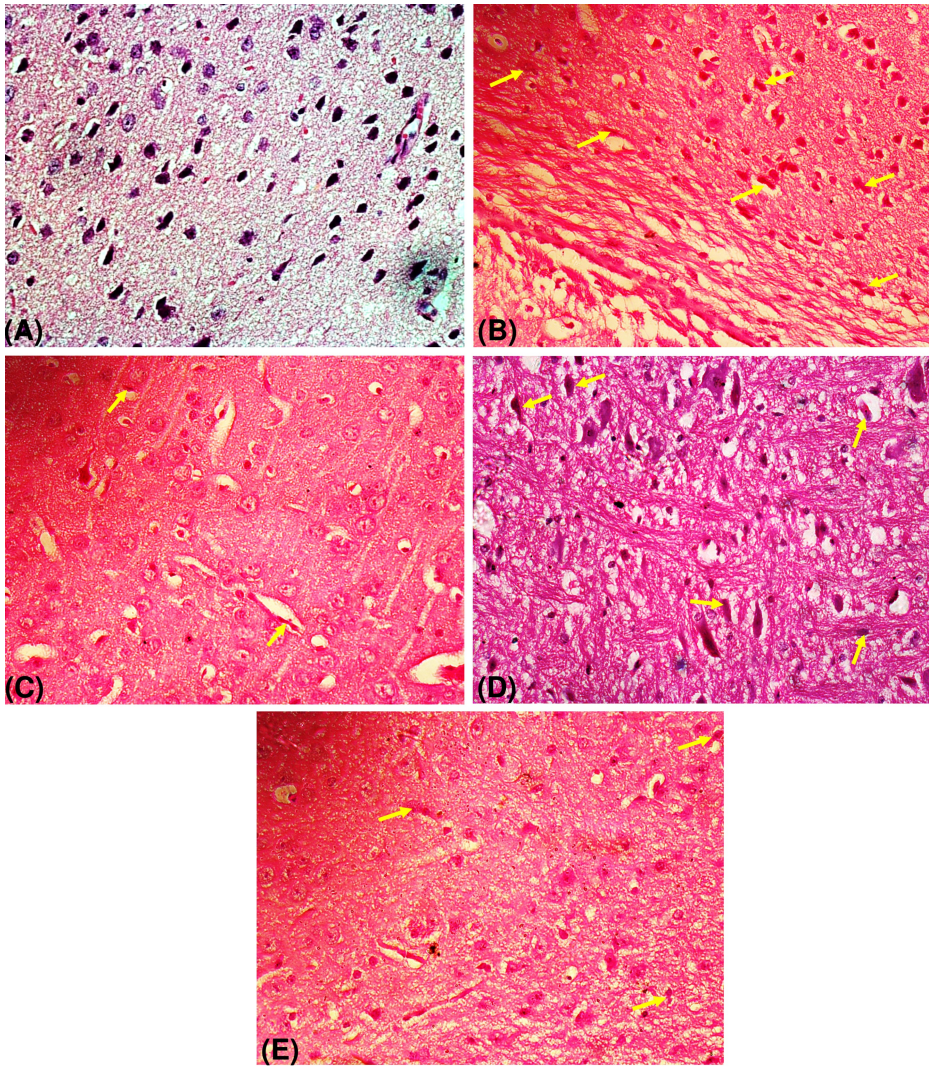

Fig. 4.18. Photomicrograph of control and treated mice brain (cortex, A-E), 40X.

showed severe chromatolysis (arrows), Gliosis and edema in cortex (Fig. 4.18.B), whereas, the hippocampus revealed severe chromatolysis of nuclear material and most of the Purkinje neurons are necrotic (Fig. 4.19.B). Mice brain exposed to donepezil showed less necrotic, degenerative changes with normal neurons and glial cells in both the cortex and hippocampus region (Fig. 4.18.C and 4.19.C). Interestingly, in the present study it was observed that high dose of CSL extract (400mg/kg BW) down regulates the injury better or similar compared to the standard donepezil (Fig. 4.18.E and 4.19.E).

4.8. Gentamicin induced nephrotoxicity

4.8.1. Acute toxicity study

CSL extract was administered orally and no mortality was observed in the experimental animals at 2000 mg/kg dose. Therefore, 1/10th (200 mg/kg) and 1/5th (400 mg/kg) of the maximum

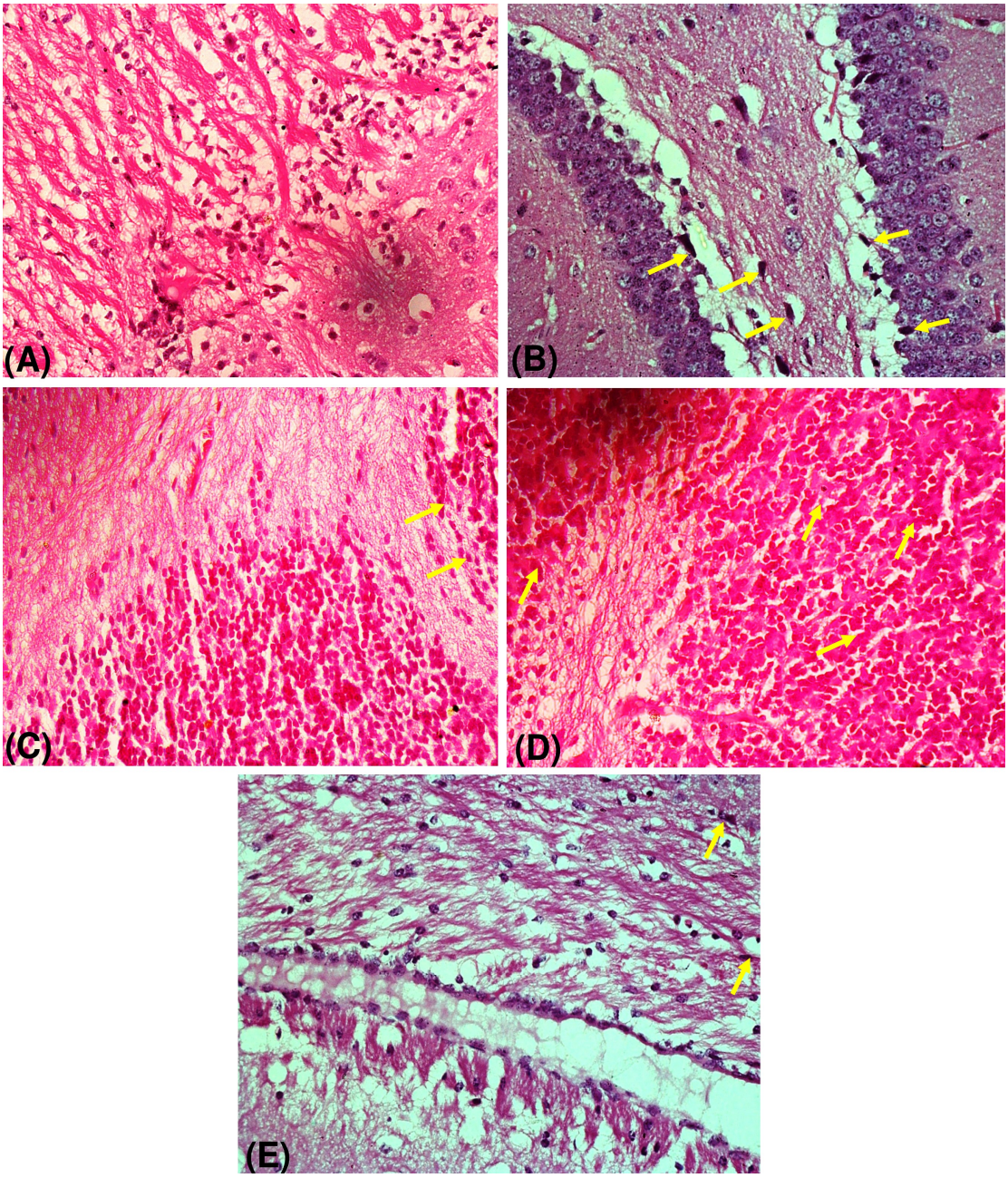

Fig. 4.19. Photomicrograph of control and treated mice brain (Hippocampus region, A-E), 40X.

Table 4.7. Effects of *Clerodendrum serratum* on the body weight of the treated rat.

	Control	Gentamicin	Cystone	CSL Low	CSL High
Initial Weight	79.06±0.33	83.33±7.57	83.66±9.07	91±2.64	86.66±1.52
Final Weight	82.33±2.51 ^{NS}	72.33±2.55 ^{NS}	92.66±2.48 ^{NS}	93.0±1.0 ^{NS}	89.66±1.52 ^{NS}
% body weight change	3.90±2.95▲	15.06±6.6▼	9.57±11.07▲	2.16±1.87▲	3.31±2.88▲

Weight (mean ± SD) in gram, ^{NS} = Non significant. Final body weight was compared with initial body weight of corresponding group. ▲ Increase weight; ▼ Decrease weight.

Table 4.8. Effects of *Clerodendrum serratum* on serum biochemical parameters of five (n=5) treated groups.

Group	Creatinine (mg/dl)	Urea (mg/dl)
Control	0.65±0.02	44.42±2.19
Gentamicin	1.78±0.12^{d}	123.31±1.88^{a}
Cystone	0.73±0.02$^{d\alpha}$	56.20±4.71$^{d\alpha}$
CSL 200 mg/kg	0.88±0.01$^{a\psi}$	94.68±4.6$^{a\psi}$
CSL 400 mg/kg	0.74±0.02$^{d\alpha}$	62.46±3.74$^{d\alpha}$

Data expressed as mean ± S.D (n=6). $^{a}p<0.05$; ^{d}p= non significant vs control group; $^{\alpha}p<0.05$; $^{\psi}p$=non significant vs gentamicin group.

dose were considered safe for the *in-vivo* studies.

4.8.2. Body weight changes

Changes in rat body weight after the treatment of gentamicin, cystone, CSL low and CSL high have been shown in Table 4.7. No significant weight gain was noticed in the treated rat when final body weight was compared with the initial body weight of the corresponding group.

4.8.3. Serum biochemical assays

In the first phase of kidney disease serum creatinine concentration is more potent indicator than the urea concentration. Parenchyma tissues in kidney are very sensitive to natural or synthetic agents such as antimicrobials, chemotherapeutic agents and analgesics which begin to increase urea concentration only after parenchyma tissue injury (Gilbert *et al.*, 1989). In the present study, serum creatinine and urea level was markedly elevated in gentamicin treated group compared to control and other dose groups (Table 4.8.). It was evident from this study that elevated creatinine and urea level in the blood was observed due to gentamicin toxicity induced kidney injury. Similar results were also observed by Nakakuki et al. (1996) and Kumar et al. (2000). Elevated creatinine and urea level were subsequently normalized due to cystone to a certain extent by administration of CSL extract.

4.8.4. In-vivo antioxidant assays

In these experiments the CSL extract showed significant inhibition of SOD (Fig. 4.20.A), catalase (Fig. 4.20.D) and GSH (Fig. 4.20.B). CSLH treatment enabled a significant increase in the percent of inhibition of catalase and reduced glutathione when compared with gentamicin treated groups. On the other hand, cystone treatment significantly increase the

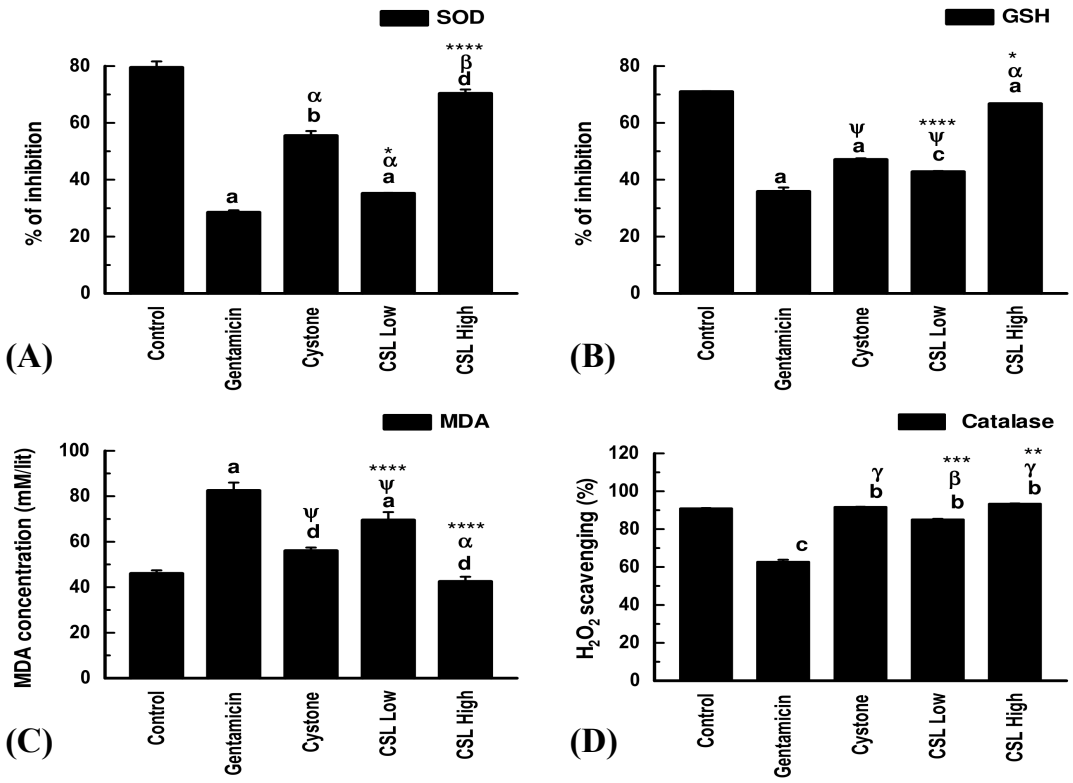

Fig. 4.20. The effect of CSL extract on **(A)** Superoxide Dismutase (SOD) activity. **(B)** Reduced Glutathione (GSH) activity. **(C)** Lipid Peroxidation (LPO) activity. **(D)** Catalase activity. Data expressed as mean ± S.D (n=6). $^{a}p<0.05$; $^{b}p<0.01$; $^{c}p<0.001$; ^{d}p= non significant vs control group; $^{\alpha}p<0.05$; $^{\beta}p<0.01$; $^{\gamma}p<0.001$; $^{\Psi}p$=non significant vs gentamicin group; *p<0.05; **p<0.01; *** p<0.001; ****p=non significant vs cystone group.

percent of inhibition compared with the gentamicin treated rat. The SOD activity in the control group was 79.50 ± 2.12% which was lowered to 28.50 ± 0.70% by gentamicin administration. The lowered SOD activity was significantly elevated by CSLH administration (70.33 ± 1.41%) when compared with the standard cystone treated group (55.50 ± 1.64%). Lipid peroxidation or MDA level in the treated groups are illustrated in Fig. 4.20.C. The MDA content was elevated from 46.00 ± 1.41 mM/litre in control to 82.5 ± 3.53 mM/litre in gentamicin group. Significant results were found when the elevated MDA level was lowered to 42.50 ± 2.12 mM/litre after CSLH administration. Gentamicin (GM) is an aminoglycoside antibiotic derived from *Micromonospora purpurea* (a gram positive bacterium found in soil or water) and is highly potent and efficient in the treatment of life threatening bacterial infections. The use of this drug is however limited by its nephrotoxic effect on the kidney (Bhatia *et al.*, 2012) which essentially excretes the drug. About 5 % of gentamicin is actively reabsorbed and

preferentially accumulated in the proximal tubular cells where it elicits its toxic effect (Mingeot-Leclercq and Tulkens, 1999; Yanagida *et al.*, 2004). Experimental evidence suggested that multiple mechanisms are involved in gentamicin nephrotoxicity such as generation of ROS and RNS and accumulation, consumption of antioxidant defence mechanisms, glomerular congestion and acute tubular necrosis leading to diminished creatinine clearance and renal dysfunction (Mingeot-Leclercq and Tulkens, 1999; Hur *et al.*, 2013). Catalase and superoxide dismutase are the major antioxidative enzymes responsible for the neutralization of free radicals. Catalase prevents the formation of highly reactive $OH^{\cdot}$ by scavenging H_2O_2, the key molecule of fenton reaction. SOD (super oxide dismutase) alternatively catalyzes the dismutation of superoxide radicals into ordinary molecular oxygen or hydrogen peroxide. Glutathione is a major antioxidant enzyme that can also serve as a redox or cell signaling regulator and guard the cells against oxidative injury by reducing H_2O_2 and scavenging reactive oxygen and nitrogen radicals. In this study, it is established that the diminished catalase, reduced glutathione and superoxide dismutase levels and elevated MDA levels were subsequently normalized by CSL administration.

4.8.5. Histopathological examination

Histopathological results demonstrate structural changes in renal tissue of different treatment groups. Histopathological examination of kidney of control rat showed the normal renal tubules and glomeruli (Fig. 4.21.A). Rat with gentamicin exposure showed severe intertubular damage, degeneration, desquamation and necrosis in tubules (Fig. 4.21.B). Rat kidneys exposed to cystone showed mild tubular epithelial changes, hyaline casts in tubules and low intertubular haemorrhage (Fig. 4.21.C). Interestingly, in the present study it was observed that high dose of CSL extract (400mg/kg BW) bring down and regulates the renal injury in a better or similar manner compared to the standard cystone (Fig. 4.21.E).

4.9. Chemical Characterizations of selected plant extracts

Since the extracts exhibited potent antioxidant, hepatoprotective, anti-neurodegenerative and nephrotoxic activity, it would be an amicable one to

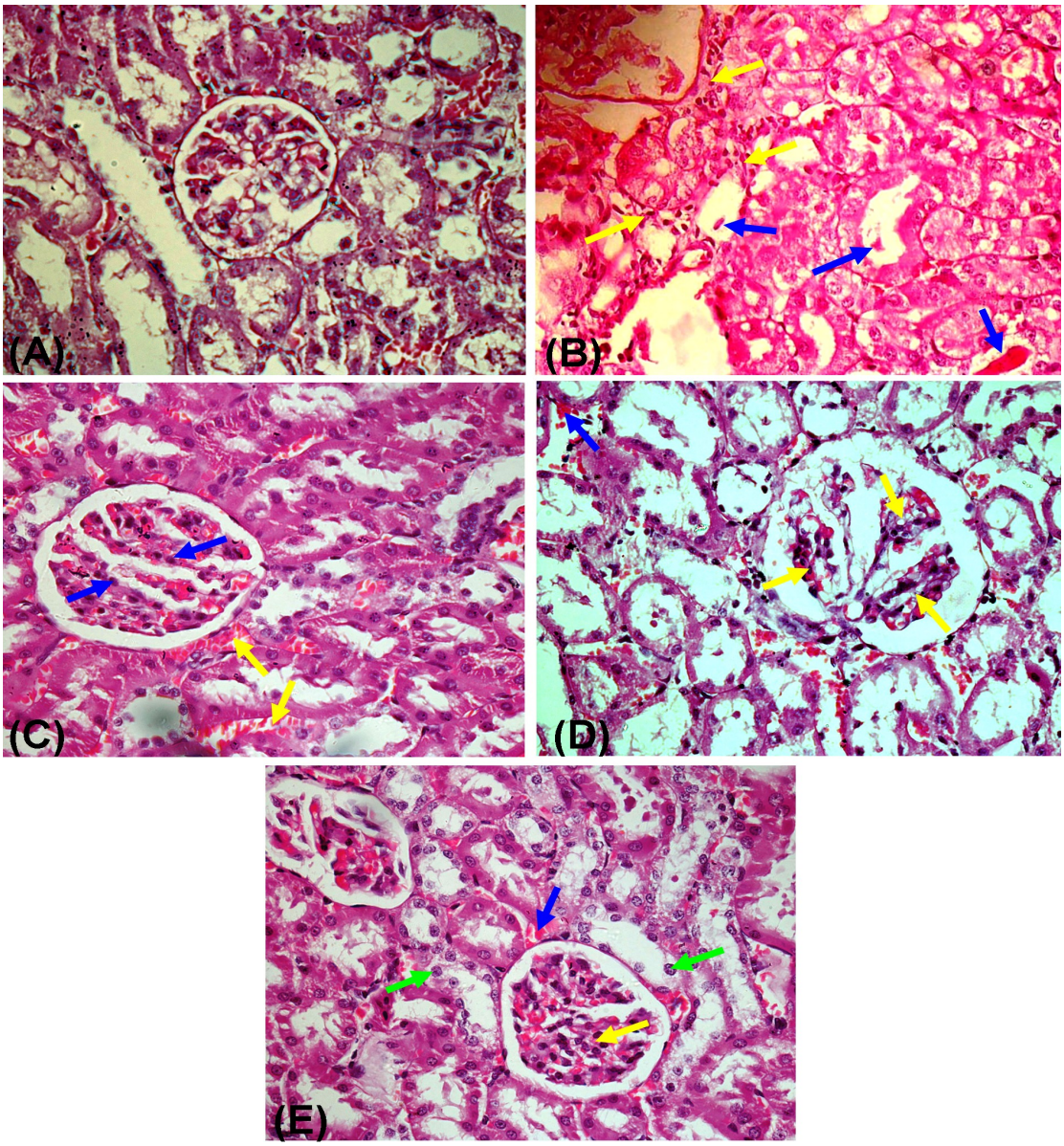

Fig. 4.21. Photomicrograph of control and treated rats kidney (A-E).

identify the active phytocompounds responsible for those activities present in the extracts. In this regard, FTIR and GC-MS analysis have been considered.

4.9.1. FT-IR analysis

Fourier transform infrared spectroscopy (FTIR) was used to analyze the functional groups (Table 4.9.) present in three *Clerodendrum* extracts and the functional groups were separated on the basis of peak ratio. The IR spectrum of CIL, VIL and CCL extracts indicated the presence of major peaks like amines, ether, alcohol and carboxylic acid at 1081 cm^{-1}, 1245 cm^{-1}, 3294 cm^{-1}, 1734 cm^{-1} respectively (Fig. 4.22).

4.9.2. GC-MS analysis

The present study was extended for the analysis pertaining to the identification

Table 4.9. FTIR absorption values and functional groups of CIL, VIL and CCL extracts.

Wave no (cm^{-1}) of CIL	Types of bond	Functional groups
721.40	Unknown	Unknown
835.74	Unknown	Unknown
1081.00	C-N	Amines
1245.71	C-O	Alcohol or Ether
1376.52	-C-H-	Alkanes
1457.90	C=C	Benzene ring
1642.01	C=N	Imine
1734.71	C=O	Carboxylic Acid
2923.48	C-H	Alkane
3294.48	O-H	Alcohol
Wave no (cm^{-1}) of VIL	**Types of bond**	**Functional groups**
721.66	Unknown	Unknown
1080.99	C-N	Amines
1248.81	C-O	Alcohol or ether
1376.83	-C-H-	Alkanes
1458.47	C=C	Benzene ring
1734.71	C=O	Carboxylic Acid
2853.79	C-H	Alkane
2923.59	C-H	Alkane
Wave no (cm^{-1}) of CCL	**Types of bond**	**Functional groups**
721.09	Unknown	Unknown
1161.35	C-O	Alcohol or ether
1376.59	-C-H-	Alkanes
1458.42	C=C	Benzene ring
1734.68	C=O	Carboxylic Acid
2853.63	C-H	Alkane
2923.76	C-H	Alkane
3392.07	O-H	Alcohol

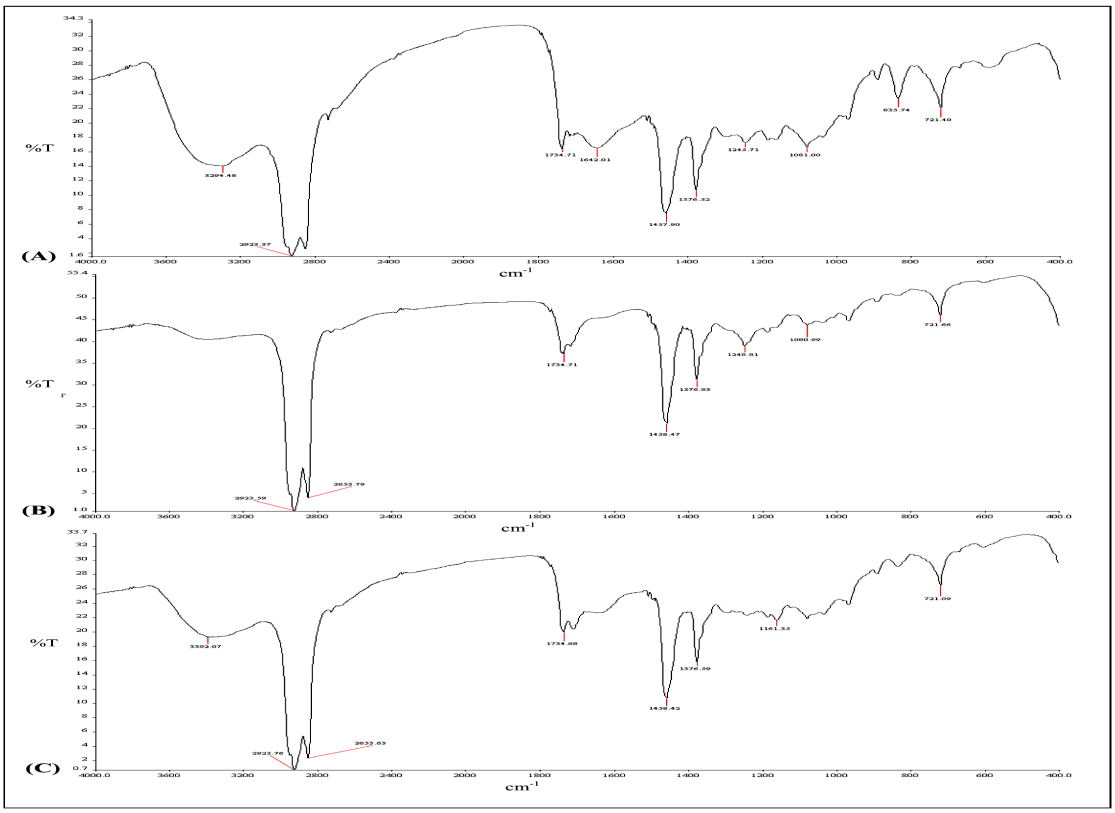

Fig. 4.22. FTIR analysis of three *Clerodendrum* sp., **(A)** *Clerodendrum indicum*; **(B)** *Volkameria inermis*; **(C)** *Clerodendrum colebrookianum.*

Table 4.10. List of phytocompounds identified in *C. indicum* and *V. inermis* leaf extract by GC-MS analysis.

Identified Compounds	Formula	Mol. Wt. †	RT
Clerodendrum indicum			
24,25-Dihydroxyvitamin D	$C_{27}H_{44}O_3$	415	18.23
2-Cyclohexen-1-one, 2-methyl-	$C_7H_{10}O$	109	18.48
Dodecanoic acid, 3-hydroxy-(β-Hydroxylauric acid)	$C_{12}H_{24}O_3$	215	18.89
Benzeneethanol, 4-hydroxy- (Tyrosol)	$C_8H_{10}O_2$	137	19.19
9-Hexadecenoic acid	$C_{16}H_{30}O_2$	253	21.89
9-Oxabicyclo[3.3.1]nonane-2,6-diol	$C_8H_{14}O_3$	157	21.98
Hexadecanoic acid, methyl ester	$C_{17}H_{34}O_2$	269	30.39
9,12-Octadecadienoyl chloride, (Z,Z)- (Linoleoyl chloride)	$C_{18}H_{31}ClO$	297	33.60
6,9,12,15-Docosatetraenoic acid, methyl ester	$C_{23}H_{38}O_2$	345	33.71
Phytol	$C_{20}H_{40}O$	295	33.93
Volkameria inermis			
Octadecane, 6-methyl-	$C_{19}H_{40}$	267	10.37
Phenol, 3,5-bis(1,1-dimethylethyl)-	$C_{14}H_{22}O$	205	21.31
1-Hexadecanol, 2-methyl-	$C_{17}H_{36}O$	255	21.60
1-Dodecanol, 3,7,11-trimethyl-	$C_{15}H_{32}O$	227	21.81
Decane, 2,3,5,8-tetramethyl-	$C_{14}H_{30}$	197	21.99
Dodecanoic acid, 1-methylethyl ester	$C_{15}H_{30}O_2$	241	24.00
3,7,11,15-Tetramethyl-2-hexadecen-1-ol	$C_{20}H_{40}O$	295	28.58
Hexadecanoic acid (Palmitic Acid)	$C_{16}H_{32}O_2$	255	32.68
9,12,15-Octadecatrienoic acid, methyl ester, (Z,Z,Z)- (Linolenic acid, methyl ester)	$C_{19}H_{32}O_2$	291	33.65
Phytol	$C_{20}H_{40}O$	295	34.10
Squalene	$C_{30}H_{50}$	409	45.15
Heptacosane	$C_{27}H_{56}$	379	48.68
Ethyl iso-allocholate	$C_{26}H_{44}O_5$	435	50.40
Retinoic acid, methyl ester	$C_{21}H_{30}O_2$	313	50.84

† =$[M-H]^-$; **RT**= Retention Time

Table 4.11. List of phytocompounds identified in *C. colebrookianum* and *C. serratum* leaf extract by GC-MS analysis.

Identified Compounds	Formula	Mol. Wt. †	RT
Clerodendrum colebrookianum			
Pentanoic acid	$C_5H_{10}O_2$	101	14.39
Dodecanoic acid	$C_{12}H_{24}O_2$	199	24.64
3,7,11,15-Tetramethyl-2-hexadecen-1-ol	$C_{20}H_{40}O$	295	28.59
Tetradecanoic acid (Myristic acid)	$C_{14}H_{28}O_2$	227	28.84
Hexadecanoic acid	$C_{16}H_{32}O_2$	255	31.71
Linolenic acid, methyl ester	$C_{19}H_{32}O_2$	291	33.66

Contd… to next page.

Contd… from previous page.

Octadecanoic acid (Stearic acid)	$C_{18}H_{36}O_2$	283	36.21
Squalene	$C_{30}H_{50}$	409	45.16
Heptacosane	$C_{27}H_{56}$	379	46.07
Stigmasterol	$C_{29}H_{48}O$	411	52.81
Clerodendrum serratum			
Dodecanoic acid	$C_{12}H_{24}O_2$	200	24.63
3,7,11,15-Tetramethyl-2-hexadecen-1-ol	$C_{20}H_{40}O$	296	28.58
Tetradecanoic acid (Myristic acid)	$C_{14}H_{28}O_2$	228	28.84
Hexadecanoic acid	$C_{16}H_{32}O_2$	256	32.72
Linolenic acid, methyl ester	$C_{19}H_{32}O_2$	292	33.65
Phytol	$C_{20}H_{40}O$	296	34.11
Linoleic acid	$C_{18}H_{32}O_2$	280	35.66
Oleic acid	$C_{18}H_{34}O_2$	282	35.77
Octadecanoic acid (Stearic acid)	$C_{18}H_{36}O_2$	284	36.21
Squalene	$C_{30}H_{50}$	410	45.16
Heptacosane	$C_{27}H_{56}$	389	51.87
Stigmasterol	$C_{29}H_{48}O$	412	53.16

† =$[M-H]^-$; **RT**= Retention Time

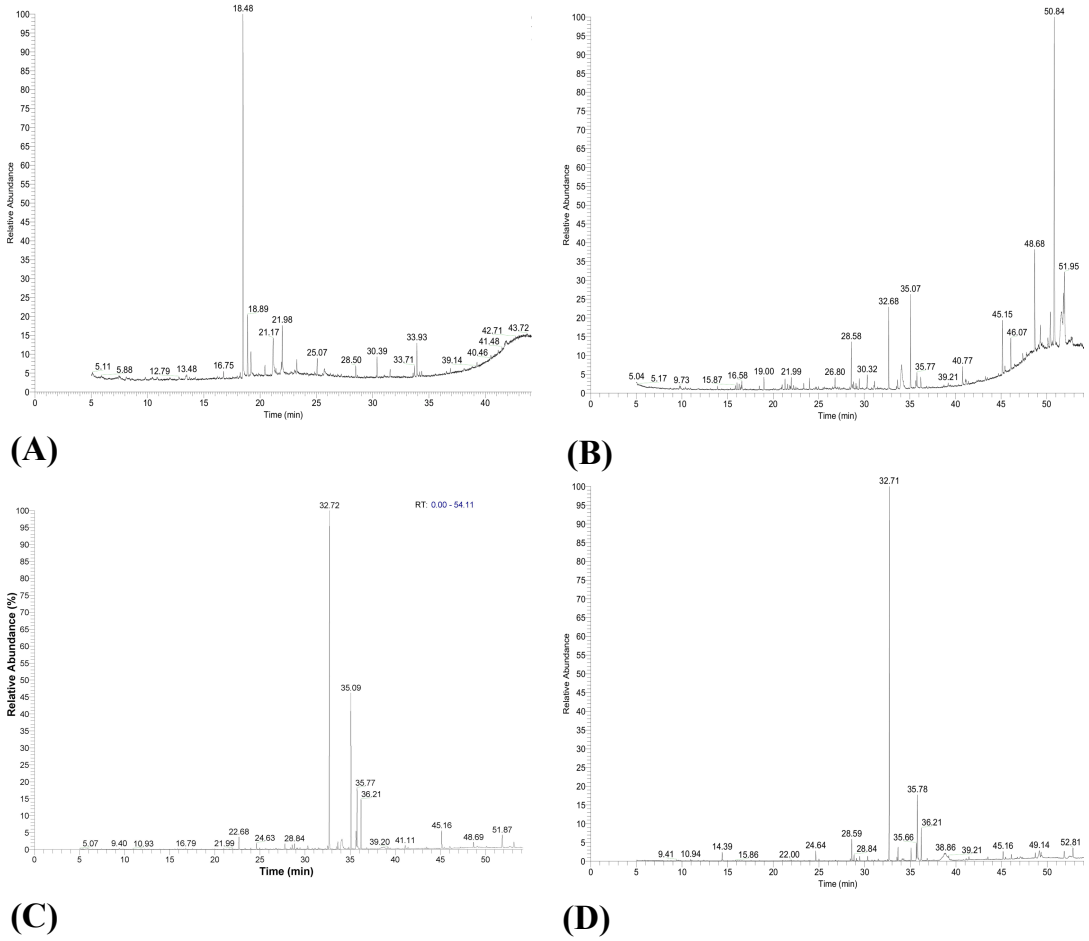

(A) **(B)**

(C) **(D)**

Fig. 4.23. GC-MS fingerprinting of four *Clerodendrum* sp., **(A)** *Clerodendrum indicum,* **(B)** *Volkameria inermis*, **(C)** *Clerodendrum serratum* and **(D)** *Clerodendrum colebrookianum.*

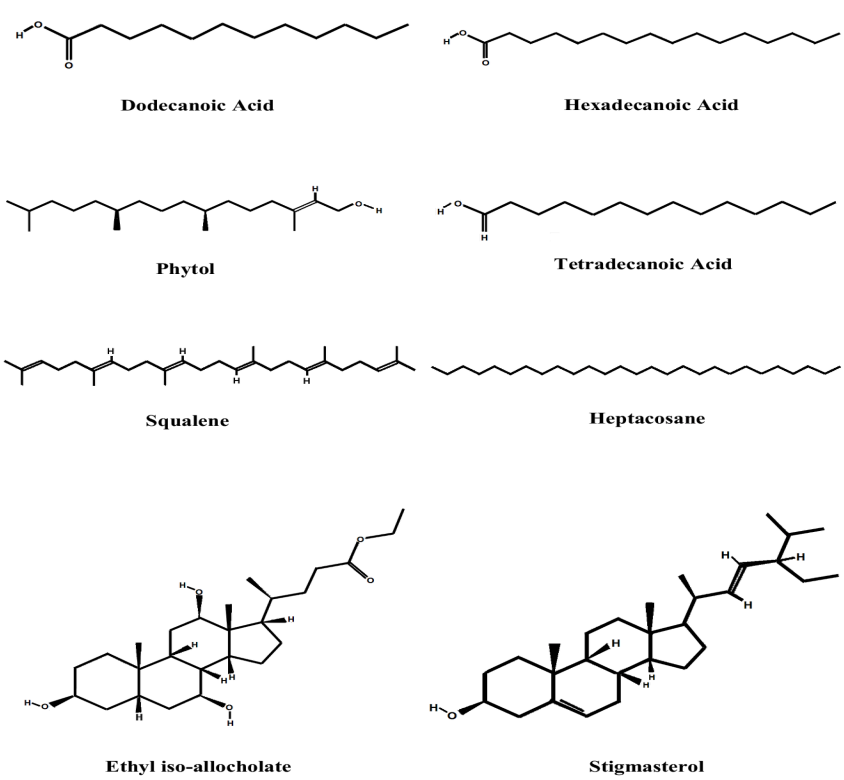

Fig. 4.24. List of some chemical compounds identified in the four *Clerodendrum* extracts by GC-MS analyses.

of active compounds in CIL, VIL, CSL and CCL using GC-MS method. A total number of forty five (45) phytocompounds have been identified in CIL (10 compounds), VIL (14 compounds), CSL (12) and CCL (10 compounds) (Fig. 4.23; Table 4.10. & Table 4.11.). A list of some important chemical compounds identified in four *Clerodendrum* extracts by GC-MS analyses has been depicted in Fig. 4.24. Different functional groups were identified through FTIR analysis which correlated well with the GC-MS data. Fatty acids like linoleic acid (LA), dodecanoic acid and hexadecanoic acid are some of the essential fatty acids that human being requires in diet (Kar *et al.*, 2016). Deficiency of linolenic acid has been reported to be associated with retardation, infertility, skin and kidney degeneration and abrupt changes in the fatty acid composition of lipids (Dobryniewski *et al.*, 2007). In addition, squalene and stigmasterol have been reported to be potent antioxidants and observed to be effective against several oxidative stress related diseases (Amarowicz, 2009; Yoshida and Niki, 2003). Hence from the above illustration, it might be inferred that CIL, VIL, CSL and CCL

extract could be regarded as a potent future antioxidative agents.

4.10. *In-silico* molecular docking

4.10.1. Molecular Docking and ROS

The molecular docking results came out with new insights. While phytochemicals were analyzed with each of the proteins, at least one compounds from each plant showed exhilarating results (Table 4.12.). 24, 25-Dihydroxyvitamin D of *C. indicum* (CIL), Ethyl iso allocholate of *V. inermis* (VIL) and Stigmasterol of *C. colebrookianum, C. serratum* (CCL and CSL) showed higher binding affinity compared to other compounds. Among them on an average stigmasterol was found to have a slight upper hand compared to the remaining compounds. However, when individual interactions were compared, 24, 25-Dihydroxyvitamin D displayed the highest binding affinity with Nrf2 protein which is a transcription factor in humans encoded by NFE2L2 gene (Nuclear factor erythroid-derived 2) (Fig. 4.25). This protein has the best interaction pattern with all the ligands. However, ap1 protein (activator protein 1) also had decent binding energies with most of the ligands (Fig. 4.26).

To understand better activities at a molecular level an *in-silico* approach was adopted. A few essential proteins deeply involved in internal antioxidant machinery as well as having implications in cell growth and proliferation cascades were thoroughly examined in a docking environment, where they were checked against the phytochemicals (ligands) present in our studied plants. The selected protein generally plays a vital role in cell division, development, apoptosis, tumor suppression and natural antioxidant properties (Kovac *et al.*, 2015). On digging further it is seen that Stigmasterol a phytochemical present in CCL and CSL had the highest

Table 4.12. Binding affinity of receptors (protein) with ligands (phytochemicals).

Ligands	Binding Affinities (kcal/mol)		
	Nrf2 (2flu)	Ap1 (1fos)	p53 (1aie)
24,25-Dihydroxyvitamin D	-9.9	-7.7	-6.7
Ethyl iso-allocholate	-9.4	-8.2	-7.3
Heptacosane	-5.4	-3.9	-4.3
Squalene	-7.5	-6.5	-5.8
Phytol	-4.9	-4.5	-3.6
Stigmasterol	-9.1	-7.9	-6.9

activity among all the compounds of all the four plants. So, stigmasterol might be one of the keys to searching the ideal antioxidant compounds while combating the free radical induced oxidative stress. The proteins like Nrf2 and ap1 which has high interactions with our phytochemicals are complexly linked to different cell signaling cascades. Among them, the Nrf2 is usually considered as a transcription factor which mediates the protection against electrophiles and oxidants and negatively regulated by cytoplasmic

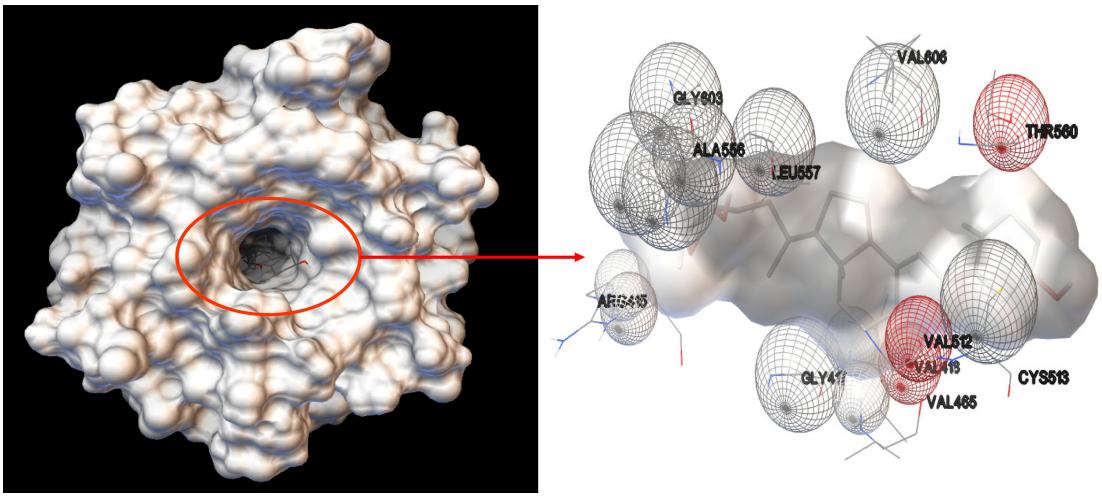

Fig. 4.25. Molecular docking image. Molecular docking (molecular surface view) between Nrf2 protein and 24, 25-Dihydroxyvitamin D: This molecular docking figure show compounds at their binding site on the left and on the right the amino acids that interact with the ligand to give resultant binding energy is shown.

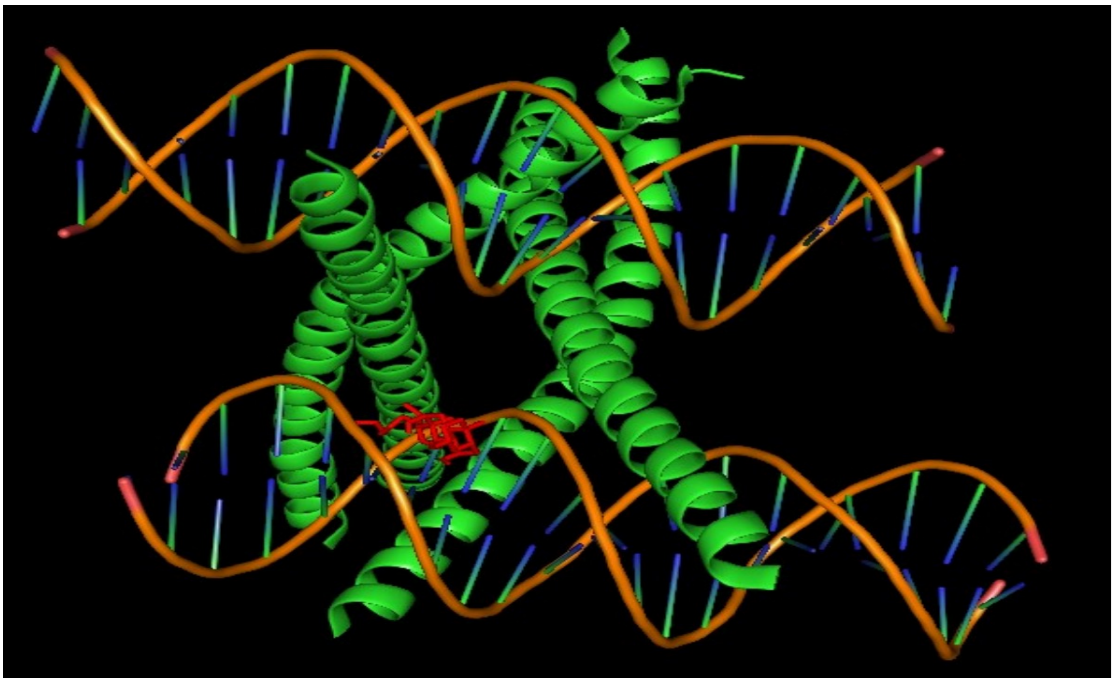

Fig. 4.26. Molecular docking (secondary structure view) between Ap1 protein and Ethyl isoallocholate.

Kelch-like ECH-associated protein 1 (Keap1) (Kovac *et al.*, 2015). Nrf2 in its highest binding state with 24, 25-Dihydroxyvitamin D shows efficient interactions at 11 amino acids positions (Fig. 4.25) (arginine at 415, glycine at 417, valine at 418 etc.). Moreover, the molecular surface view of the interaction shows the ligand deeply embedded inside a binding pocket (Fig. 4.25). Such an interaction of -9.9 kcal/ mol binding affinity and excellent conjugation are ideal in nature. Compounds like Stigmasterol and 24, 25-Dihydroxyvitamin D can therefore be ideal drugs against these targets. The Ap1 and p53 protein showed good interactions also has DNA binding ability which can get triggered when there is an increase in production of ROS molecules. They themselves are regulated by different cascades, for example, an ap1 family of transcription factor consists of Jun, Fos and ATF-2 homo and heterodimers (Zwacka *et al.*, 1998) which regulate their expression. However, the problem occurs as all these redox sensitive pathways can cause cell injury and cell and organ remodeling through the production of cytokines and growth factors. Therefore, therapeutic strategies are considered rational for reducing oxidative stress. Our phytochemicals have excellent antioxidant properties as well as they can bind to essential transcription factors which are otherwise helpful but can be hazardous to the cell in case of additional oxidative stress (Buldak *et al.*, 2014). Thus, these herbal alternatives can provide essential antioxidants as well as have no evident toxic effect even at the face of oxidative stress. Moreover, we can keep most of the growth enhancing and cell proliferating transcription factors away as shown by the *in-silico* binding affinity thus these phytocompounds can be proposed for proper cytostatic therapy.

4.10.2. Molecular Docking and hepatotoxic activity

The bioactive compounds of CIL, VIL and CCL were checked for possible interactions with several proteins playing the essential role in different metabolic pathways of humans and other major vertebrates. The proteins were chosen those have relationship with the health of the liver. These proteins acted as receptors required for molecular docking experiments. The ligands required to conduct the experiment are the compounds identified by GC-MS analysis of the plant extract. Upon a series of receptor-

Table 4.13. Binding affinity of receptors (protein) with ligands (phytochemicals).

Ligands	Binding Affinities (kcal/mol)	
	Hepatitis BX (3i7h)	NF-κβ (1nfi)
24,25-Dihydroxyvitamin D	-5.7	-5.4
Ethyl iso-allocholate	-8.4	-7.4
Heptacosane	-4.9	-3.8
Squalene	-6.3	-4.9
Phytol	-5.2	-3.8
Stigmasterol	-8.7	-6.9

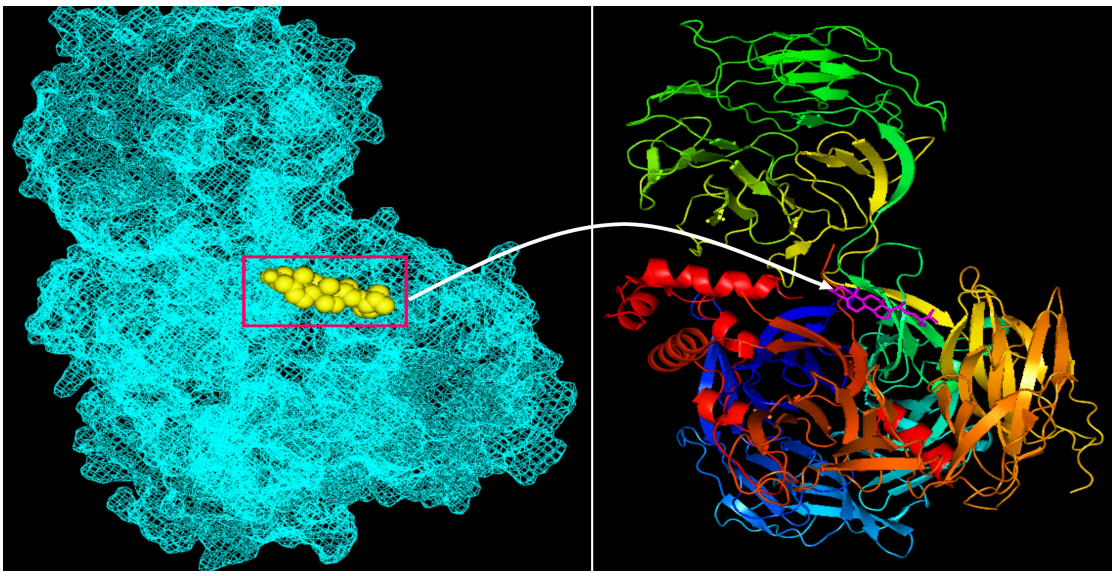

Fig. 4.27. Molecular docking interactions of Stigmasterol with Hepatitis BX (3i7h).

ligand interaction study, it was identified that each of the ligands has different binding affinity with the selected proteins. The highest binding affinity was found between Stigmasterol and a protein with PDB ID 3i7h which is the crystal structure of DDB1 in complex with H-Box Motif of HBX (Fig. 4.27 and Table 4.13.). NFκβ protein and Ethyl iso-allocholate also has good binding affinity and as seen in the secondary structure views (Fig. 4.28).

Hepatitis BX may act as the precursor for Hepatocellular carcinoma (HCC). Hepatitis BX promotes the expression of insulin-like growth factor (IGF) in HCC. Thus blocking this protein with this phytochemical can reduce the chances of development of HCC in case of liver diseases. Proteins like NF-κB also showed good interactions with these phytochemicals. NF-κB controls cytokine production and cell survival, but in certain cases its regulation is related to cancer, inflammation and

autoimmune diseases. Phytochemicals from the CIL, VIL and CCL extract act as suitable ligand for all these receptors. So, whether it is because of the individual bioactive phytochemical or the result of synergestic effects of all the biochemicals, the plants can be considered to have medicinal benefits against hepatotoxicity.

4.10.3. Molecular Docking and neurodegeneration

Despite of having immense antioxidant and anti-neurodegenerative properties

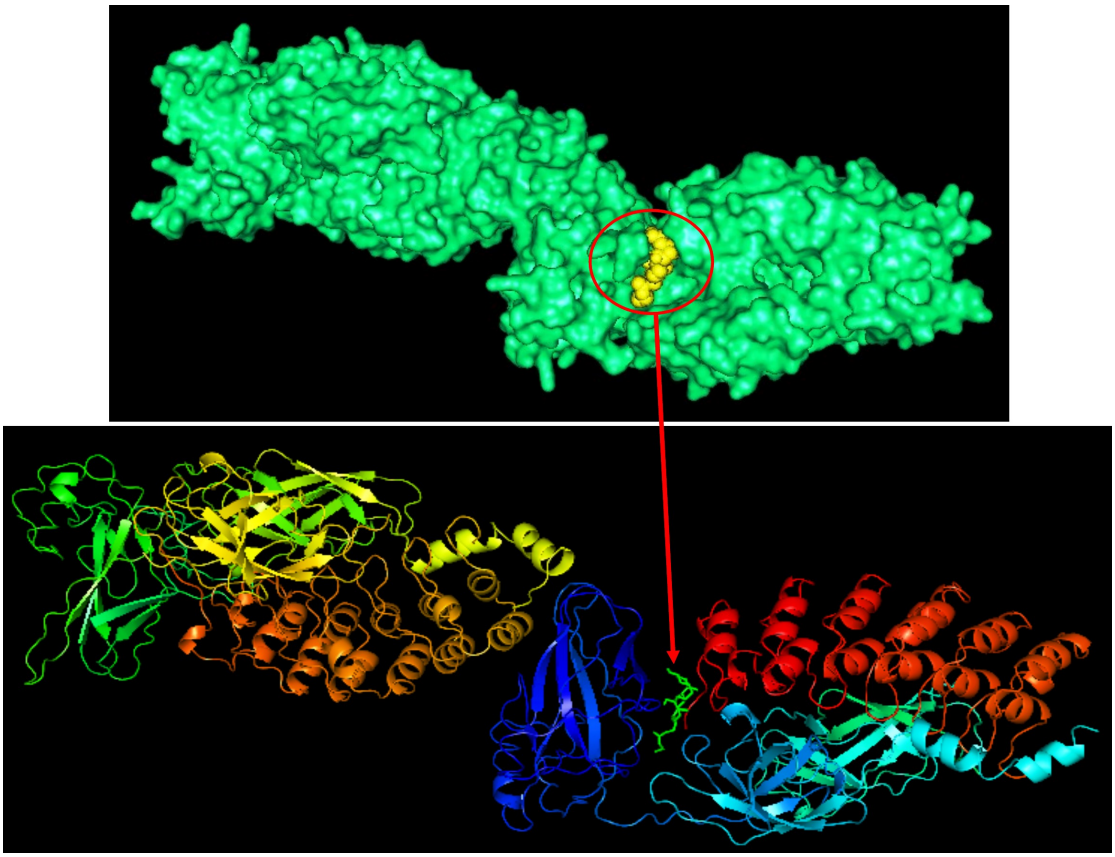

Fig. 4.28. Molecular surface view of NF-κβ (1nfi) protein with Ethyl iso-allocholate.

Table 4.14. Binding affinity of receptors (protein) with ligands (phytochemicals).

Ligands	Binding Affinities (kcal/mol)
	Dopamine receptor D3 (3pbl)
Dodecanoic acid	-4.2
3,7,11,15-Tetramethyl-2-hexadecen-1-ol	-4.1
Tetradecanoic acid	-4.5
Hexadecanoic acid	-3.6
Phytol	-4.4
Linoleic acid	-2.9
Oleic acid	-3.3
Octadecanoic acid	-3.5
Squalene	-5.7
Heptacosane	-5.2
Stigmasterol	-6.1

found in selected plant extract (CSL) due to presence of several active metabolites including Squalene, Heptacosane and stigmasterol etc., these were considered as the potential drug target ligands against neurodegenerative disorders (NDs). As a part of drug target establishment, molecular docking was first performed to explore the binding pattern of the above mentioned target compounds with human brain membrane protein (dopamine receptor D3 protein; ID-3pbl). The D3 protein, localized to the limbic areas of the brain, was selected due to its prominent role in cognition, emotional and endocrine functions and hence, it might be the chief target of antipsychotic therapy involving dopamine antagonists (Nakajima *et al.*, 2013). Results obtained from docking revealed different binding sites with different affinities (Table 4.14.). The *in -silico* insight in this case shows that the compound Stigmasterol shows the best results with a binding affinity of -6.1 kcal/mol in autodock vina (Fig. 4.29), although, other promising compound like Squalene and Heptacosane are not too far behind. Strong binding pattern of these ligand compounds with dopamine receptor D3 protein signified their possible role in the treatment of neurodegeneration.

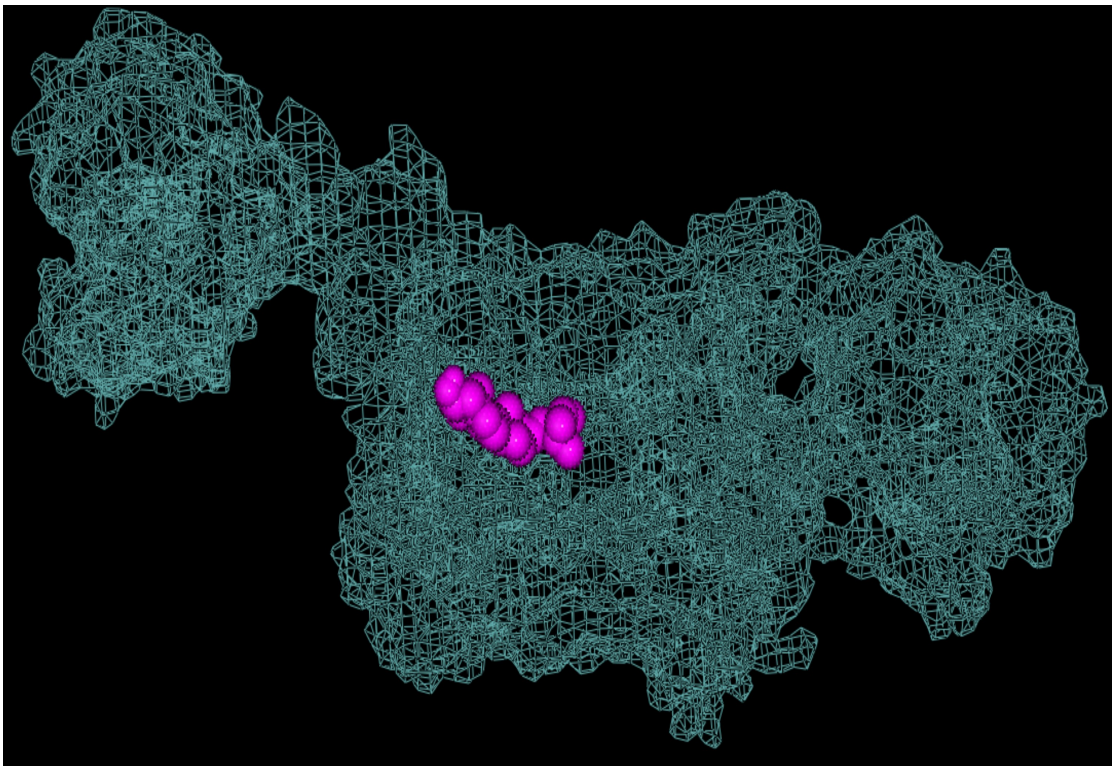

Fig. 4.29. Molecular docking representation of dopamine receptor D3 (3pbl) protein with Stigmasterol.

Table 4.15. Binding affinity of receptors (protein) with ligands (phytochemicals).

Ligands	Binding Affinities (kcal/mol)
	Polycystic Kidney Disease protein 2 (5t4d)
Dodecanoic acid	-4.7
3,7,11,15-Tetramethyl-2-hexadecen-1-ol	-6.1
Tetradecanoic acid	-4.7
Hexadecanoic acid	-5.8
Phytol	-5.2
Linoleic acid	-4.8
Oleic acid	-4.8
Octadecanoic acid	-4.9
Squalene	-7.5
Heptacosane	-6.0
Stigmasterol	-8.6

4.10.4. Molecular Docking and nephrotoxicity

The molecular docking result shows an overall good binding affinity (Table 4.15.). The plant extract (CSL) selected here provided loads of promising bioactive phytochemicals. Therefore, we wanted to reinvestigate their potential from the point of view of renal health. We already have exciting

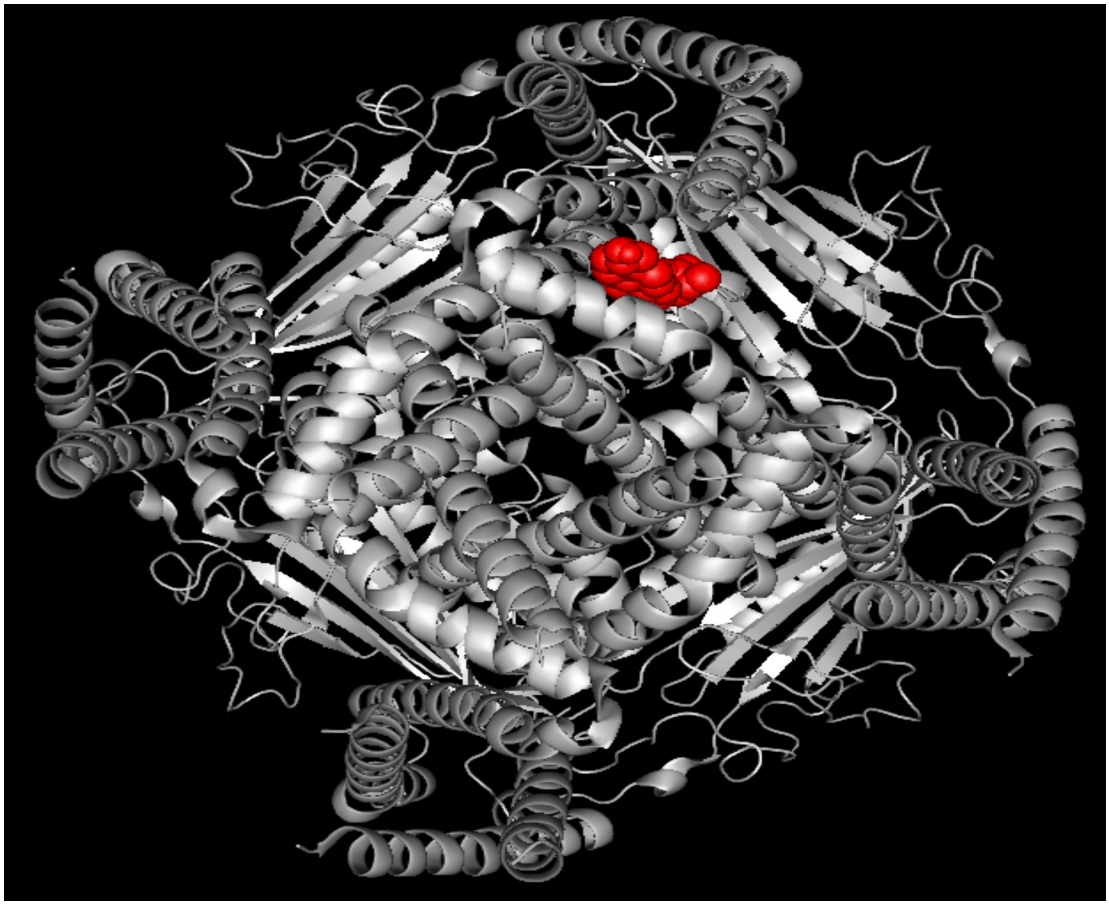

Fig. 4.30. *In-silico* docking representation of stigmasterol with Polycystic Kidney Disease protein 2 (5T4D).

result in these aspect considering results from the histopathological experiment and *in-vivo* enzymatic assays. The *in-silico* insight in this case shows that the compound stigmasterol shows the best results with a binding affinity of -8.6 kcal/mol in autodock vina (Fig. 4.30), although, other promising compound like squalene and 3,7,11,15-Tetramethyl-2-hexadecen-1-ol acid are not too far behind. The protein in consideration is Polycystic kidney disease protein 1-like 2 (PKD2) that is responsible for autosomal dominant polycystic kidney disease. This is one of the most important proteins responsible for multiple cyst formation in kidney. The treatment of CSL extract already shows promising result in the *in-vivo* experiments so in the light of *in-silico* experiments we can confirm that specific compounds like stigmasterol and squalene might be the reason behind such effect. The query still remains whether stigmasterol alone is capable of such effect or is it the combinatorial action as seen in most of the herbal formulations.

4.11. Study of solvent fraction

4.11.1. Characterization of the compounds

The structures of all the compounds were elucidated on the basis of physical and spectroscopic analysis and by comparing with the spectral data of already reported compounds. The analytical data of the compounds along with physical properties is listed in Table 4.16.

4.11.2. FTIR analysis

The FT-IR spectrum of fraction-1 showed three C-H stretching bands at 2913, 2965 and 2852 cm^{-1} and four skeletal vibrational bands at 1376, 1440, 1107 and 832 cm^{-1} (Fig. 4.31A). The band at 1666 cm^{-1} was due to C=C stretching (Hall *et al.*, 2016; Chun *et al.*, 2013). The recorded infrared spectrum of fraction-1 was compared with the literature spectral data and its quiet similar to the spectra squalene (Hall *et al.*, 2016; Chun *et al.*, 2013).

The spectrum of fraction-2 possesses a band at 2989 cm^{-1} attributable to the carbon hydrogen bonds of the unsaturated linkage (methyl ester) (Wu

Table 4.16. Analytical and Physical data of fraction-1 and fraction-2.

Compound	% Found		Physical State	Colour	Amount Yield (mg)
	C	H			
Fraction 1	87.21	11.93	Solid	Dark Brown	251.9
Fraction 2	78.01	11.31	Solid	Dark Brown	211.9

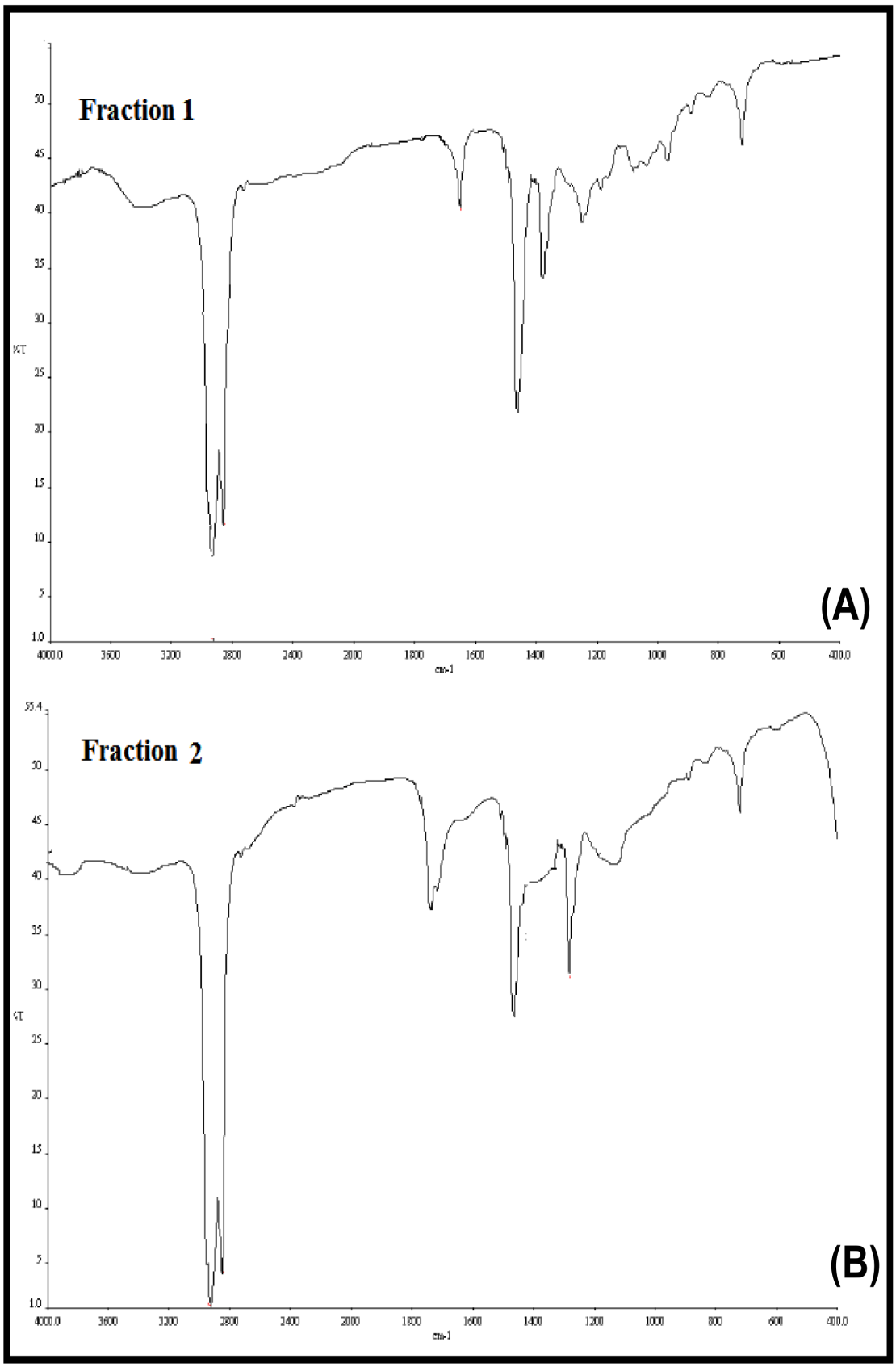

Fig. 4.31. FTIR spectra of **(A)** fraction-1 and **(B)** fraction-2.

et al., 2009). Peaks at 1721cm^{-1} and 1744cm^{-1} were assigned for -C-H stretching vibration of CH_2 group (Fig. 4.31B) (Wu *et al.*, 2009). Low intensity bands at 2134cm^{-1} and 2183cm^{-1} were assigned for =C-H stretching and -C=C stretching of HC=CH. While peak at 2347cm^{-1} was assigned for CH_2 symmetric stretching. The obtained spectrum of fraction-2 is compared with the literature data and it is similar to the spectra of 9, 12, 15-Octadecatrienoic acid, methyl ester (linolenic acid methyl ester) (Wu *et al.*, 2009).

4.11.3. NMR Spectra

The ^{13}C NMR spectra of fraction-1 displayed fifteen signals which were distinguished as four methyls (25.51, 17.60, 16.05 and 16.01 ppm), three quaternary carbons (135.11, 134.90 and 131.26 ppm), five allylic methylenes (39.77, 39.74, 28.29, 26.16 and 26.11 ppm) and three ethylenic methines (125.31, 124.23 and 124.28 ppm) (Fig. 4.32B) (Pogliani *et al.*, 1994). The ^{1}H NMR spectra of fraction -1 exhibited signals for vinylic protons at δ5.12-5.16, methylene protons at δ1.99-2.07 and methyl protons at δ1.60 -1.68 (Fig. 4.32A) (Pogliani *et al.*, 1994).

The ^{1}H NMR spectra of fraction-2 showed signals for the olefinic protons

Table 4.17. ^{1}H, ^{13}C chemical shift of compound fraction-1 and fraction-2.

	C_i/H_i	δ(C_i) (ppm)	δ(H_i) (ppm)		H_i	δ(H_i) (ppm)
	Me1t	25.51	1.68		20	0.81
	Me2	17.60	1.60		19	1.69
	2q	131.26			18	1.68
	3	125.31	5.14		17	1.69
	4	26.16	2.07		9	1.73
	5	39.77	1.99		8	1.75
	6q	135.11			7	1.76
Fraction 1	Me6	16.05	1.61	**Fraction 2**	6	1.81
	7	124.23	5.12		5	1.96
	8	26.11	2.06		18	2.06
	9	39.74	2.01		10	2.18
	10q	134.90			4	2.72
	Me10	16.01	1.62		13	2.83
	11	124.28	5.16		11,12,14	5.11
	12	28.29	2.02		15	5.45

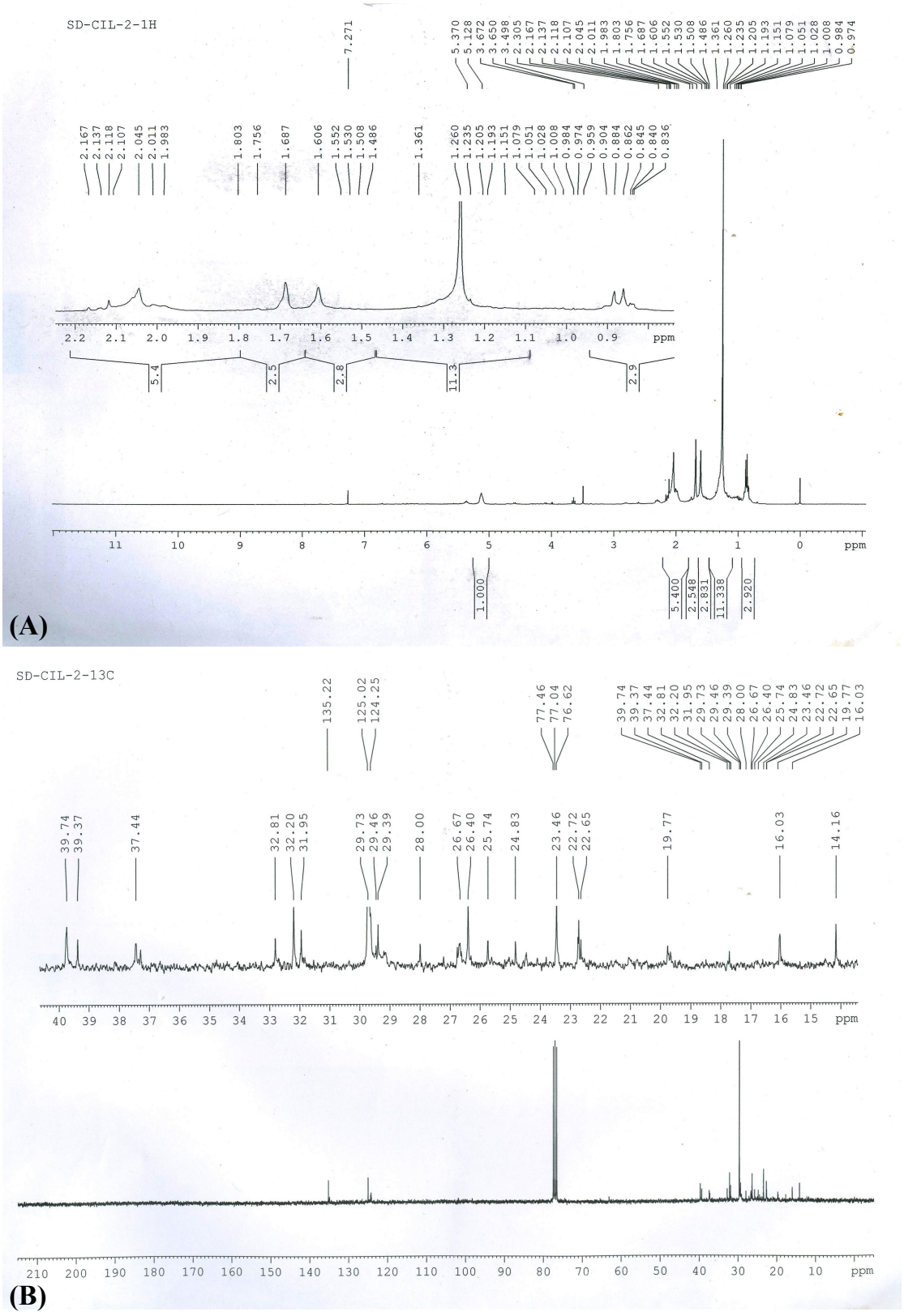

Fig. 4.32. ^{1}H NMR spectra **(A)** and ^{13}C NMR spectra **(B)** of fraction-1 (Squalene).

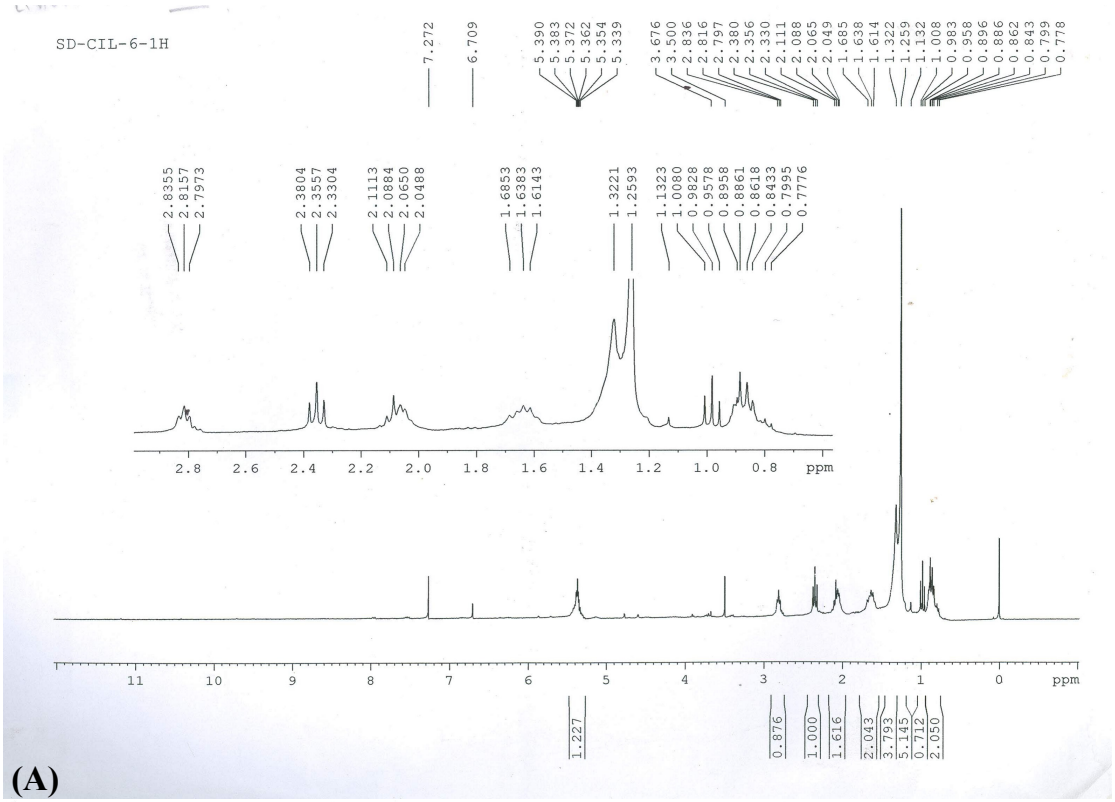

(A)

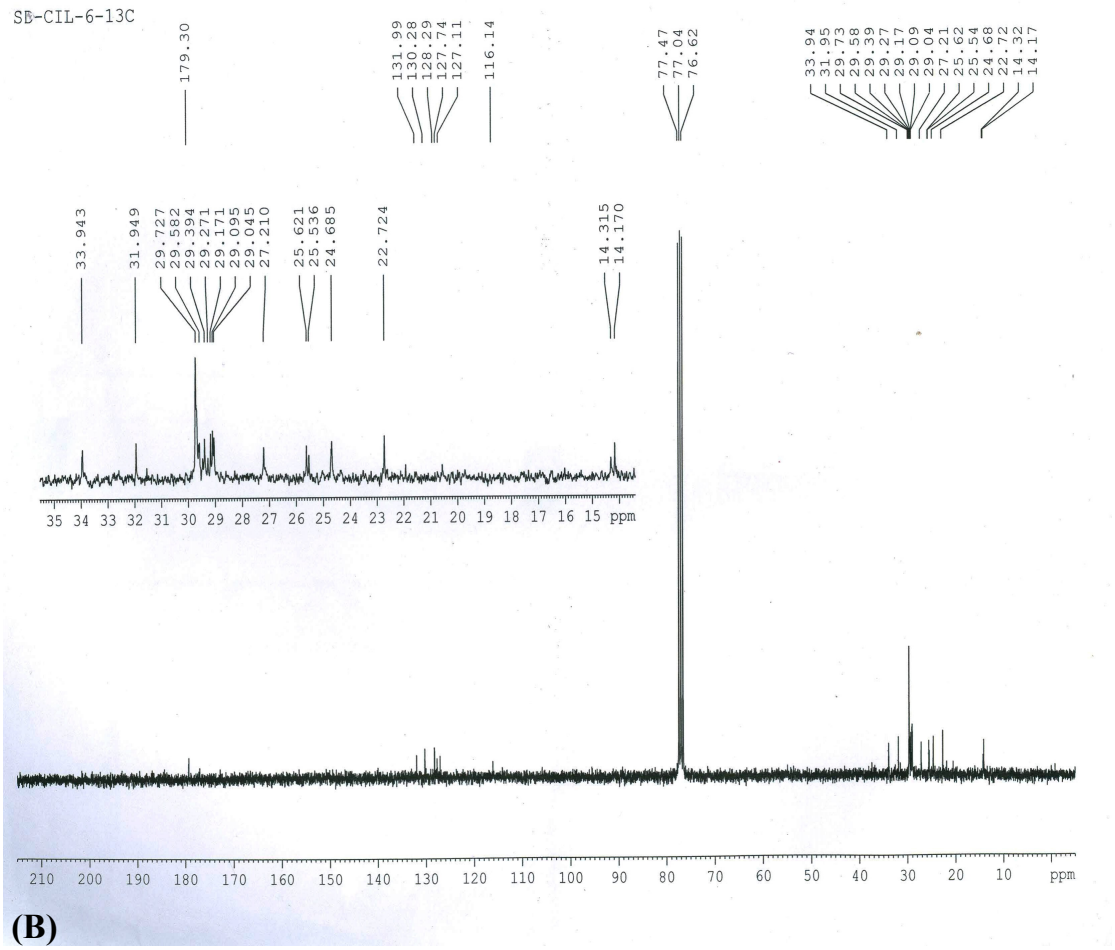

(B)

Fig. 4.33. ^{1}H NMR spectra **(A)** and ^{13}C NMR spectra **(B)** of fraction-2 (linolenic acid methyl ester).

at δ5.30-5.45 ppm, methylene protons at δ1.69-2.30, protons linked to the allylic carbons at δ2.03-2.18 ppm, protons correspond to the bis-allylic carbons at δ2.72-2.83 ppm and for the protons of terminal methyl group at δ0.81-0.93 ppm (Fig. 4.33A and 4.33B) (Davis *et al.*, 1999).

Both ^{1}H and ^{13}C NMR spectra of fraction-1 and fraction-2 (Table 4.17.) are compared with the available literature spectral data and it is found to be similar to the spectra of Squalene for fraction-1 and 9,12,15-Octadecatrienoic acid, methyl ester (linolenic acid methyl ester) for fraction-2 (Pogliani *et al.*, 1994; Davis *et al.*, 1999).

4.11.4. In-vitro antioxidant activity

In the present study, fraction-1 and fraction-2 exhibited potent phenol and flavonoid content (Table 4.18.) and free radical scavenging activity. Among the two fractions, fraction-2 showed higher DPPH scavenging activity (64.42±0.60% at 200µg/ml) than the respective standard ascorbic acid (58.50±0.02% at 200µg/ml) (Fig. 4.34.A). Highly significant nitric oxide scavenging activity was also observed in case of fraction-2 (fraction-1 51.09±1.23%, fraction-2 59.67±0.62% at 200 µg/ml) (Fig. 4.34.B) in comparison to the respective standard curcumin (100±0.0 at 200 µg/ml). Hydrogen peroxide scavenging assays of the two fractions showed that the activity of fraction-2 is higher than the fraction-1 (fraction-1 42.79±0.43%, fraction-2 49.00±0.41% at 200 µg/ml) (Fig. 4.34.C) in comparison to Sodium pyruvate (7.78±0.90% at 200 µg/ml). Ferric reducing power assay of the fractions as observed from Fig. 4.34.D, showed their excellent reducing power activity, among which fraction-2 had maximum reducing power when compared with fraction-1 and the standard BHT under study. Detailed IC_{50} values of the respective *in-vitro* antioxidant tests are enlisted in Table 4.19.

Natural antioxidants are of immense importance as nutrients and health supplements. Clinical trials have revealed that there is an inverse correlation between the intake of fruits and vegetables and the occurrence of

Table 4.18. Polyphenol contents of the two fractions.

	Phenol (mg/g GAE)	**Flavonoid (mg/g QE)**
Fraction-1	215.34	112.21
Fraction-2	330.25	125.67

Table 4.19. IC_{50} values of each fraction with their respective standard used in the present study.

Parameters	Fraction-1	Fraction-2	Standard
DPPH	194.00±2.31***	164.56±1.15***	203.2±1.9 (Ascorbic Acid)
Nitric Oxide	178.18±3.54***	128.58±2.50***	61.17±0.41 (Curcumin)
Hydrogen Peroxide	295.52±11.49**	289.30±5.90**	2185.2±187.4 (Sodium Pyruvate)

Units in µg/ml. Data expressed as mean ± S.D (n=6). **p<0.01; ***p<0.001 when compared with standard.

disorders such as inflammation, cardiovascular disease, cancer, ageing and depression etc. (Durackova, 2010). Enhanced quantity of phenol and flavonoid content in two fractions, especially fraction-2 prompted us towards screening of its detailed therapeutic and medicinal properties including free radical scavenging activities and chemical characterization. Free radical DPPH accept an electron or hydrogen radical to become stable which reacts with a reducing agent to form a new bond, thus, changing the colour of the solution. Being an antioxidative agent,

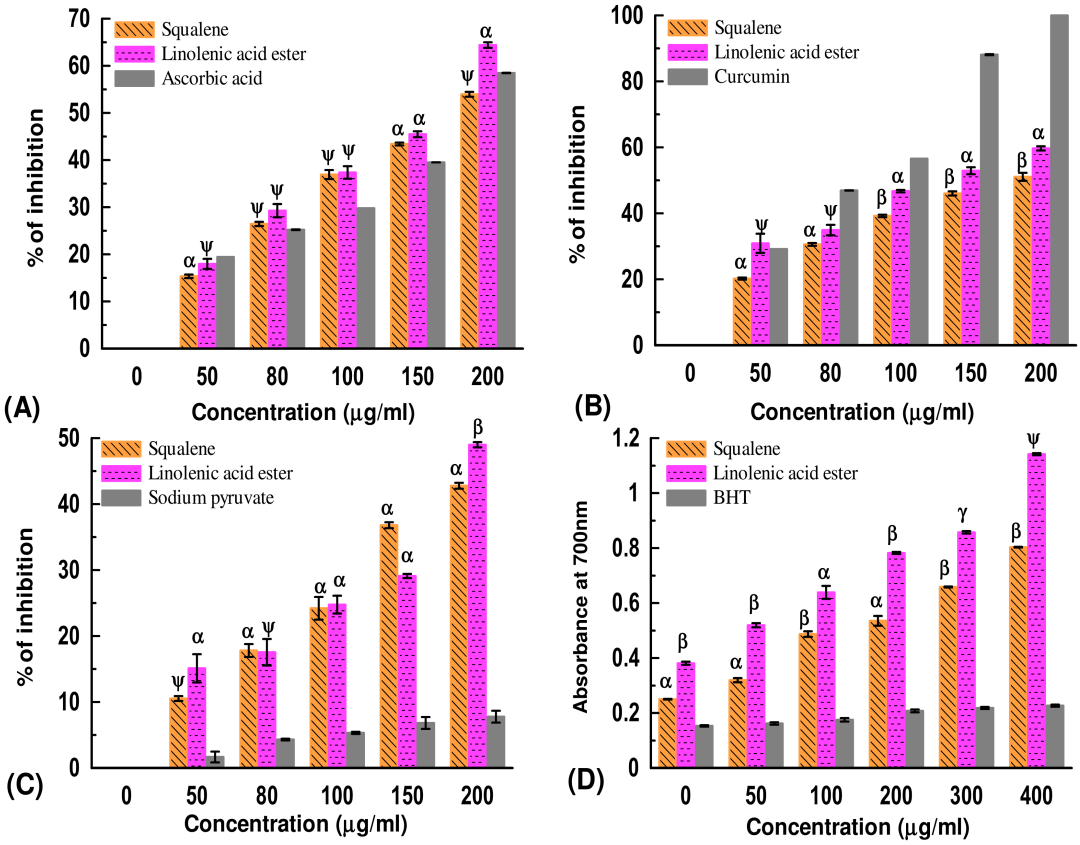

Fig. 4.34. Antioxidant activity of two isolated compound squalene and linolenic methyl acid ester **(A)** DPPH activity; **(B)** Nitric oxide; **(C)** Hydrogen peroxide and **(D)** Reducing power assay. [Data expressed as mean ± S.D (n=3). $^{\alpha}p<0.05$; $^{\beta}p<0.01$; $^{\gamma}p<0.001$; $^{\psi}$-Non significant when compared with standard].

Table 4.20. Antimicrobial activity of isolated compound.

Sample	Concentration (mg/ml)	Diameter of zone of inhibition (mm.)			
		B. subtilis	***S. aureus***	***E. coli***	***P. aeruginosa***
Fraction-1	10	11.5±0.7	12.5±1.41	13±1.41	13.5±0.7
Fraction-2	10	14±1.41	14±1.41	16±2.82	18.5±0.7
DMSO		8.5±0.7	8.5±0.7	8.5±0.7	8.5±0.7

fraction-2 exerts decrease coloration with higher concentration (Huang *et al.*, 2005). Nitric oxide (NO) is a destructive free radical, damaging several biological molecules in human body which in turn produce another detrimental molecule, peroxynitrite ($ONOO^-$) upon reaction with superoxide radical. We found that NO scavenging activity of fraction-2 was pretty higher than the others signifying its positive affection towards superoxide anion hindering the formation of peroxynitrite. Hydrogen peroxide (H_2O_2), another oxidative agent, accumulates in cells and converts into Hydroxyl radical ($OH^{\bullet}$) (Ray and Husain, 2002; Valko *et al.*, 2004). Fraction-1 and fraction-2 was found to be a potent H_2O_2 quencher to

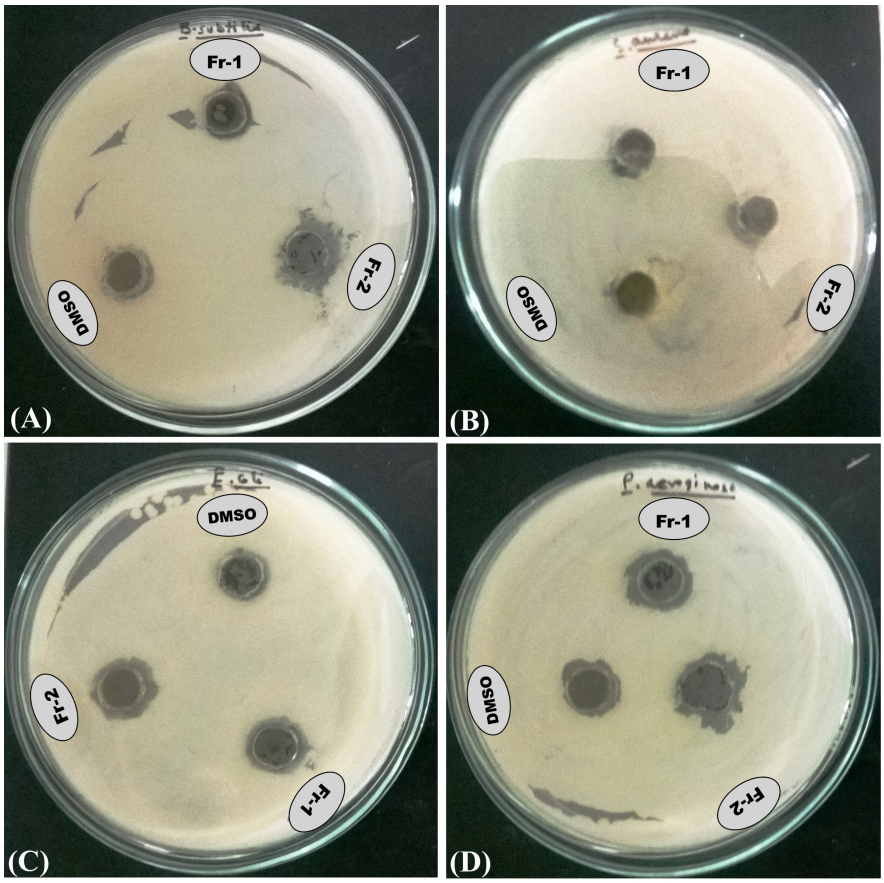

Fig. 4.35. Zone of inhibitions/Antimicrobial activity of two isolated compound squalene and linolenic acid methyl ester against various pathogens **(A)** *B. subtilis*; **(B)** *S. aureus*; **(C)** *E. coli* and **(D)** *P. aeruginosa* using agar well diffusion assay.

nullify the effect of ROS and might have potential to prevent different types of oxidative stress related disorders (Lapidot *et al.*, 2002).

4.11.5. Antimicrobial activity of the solvent fractions

The two fractions (Fraction-1 and fraction-2) were tested against two pathogenic gram positive bacteria *Bacillus subtilis*, *Staphylococcus aureus* and two pathogenic gram negative bacteria *Escherichia coli*, *Pseudomonas aeruginosa* etc. Fraction-1 and fraction-2 showed significant antimicrobial activities (zone of inhibition in mm) against *B. subtilis, E. coli* and *P. aeruginosa* (Table 4.20.; Fig. 4.35) whereas, both the fraction showed moderate activity against *S. aureus*. These active compounds, as natural or synthetic, had demonstrated the capacity to modulate the antibiotic activity. Fraction-1 and fraction-2 is such a compound has a potential to inhibit the bacterial efflux systems, enhancing the antibiotic activity. Similar results were also observed by Shakhatreh et al. (2016) and Sampaio et al. (2014). On the basis of result obtained in this present investigation we conclude that the compound showed potent anti-bacterial activity. This implied that both gram positive and gram negative bacteria were susceptible to such active compounds. The obtained results may provide a support to protect against bacterial disorder and these compounds might prove beneficial as a novel drug candidate against bacterial infection in future.

4.12. *In-vitro* regeneration through tissue culture

4.12.1. Establishment of aseptic culture

Fungal and bacterial contamination was the main problem during the early stage of the culture initiation. To avoid this problem various surface sterilants (tween 20, 70 % ethanol, 0.1% mercuric chloride solution) were used, but it could not eliminate the contaminants totally. Almost similar methods like 70 % ethanol and 0.1 % mercuric chloride ($HgCl_2$) have been used to disinfect the explants of *Clerodendrum inerme* (Srinath *et al.*, 2009). Labolene (5%) in combination with 0.1% $HgCl_2$ has been used in the tissue culture study of *Clerodendrum serratum* by Sharma and his co workers (2009).

4.12.2. Callus induction

In-vitro maintained nodal explants started swelling within 6–8 days and

Table 4.21. Effect of different concentrations of BAP with the optimal concentrations of NAA on callus induction from nodal segments of *C. thomsoniae.*

Medium	Plant growth regulators (mg/l)		Callus induction frequency (%)	Mean weight of the callus (gm)
	BAP	NAA		
MS	0	0	0	0.0
	1	0.5	25	0.11±0.015
	2	0.5	85	0.56±0.076
	3	0.5	40	0.3±0.02
	4	0.5	30	0.2±0.025

fully developed callus like structures were observed after 12-15 days of inoculation. All the calli were observed to be initiated from the cutting edge of the explants (Fig. 4.36.A). The calli formed were fast growing, yellowish green and compact. Though in our tissue culture studies, MS and WPM were used for preliminary screening, but better responses were observed in cultures of MS media. So, for propagation of *C. thomsoniae* only MS was employed for further regeneration. This indicates that some of the essential component required by *Clerodendrum* for its regeneration is

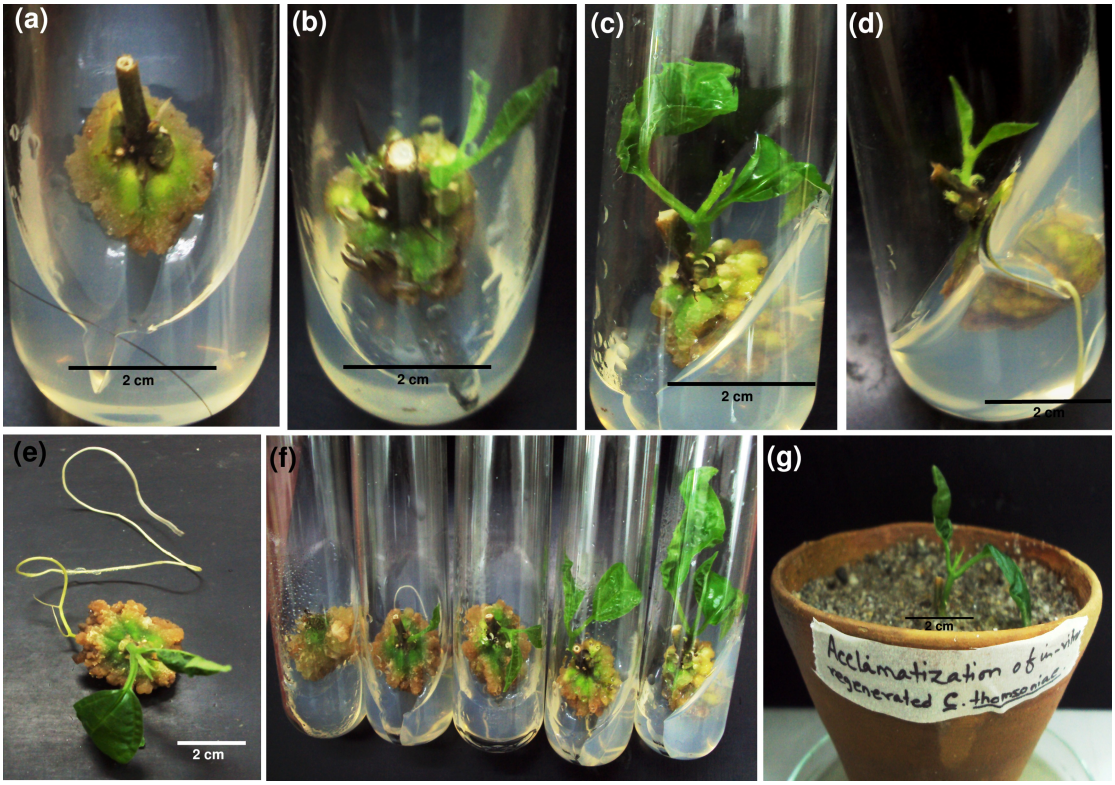

Fig. 4.36. Stages of callus induction and regeneration. **(A)** Callus induction, **(B)** Formation of *in-vitro* shoot, **(C)** Development of leaves, **(D)** *In-vitro* root induction, **(E)** Plantlet with well developed roots, **(F)** Different stages of shoot induction, **(G)** Acclimatization of plant in clay pot containing mixture of soil and sand.

not available in WPM (Nataraj *et al.*, 2016). Similar observation on other species of *Clerodendrum* tissue culture is available. Callus was induced only when nodal explants were inoculated in MS medium supplemented with BAP and NAA. The callus induction frequency was found optimum in MS medium supplemented with 2 mg/l BAP and 0.5 mg/l NAA (85%), followed by 40% with 3 mg/l BAP and 0.5 mg/l NAA (Table 4.21.). Further increase in the hormone concentration resulted in reduction of callus formation. In our present study, the highest callus weight (0.56±0.076gm) was noted with 2 mg/l BAP and 0.5 mg/l NAA followed by 3 mg/l BAP and 0.5 mg/l NAA (0.3±0.02gm) (Table 4.21.).

4.12.3. Shoot regeneration

The regenerative ability of the compact calli was studied by the application of two important plant hormones cytokinins and auxin. After 2 weeks of the culture, most of the calli turned green and emergence of shoot primordia took place (Fig. 4.36.B and C). The number and length of shoots varied with the concentration of phytohormones used. MS medium supplemented with 2 mg/l BAP in combination with 0.5 mg/l NAA produced the highest number of shoot buds (13±1.5) followed by 3 mg/l BAP in combination with 0.5 mg/l NAA (9.5±0.5) (Table 4.22.). BAP is most commonly used cytokinin mainly due to twofold reasons, firstly, it is cheap and secondly, it can be autoclaved (Thomas and Blakesley, 1987). The highest shoot length (3.5±0.5 cm) was noted with 2 mg/l BAP and 0.5 mg/l NAA followed by 2.3±0.15 cm with 3 mg/l BAP in combination with 0.5 mg/ l NAA. In the present workflow, BAP was found to be rather effective in case of shoot multiplication. These findings are in accordance with the earlier work on *in-vitro* propagation of other *Clerodendrum* species like *C. inerme*

Table 4.22. Influence of different concentrations of plant growth regulators on regeneration of shoot buds and elongation of proliferated shoots from callus of *C. thomsoniae.*

Medium	Plant growth regulators (mg/l)		Mean no. of shoots/callus	Mean Shoot length (cm)
	BAP	NAA		
MS	0	0	0.0	0.0
	1	0.5	6.5±0.5	$1.33\pm0.3^{**}$
	2	0.5	13±1.5	$3.5\pm0.5^{**}$
	3	0.5	9.5±0.5	$2.3\pm0.15^{**}$
	4	0.5	4±1.0	1.6 ± 0.07^{NS}

Data expressed as mean ± S.D (n=3). **p<0.01; ^{NS}-Non significant when compared with mean no. of shoots/callus.

(Srinath *et al.*, 2009), *C. serratum* (Sharma *et al.*, 2009), *C. colebrookianum* (Mao *et al.*, 1995), *C. inerme* (Baburaj *et al.*, 2000) where BAP has been widely used and was found to be effective.

In our present experiment, it was noted that root development took place without changing the medium and hormones. In BAP assisted with MS, rooting was initiated little later 10 ± 3 days after shoot development. About 90 % of shoots rooted in MS medium supplemented with 2 mg/l BAP in combination with 0.5 mg/l NAA. The highest number of roots (3.5±0.5) and maximum length of roots (21.3±1.52 cm) were recorded with 2 mg/l BAP with 0.5 mg/l NAA followed by 3 mg/l, 4mg/l BAP (Table 4.23.; Fig. 4.36.D and E).

4.12.4. Acclimatization

The *in-vitro* propagated plantlets with a well developed shoot and root system were successfully transferred to clay pots containing sandy soil and farm yard manure in a ratio of 1:1 (v/v) exhibited 70 % survival rate and grew in the greenhouse **(**Fig. 4.36.G). After a month, these acclimatized plants were successfully transferred to the field.

4.12.5. Genetic fidelity testing

In the present study, plantlets were produced indirectly from the nodal explants through the formation of callus. No differences were observed between field grown plant and plantlets regenerated from nodal explants through callus by RAPD and ISSR analysis. A total of 30 RAPD and 15 ISSR primers were used to screen somaclonal variations, out of which only 10 RAPD and ISSR primers produced clear and scorable amplification products. A total of 65 scorable bands were obtained from the RAPD analysis, whereas ISSR primers produced 75 distinct and scorable bands (Table 4.24.). The number of

Table 4.23. Effect of different concentrations of BAP and NAA on rooting of *in-vitro* raised elongated roots in *C. thomsoniae.*

Medium	Plant growth regulators (mg/l)		Mean no. of roots/explant	Mean root length (cm)
	BAP	NAA		
MS	0	0	0.0	0.0
	1	0.5	1.33±0.35	7.8±0.76**
	2	0.5	3.5±0.5	21.3±1.52**
	3	0.5	1.9±0.13	13±1.0**
	4	0.5	1.7±0.05	10.5±0.5**

Data expressed as mean ± S.D (n=3). **p<0.01 when compared with mean no. of roots/explants.

bands varied from 3-13 in case of RAPD primers and 3-12 in case of ISSR primers respectively. All the bands generated were found to be monomorphic i.e. bands generated through both RAPD and ISSR analyses were common in parental genotypes and the *in-vitro* raised plantlets. A representative of RAPD and ISSR profile is depicted in Fig. 4.37. The size of the bands ranged in between 220-1646 bp and 139-1,340 bp in case of RAPD and ISSR primers respectively. Sharma and his coworkers (2009) studied the clonal fidelity of *in-vitro* raised *C. serratum* where they used 6 decamer RAPD primers to establish the genetic stability among the micropropagated plantlets. Mishra and her coworkers (2015) and Goyal et al. (2015) reported that RAPD and ISSR fingerprints are very crucial to detect clonal fidelity of *in-vitro* raised plantlets.

Table 4.24. PCR amplification using RAPD and ISSR primers.

Primer ID	Primer sequence (5'-3')	Total bands amplified	No. of monomorphic bands	Band size (bp)
OPA 01	CAGGCCCTTC	4	4	324-1310
OPA 02	TGCCGAGCTG	8	8	325-1646
OPA 03	AGTCAGCCAC	13	13	224-1434
OPA 07	GAAACGGGTG	3	3	220-1128
OPA 08	GTGACGTAGG	5	5	357-1453
OPA 09	GGGTAACGCC	4	4	286-1218
OPA 10	GTGATCGCAG	7	7	346-1605
OPA 11	CAATCGCCGT	5	5	383-1383
OPA 12	CAGCACCCAC	9	9	459-1544
OPA 18	AGGTGACCGT	7	7	363-1589
Total bands		**65**	**65**	
UBC 807	(AG)8T	7	7	226-949
UBC 808	(AG)8C	8	8	139-1340
UBC 810	(GA)8T	12	12	225-935
UBC 811	(GA)8C	6	6	185-847
UBC 813	(CT)8T	3	3	250-975
UBC 815	(CT)8G	4	4	425-1260
UBC 818	(CA)8G	8	8	326-1030
UBC 822	(TC)8A	8	8	288-1250
UBC 824	(TC)8G	8	8	235-1225
UBC 825	(AC)8T	11	11	323-1110
Total bands		**75**	**75**	

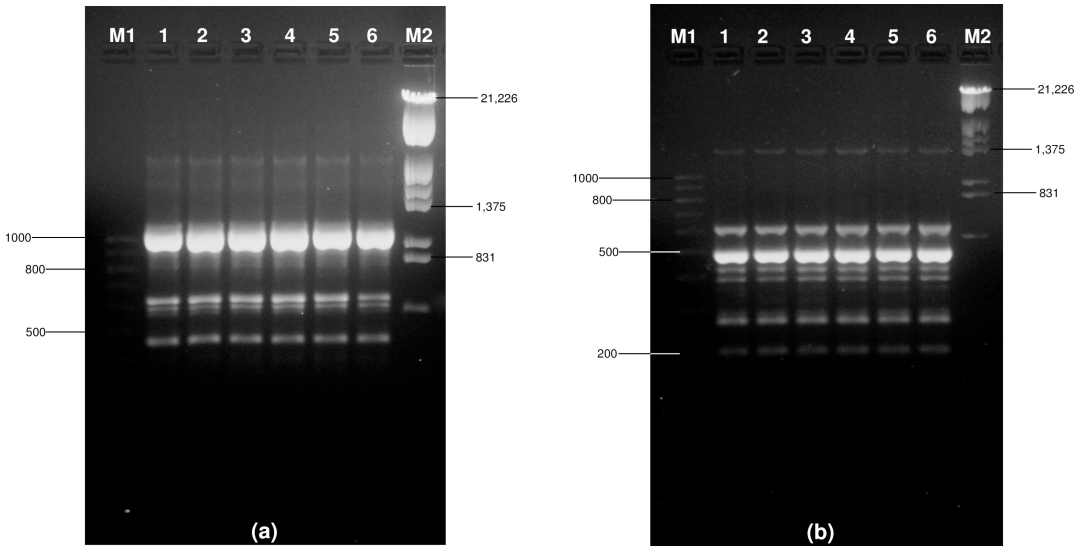

Fig. 4.37. DNA fingerprinting pattern of *in-vitro* callus regenerated plantlets of C. thomsoniae. **(A)** using RAPD primer OPA 13 and **(B)** using ISSR primer UBC 808. Lane 2–6: micropropagated plantlets compared with field grown plant (lane1); Lane M1: 100 bp molecular marker; Lane M2: λ-DNA/EcoRI/HindIII double digest DNA ladder.

4.12.6. GC-MS analysis

The present study was extended for the analysis pertaining to the identification of active compounds in field grown plant and tissue culture plant using GC-MS method. A total number of nineteen (19) and twenty seven (27) phytocompounds have been identified in field grown plant and tissue culture plant respectively (Table 4.25.), which corresponds to Fig. 4.38 and the screened phytometabolic constituents have been provided in Table 4.26. Ten compounds are common between field grown plant and tissue culture plant, but interestingly seventeen (17) compounds were exclusively present in tissue culture plant of which a number of compounds are of potential therapeutic significance. Several phytochemicals belonging to long chain fatty moiety and their derivatives such as Hexadecanoic acid; Dodecanoic acid; Tetradecanoic acid; Heptanedioic acid; Octanedioic acid; Adipic acid etc has been identified in the samples. Interestingly, these long chain fatty acids play an important role in plant development (Bach and Faure, 2010). linoleic acid (LA), oleic acid (OA), squalene and stigmasterol are the main bioactive compounds having different medicinal properties. LA is one of the essential fatty acids that human need in diet. Deficiency of LA may lead to growth retardation, infertility, skin and kidney degeneration and abrupt changes in fatty acid composition of lipids (Dobryniewski *et al.*, 2007). Besides,

Table 4.25. List of phytocompounds identified in *C. thomsoniae* leaf extract (field grown plant and tissue culture plant) by GC-MS analysis.

Compound name	Formula	Mol. Wt. †	Field grown plant	Tissue culture plant
Acetic acid	$C_2H_4O_2$	55	×	√
Propanoic acid	$C_3H_6O_2$	73	×	√
3-Hydroxy-2-butanone	$C_4H_8O_2$	87	×	√
Glyceric acid	$C_3H_6O_3$	89	√	×
3-Hydroxybutyric acid	$C_4H_8O_3$	103	×	√
Diethylene glycol	$C_4H_{10}O_3$	105	×	√
2-Furancarboxylic acid	$C_5H_4O_3$	111	×	√
2-Hexenoic acid	$C_6H_{10}O_2$	113	√	√
Butanedioic acid	$C_4H_6O_4$	117	√	√
1,2,3-Benzenetriol (Pyrogallol)	$C_6H_6O_3$	125	×	√
Pyroglutamic acid	$C_5H_7NO_3$	127	×	√
Pentanedioic acid (Glutaric acid)	$C_5H_8O_4$	131	√	√
Malic acid	$C_4H_6O_5$	133	√	×
1,2-Ethanediol, phenyl	$C_8H_{10}O_2$	137	×	√
Benzoic acid, 3-hydroxy (m-Salicylic acid)	$C_7H_6O_3$	137	×	√
4-Hydroxyphenylethanol (Tyrosol)	$C_8H_{10}O_2$	137	×	√
Adipic acid	$C_6H_{10}O_4$	145	×	√
Heptanedioic acid (Pimelic acid)	$C_7H_{12}O_4$	159	×	√
Octanedioic acid (Suberic acid)	$C_8H_{14}O_4$	173	×	√
1-Dodecanol	$C_{12}H_{26}O$	185	×	√
Azelaic acid	$C_9H_{16}O_4$	187	√	√
Dodecanoic acid	$C_{12}H_{24}O_2$	200	√	√
Ethyl tartrate	$C_8H_{14}O_6$	205	×	√
Tetradecanoic acid	$C_{14}H_{28}O_2$	227	√	√
Hexadecanoic acid (Palmitic acid)	$C_{16}H_{32}O_2$	255	√	√
Heptadecanoic acid	$C_{17}H_{34}O_2$	269	√	×
Linoleic acid	$C_{18}H_{32}O_2$	279	√	√
Oleic acid	$C_{18}H_{34}O_2$	281	×	√
Stearic acid	$C_{18}H_{36}O_2$	283	√	×
2-Hexadecen-1-ol, 3,7,11,15-tetramethyl	$C_{20}H_{40}O$	295	√	×
Eicosanoic acid	$C_{20}H_{40}O_2$	311	√	×
Palmitelaidic acid, trimethylsilyl ester	$C_{19}H_{38}O_2Si$	325	√	×
Heptacosane	$C_{27}H_{56}$	379	√	×
Squalene	$C_{30}H_{50}$	409	√	√
Stigmasterol	$C_{29}H_{48}O$	412	√	√
α-Tocopherol	$C_{29}H_{50}O_2$	429	√	×

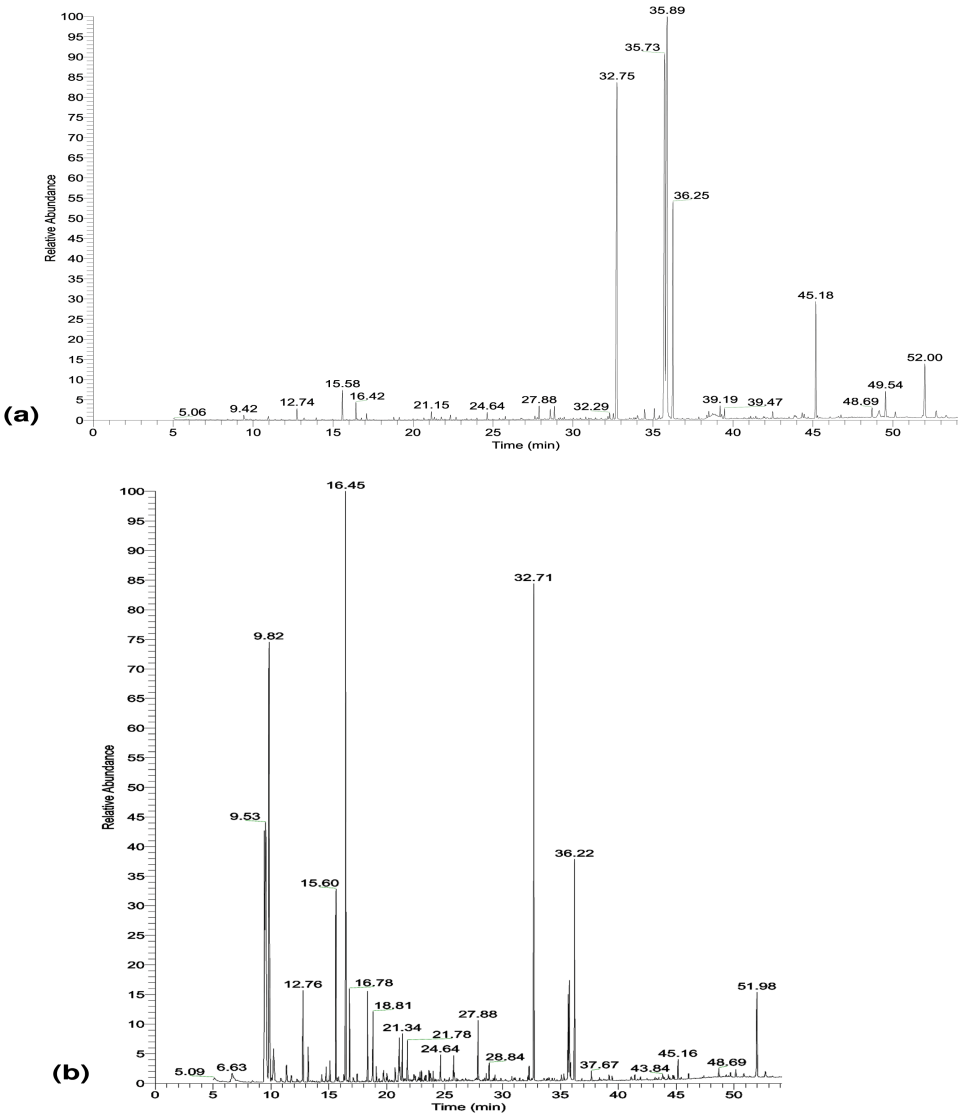

Fig. 4.38. GC-MS fingerprinting of **(A)** field grown plant and **(B)** tissue culture plant.

Table 4.26. Compounds with potential medicinal value identified in *C. thomsoniae* tissue culture plant.

Compound name	Activity	Reference
3-Hydroxybutyric acid	Anti-stress activity	Sleiman et al. (2016)
Azelaic acid	Effective in the treatment of postinflammatory hyperpigmentation and melasma	Breathnach (1995)
n-Hexadecanoic acid	Anti-oxidant, Hypocholesterolemic	Aparna et al. (2012); Sutha et al. (2010).
Linoleic acid	Anti-cancer	Tsuzuki et al. (2004); Cesano et al. (1998).
Oleic acid	Aanticancer	Martín-Moreno et al. (1994); Reddy and Maeura (1984).
Squalene	Anti-oxidant, anticancer activity	Amarowicz (2009); Yoshida and Niki (2003).
Stigmasterol	Anti-oxidant, anticancer activity	Amarowicz (2009); Yoshida and Niki (2003).

LA has been reported to suppress human tumor (Tsuzuki *et al.*, 2004) and lung tissue cancer (Cesano *et al.*, 1998). Another metabolite, OA has been reported to have potential protective effect against breast cancer and colon carcinomas in rats (Martin-Moreno *et al.*, 1994; Reddy and Maeura, 1984). 3-Hydroxybutyric acid has anti-stress activity (Sleiman *et al.*, 2016). In addition, squalene and stigmasterol were reported as potent antioxidants as well as beneficial against several carcinogens (Amarowicz, 2009); (Yoshida and Niki, 2003). Hence, it seems likely that the tissue culture plant contain plenty of medicinally important constituents which might be a good source of natural medicine.

4.12.7. Molecular docking

The compounds detected by GC-MS for the field grown plant and the tissue cultured progeny largely contain the same set of phytocompounds indicating that the basic chemical architecture of both is same. However, some of the compounds present in tissue cultured plant were missing in the field grown plant (Table 4.25.). Among them interestingly 3-Hydroxybutyric acid and Pyroglutamic acid are also present. They are both reported for anti-stress activity and their presence indicates the intelligent development scheme for the micropropagated progeny (Pepeu and Spignoli, 1989; Sleiman *et al.*, 2016). To further understand their chemical behavior from a different perspective we conducted *in-silico* molecular

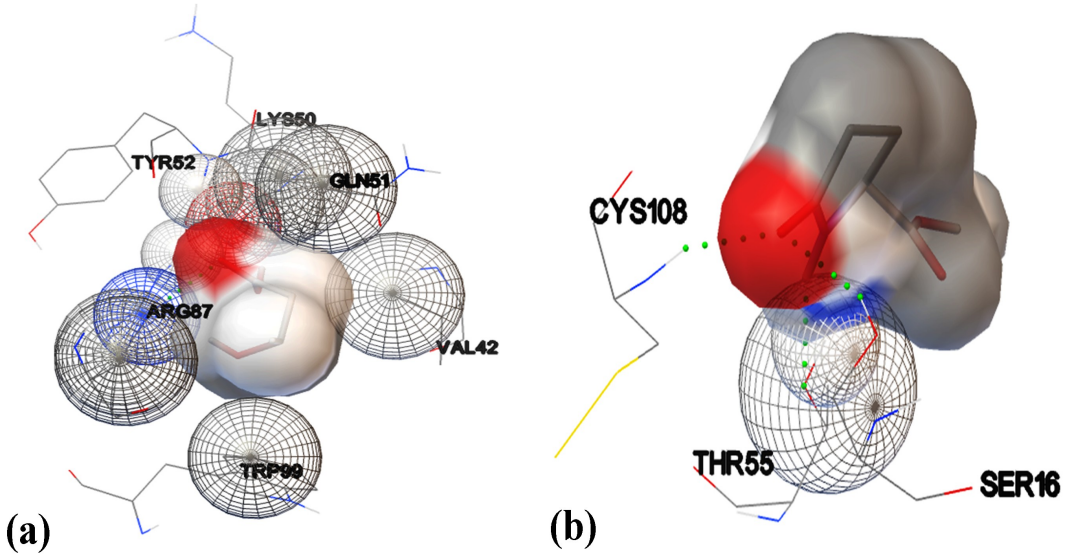

Fig. 4.39. Molecular surface view of BDNF protein with **(A)** 3-Hydroxybutyric acid and **(B)** Pyroglutamic acid docked into its binding site.

docking tests. Here the receptor protein used is Brain-derived neurotrophic factor (BDNF), which is reported to have an upper hand in depression and stress related lifestyle hazards (Sleiman *et al.*, 2016). The two compounds are seen to have good interactions with our BDNF receptor, 3-Hydroxybutyric acid has a binding affinity of -4.4 kcal/mol and Pyroglutamic acid has a binding affinity of -4.7 kcal/mol (Fig. 4.39). So, it can be inferred that the 3-Hydroxybutyric acid and Pyroglutamic acid present in the micropropagated plants can have a potential to bind with BDNF receptor. Hence, besides having all the therapeutic uses of the plant itself, the tissue cultured plants can possess an added anti-stress property in itself.

4.13. Study of Molecular diversity

4.13.1 DNA isolation

Clerodendrum DNA was isolated using the standard protocol of Doyle and Doyle (1987) with minor modifications. The DNA-CTAB complex provided a network of whitish precipitate of nucleic acids after proper removal of impurities and further used for downstream processing. Agarose gel analysis of those DNA thus obtained exhibited distinct and clear bands.

Crude DNA is basically mixed with many contaminants including RNA, protein and polysaccharides etc. which lead to enzymatic reaction with DNA. Therefore, DNA purification is prerequisite step before performing downstream analysis like PCR amplification, DNA restriction and gene cloning. Inclusion of CTAB method in DNA extraction process helps to eliminate polysaccharides from DNA precipitations to a large extent. Subsequently, extraction with phenol:chloroform:isoamyl alcohol indicates the removal of protein impurities from the DNA samples. Further, RNAase enzyme is used to remove RNAs from samples.

In the present study, 2 different types of quantification methods were followed to analyze the quality of DNA. First one is spectrophotometric method and the other one is agarose gel electrophoresis. In spectrophotometric method, the DNAs were quantified in a UV spectrophotometer with 260 nm and 280 nm filters. The results were calculated as the ratio of A_{260}/A_{280} after performing of six replicates and the samples considered only showing a ratio of around 1.8 (Table 4.27.).

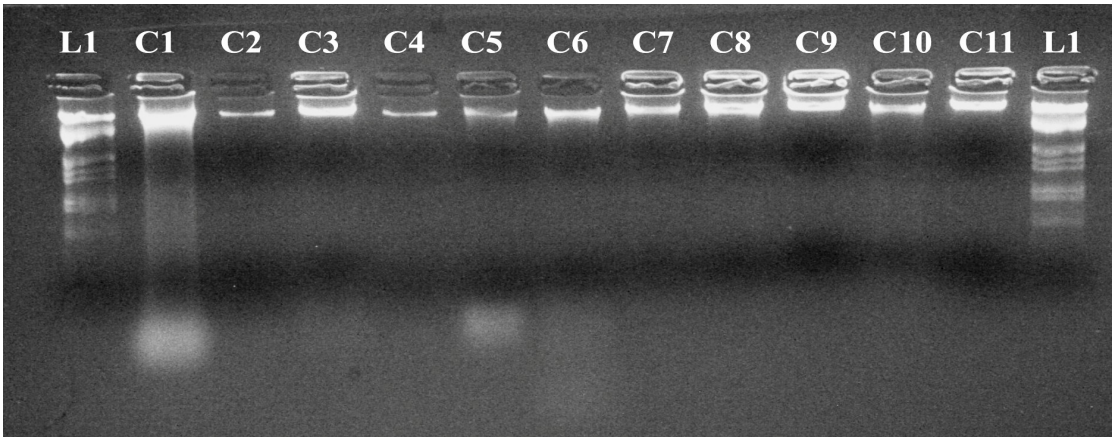

Fig. 4.40. Crude DNA of all the *Clerodendrum* samples (Lane C1- C11: different samples of *Clerodendrum* under study, Please refer table 3.1 for the name of species); L1: λ DNA/ EcoRI/HindIII double digest DNA ladder.

Table 4.27. List of samples showing their purity.

Sample ID	A_{260}/A_{280} ratio (purity)
CL-1	1.83
CL-2	1.80
CL-3	1.83
CL-4	1.77
CL-5	1.78
CL-6	1.85
CL-7	1.88
CL-8	1.83
CL-9	1.78
CL-10	1.79
CL-11	1.75

In gel electrophoresis, the intactness of the DNA was determined with the help of 0.8% Agarose gel electrophoresis using λ-DNA/EcoRI/HindIII double digest indicating molecular weight of the sample DNA (Fig. 4.40). The samples with relatively larger bands were chosen for further downstream process.

Hence, the combination of the above mentioned three steps i.e. extraction, purification and quantification allowed sufficient amount of pure DNA from the leaves of different *Clerodendrum* species for PCR amplification.

4.13.2 RAPD analysis

RAPD is a routinely used technique to evaluate the genetic relationship among species, varieties and cultivars. Initially, 45 different decamer primers have been used to study the genetic diversity (RAPD analysis) of 11 species of *Clerodendrum*. Out of the 45 primers screened, 39 resulted distinct and scorable bands ranging from 124 bp to 1980 bp (Table 4.28.).

A total of 495 bands were generated of which all are polymorphic bands. Interestingly, the percentage of polymorphism was found to be 100% and the number of polymorphic bands (Table 4.28.) generated by each decamer primers ranged in between 04

Table 4.28. Total number and size of amplified bands, number of monomorphic and polymorphic bands generated and percentage of polymorphism generated by the RAPD primers.

Primer ID	Sequence (5′-3′)	Total bands amplified	Monomorphic bands	Polymorphic bands	% polymorphism	Band size (bp)
OPA01	CAGGCCCTTC	16	0	16	100%	324-1410
OPA02	TGCCGAGCTG	18	0	18	100%	325-1656
OPA03	AGTCAGCCAC	**27**	0	27	100%	**124**-1444
OPA04	AATCGGGCTG	21	0	21	100%	195-1367
OPA05	AGGGGTCTTG	14	0	14	100%	288-1750
OPA07	GAAACGGGTG	24	0	24	100%	220-1238
OPA08	GTGACGTAGG	14	0	14	100%	367-1533
OPA09	GGGTAACGCC	13	0	13	100%	276-1118
OPA10	GTGATCGCAG	17	0	17	100%	346-1600
OPA11	CAATCGCCGT	14	0	14	100%	393-1483
OPA12	TCGGCGATAG	16	0	16	100%	249-1733
OPA13	CAGCACCCAC	11	0	11	100%	239-1175
OPA14	TCTGTGCTGG	10	0	10	100%	323-1165
OPA15	TTCCGAACCC	17	0	17	100%	483-1600
OPA16	AGCCAGCGAA	13	0	13	100%	329-1620
OPA17	GACCGCTTGT	13	0	13	100%	347-1445
OPA18	AGGTGACCGT	20	0	20	100%	285-1523
OPA19	CAAACGTCGG	20	0	20	100%	268-**1980**
OPA20	GTTGCGATCC	15	0	15	100%	285-1523
OPB01	GTTTCGCTCC	12	0	12	100%	350-1440
OPB04	GGACTGGAGT	15	0	15	100%	375-1470
OPB05	TGCGCCCTTC	08	0	08	100%	753-1450
OPB06	TGCTCTGCCC	11	0	11	100%	360-1445
OPB07	GGTGACGCAG	14	0	14	100%	314-1200
OPB08	GTCCACACGG	10	0	10	100%	250-1150
OPB10	CTGCTGGGAC	11	0	11	100%	628-1630
OPB11	GTAGACCCGT	16	0	16	100%	190-1600
OPB12	CCTTGACGCA	08	0	08	100%	185-1500
OPB13	TTCCCCCGCT	**04**	0	04	100%	350-1450
OPF09	CCAAGCTTCC	11	0	11	100%	561-1255
OPG19	GTCAGGGCAA	11	0	11	100%	446-1443
OPH04	GGAAGTCGCC	14	0	14	100%	375-1330
OPN05	ACTGAACGCC	15	0	15	100%	425-1430
OPN13	AGCGTCACTC	10	0	10	100%	483-1175
OPN19	GTCCGTACTG	12	0	12	100%	159-1570
	Total	**495**	**0**	**495**	**100%**	

(OPB13) and 27 (OPA03). The RAPD profile of the 11 accessions of *Clerodendrum* generated using primers OPA 12, OPA 16, OPA 18 and OPN 19 are represented in Fig. 4.41.(A-D). A similarity matrix was further drawn using Dice coefficient of similarity (Nei and Li, 1979) ranging from 0.60 to 0.85 (Table 4.29.). The lowest similarity was observed between *C. japonicum* and *C. serratum*, while the highest value was recorded between *C. speciaosum* and *C. infortunatum*. A dendrogram was constructed on the basis of the data obtained from RAPD analysis using NTSYSpc (Fig. 4.42). In fact, RAPD markers are the most suitable ones to analyze the genetic variation of both intra and inter-population (Li *et al.*, 2010). The dendrogram prepared from RAPD analysis revealed that *C. indicum*, *C. speciaosum*, *C. thomsoniae*, *C. splendens*, *C. fragrans* and *C. bracteatum* formed a group (1st clade) in which members of *C. inerme*, *C. colebrookianum*, *C. japonicum* and *C. infortunatum* formed another group (2nd clade). *C. speciaosum* and *C. thomsoniae* shared a node at 85% whereas *C. indicum* exhibited a cluster with *C. speciaosum* and *C. thomsoniae* sharing a node at 71% and 73% respectively. In the second clade, *C. inerme* and *C. colebrookianum* shared a node at 69%. In addition, *C. serratum* appeared as a distinct outgroups in the dendrogram. The correspondence analysis of both 2D (Fig. 4.43.A) and 3D (Fig. 4.43.B) plotting and corroborated the cluster analysis result. Hence, it might be inferred that RAPD markers are praiseworthy for analyzing genetic variations among the species and could be utilized as molecular taxonomic characters to analyze the genetic relationships among the species of *Clerodendrum*.

4.13.3 Inter Simple Sequence Repeat analysis

We accessed phylogenetics among the 11 accessions of *Clerodendrum* using DNA based technique complemented with 15 ISSR primers. Initially, fifteen ISSR primers were screened and all the primers showed positive response to generate distinct, scorable bands (Table 4.30.). Among the primers used, the primer UBC 836 produced 11 bands while UBC 810 amplified the highest number of bands i.e. 20. A total of 229 amplified bands were produced by the 15 primers of which all the 229 were polymorphic. The frequency of polymorphism was found to be 100%. The band size ranged between 111 bp

Table 4.29. The similarity matrix obtained using Dice coefficient of similarity among the 11 species of *Clerodendrum* based on RAPD profiling.

	CL-1	CL-2	CL-3	CL-4	CL-5	CL-6	CL-7	CL-8	CL-9	CL-10	CL-11
CL-1	1										
CL-2	0.68	1									
CL-3	0.68	0.66	1								
CL-4	0.67	0.63	0.66	1							
CL-5	0.71	0.68	0.65	0.75	1						
CL-6	0.73	0.68	0.65	0.68	**0.85**	1					
CL-7	0.67	0.66	0.67	0.63	0.66	0.68	1				
CL-8	0.65	0.68	**0.60**	0.64	0.66	0.66	0.62	1			
CL-9	0.69	0.69	0.69	0.65	0.70	0.70	0.69	0.64	1		
CL-10	0.70	0.65	0.62	0.63	0.68	0.70	0.67	**0.60**	0.66	1	
CL-11	0.67	0.65	0.65	0.63	0.67	0.67	0.66	0.61	0.68	0.73	1

For details on sample ID CL-1 to CL-11 please refer table 3.1.

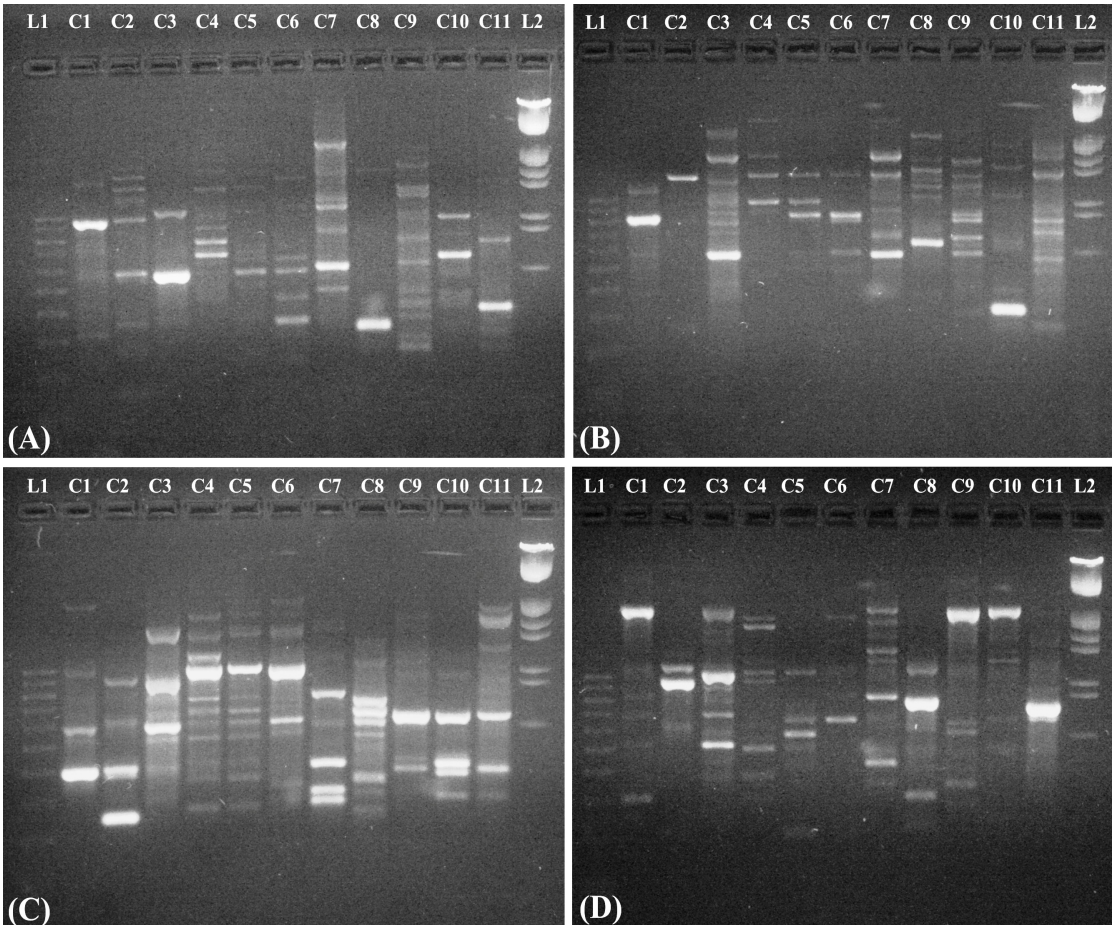

Fig. 4.41. Representatives of RAPD profiling of 11 accessions of *Clerodendrum* amplified with **(A)** OPA12, **(B)** OPA 16, **(C)** OPA 18 and **(D)** OPN 19 primers. Lane L1: 100 bp molecular marker; Lane C1-C11 different accessions of *Clerodendrum* under study (refer table 3.1); Lane L2: λ-DNA/EcoRI/HindIII double digest DNA ladder.

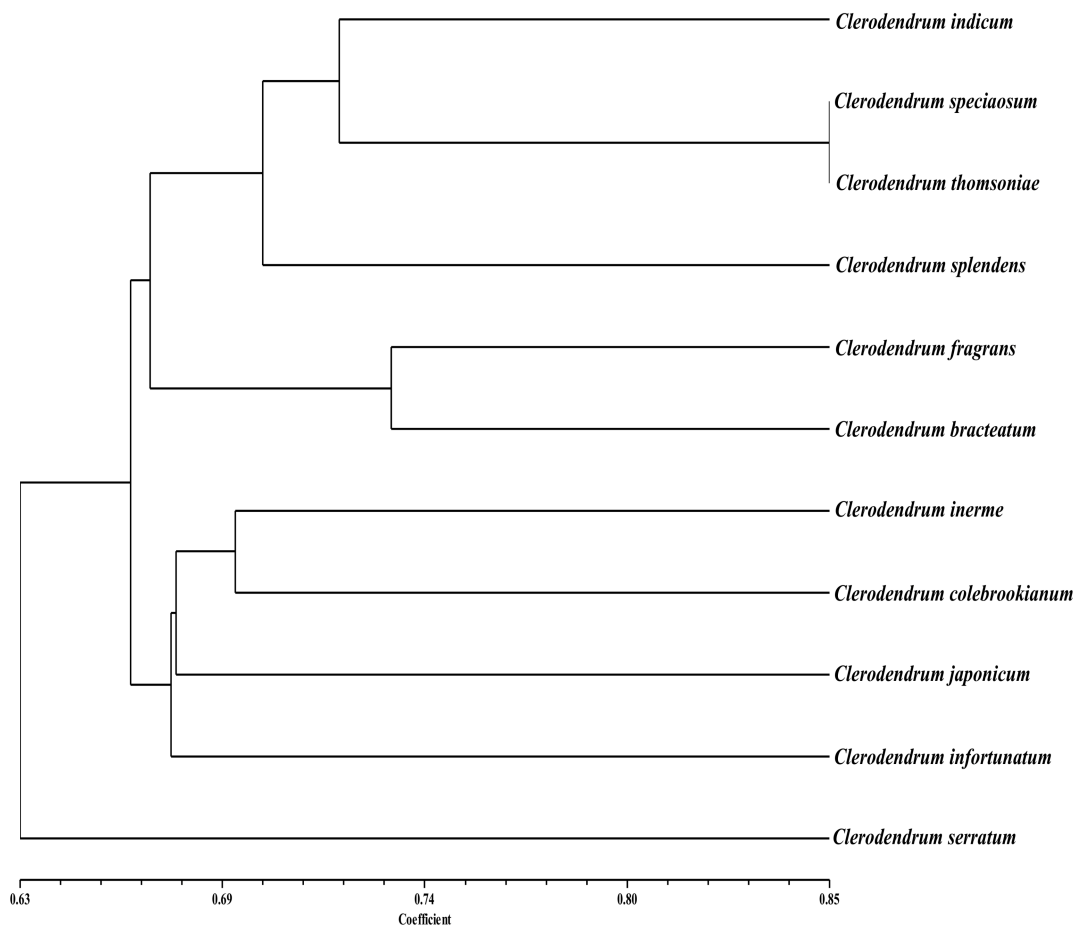

Fig. 4.42. Dendrogram obtained from UPGMA cluster analysis of RAPD markers illustrating the genetic relationships among the 11 accessions of *Clerodendrum*.

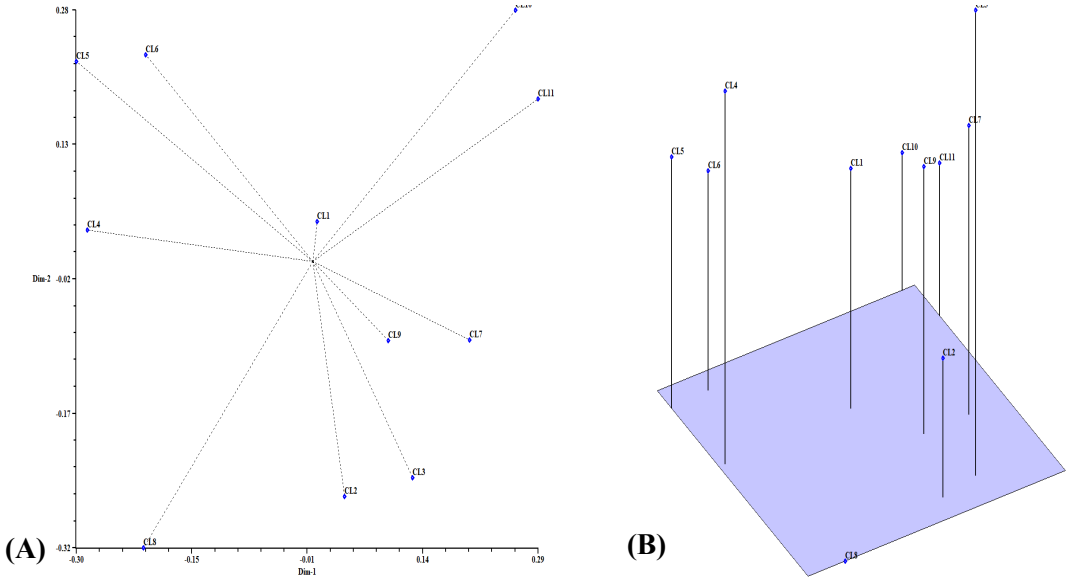

Fig. 4.43. Principal coordinate analysis of 11 species of *Clerodendrum* based on RAPD analysis data. **(A)** 2-dimensional plot and **(B)** 3-dimensional plot.

Table 4.30. Total number and size of amplified bands and number of polymorphic bands generated by ISSR primers.

Primer ID	Sequence (5'-3')	Total bands amplified	Polymorphic bands	% of polymor-phism	Band size (bp)
UBC807	(AG)8T	15	15	100%	216-949
UBC808	(AG)8C	15	15	100%	190-848
UBC810	(GA)8T	**20**	20	100%	235-925
UBC811	(GA)8C	13	13	100%	195-840
UBC813	(CT)8T	16	16	100%	250-975
UBC815	(CT)8G	18	18	100%	**111**-1333
UBC818	(CA)8G	14	14	100%	320-1023
UBC822	(TC)8A	15	15	100%	278-**1350**
UBC824	TC(8)G	14	14	100%	245-1215
UBC825	(AC)8T	13	13	100%	313-1100
UBC834	(AG)8YT	16	16	100%	350-1050
UBC836	(AG)8YA	**11**	11	100%	131-986
UBC841	(GA)8YC	17	17	100%	154-1336
UBC856	(AC)8YA	18	18	100%	170-1267
UBC873	(GACA)4	14	14	100%	275-1250
	Total	**229**	**229**	**100%**	

to 1350 bp. A representative of ISSR profile of the 11 accessions of *Clerodendrum* generated with UBC 811, UBC 815, UBC 841 and UBC 873 primer is depicted in Fig. 4.44 (A-D). Nei's genetic similarity between each pair of species ranged in between 0.53 to 0.88 (Table 4.31.). The lowest was found between *C. japonicum* and *C. serratum* while the highest value was recorded between *C. speciaosum* and *C. thomsoniae*.

The dendrogram constructed based on the data from the ISSR based random primers (Fig. 4.45) showed that most of the *Clerodendrum* species clustered together whereas, *C. serratum* appeared as a distinct outgroup in the dendrogram. In this dendrogram, *C. indicum* and *C. japonicum* shared a node at 66% whereas *C. speciaosum* and *C. thomsoniae* sharing a node at 88% respectively. The correspondence analysis of both 2D (Fig. 4.46.A) and 3D (Fig. 4.46.B) plotting and corroborated the cluster analysis result. Thus it can be inferred from the ISSR marker study that not only morphological features must be considered for the taxonomy of *Clerodendrum* but multidisciplinary approach including the molecular techniques must be employed to have correct taxonomic demarcation.

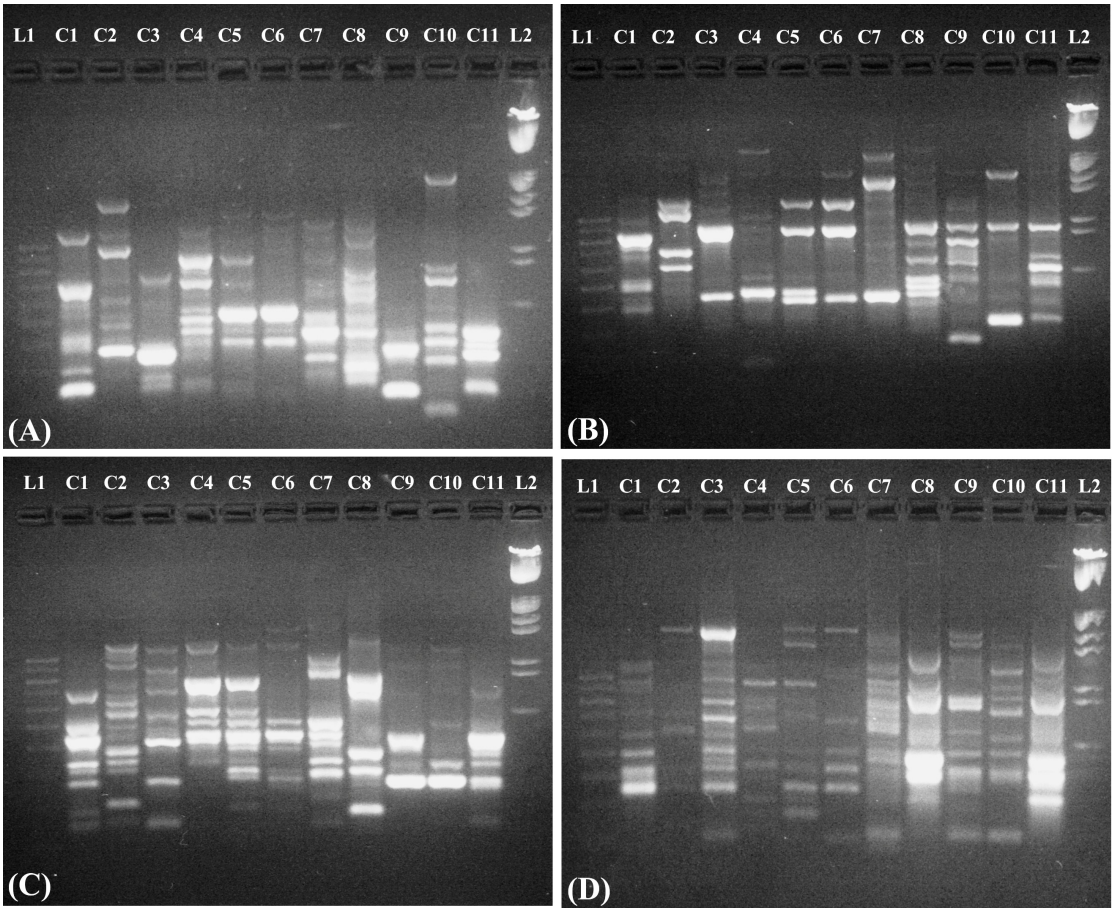

Fig. 4.44. ISSR banding patterns of 11 accessions of *Clerodendrum* generated by **(A)** UBC811, **(B)** UBC 815, **(C)** UBC 841 and **(D)** UBC873 primers. Lane L1: 100 bp molecular marker; Lane C1-C11 different accessions of *Clerodendrum* under study (please refer table 3.1 for the species); Lane L2: λ-DNA/EcoRI/HindIII double digest DNA ladder.

Table 4.31. The similarity matrix obtained using Dice coefficient of similarity among the 11 species of *Clerodendrum* based on ISSR profiling.

	CL-1	**CL-2**	**CL-3**	**CL-4**	**CL-5**	**CL-6**	**CL-7**	**CL-8**	**CL-9**	**CL-10**	**CL-11**
CL-1	1										
CL-2	0.60	1									
CL-3	0.66	0.64	1								
CL-4	0.60	0.70	0.64	1							
CL-5	0.61	0.65	0.64	0.79	1						
CL-6	0.61	0.64	0.62	0.72	**0.88**	1					
CL-7	0.64	0.62	0.61	0.66	0.65	0.66	1				
CL-8	0.60	0.59	**0.53**	0.61	0.60	0.60	0.66	1			
CL-9	0.64	0.62	0.63	0.66	0.64	0.65	0.68	0.66	1		
CL-10	0.65	0.64	0.62	0.68	0.70	0.59	0.69	0.66	0.71	1	
CL-11	0.62	0.62	0.62	0.66	0.66	0.65	0.62	0.62	0.71	0.79	1

For details on sample ID CL-1 to CL-11 please refer table 3.1.

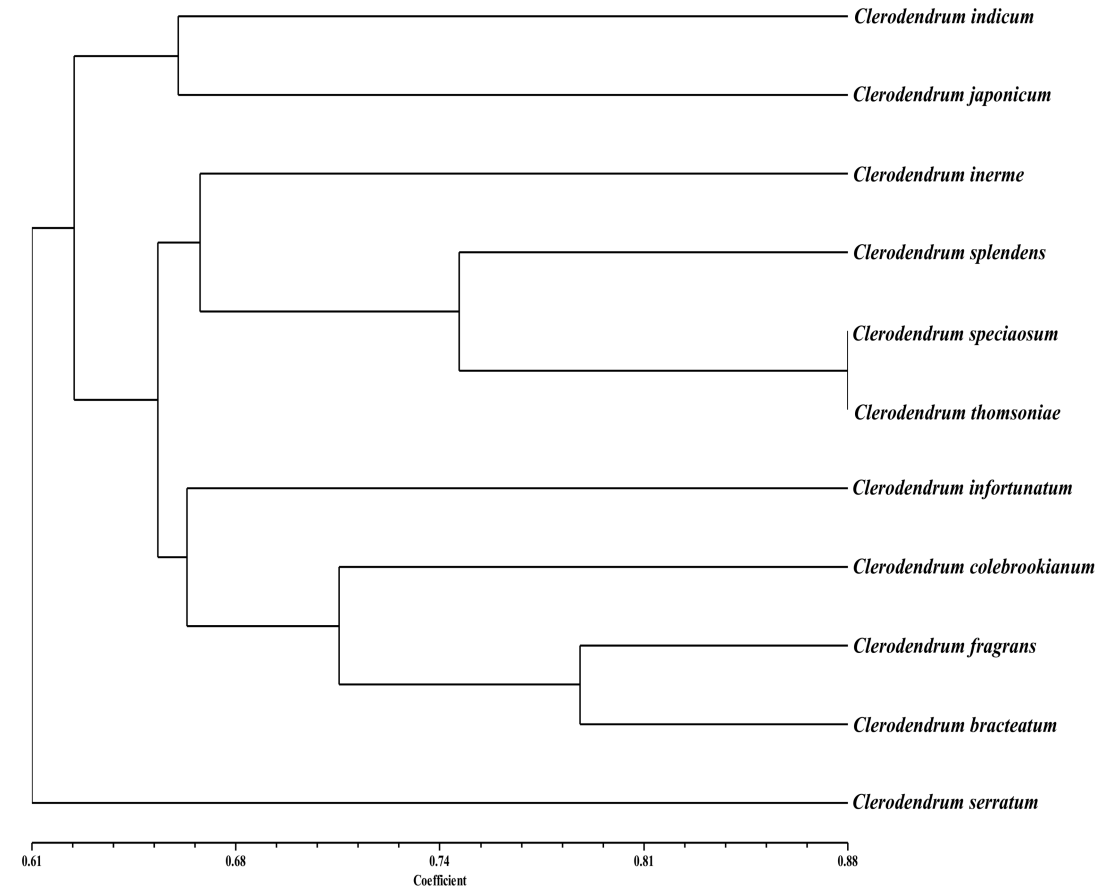

Fig. 4.45. Dendrogram generated from the cluster analysis of ISSR markers of 11 *Clerodendrum* accessions.

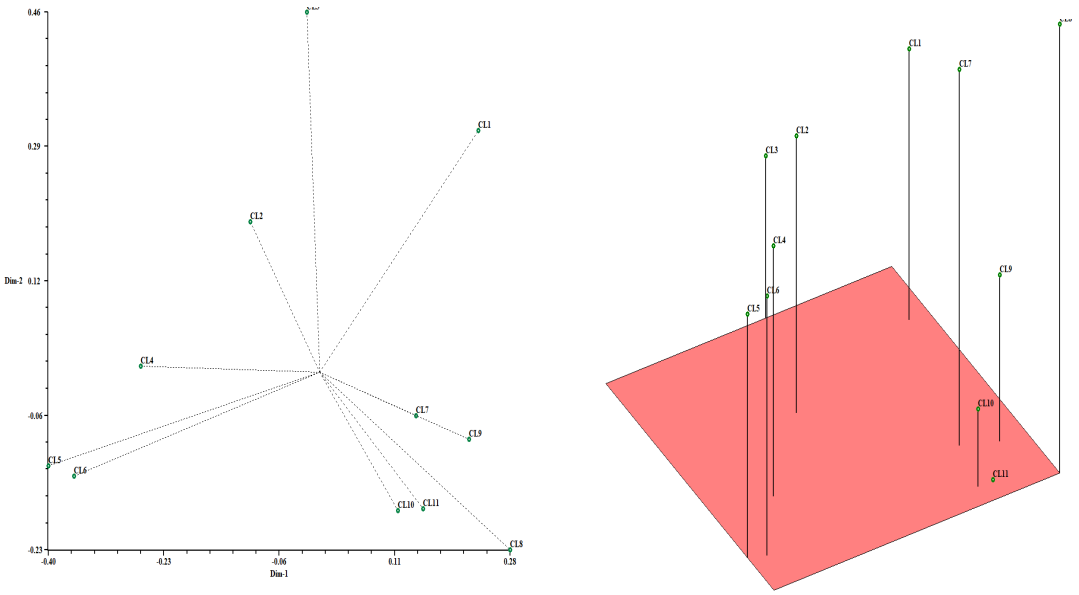

(A) **(B)**

Fig. 4.46. Principal coordinate analysis of 11 species of *Clerodendrum* based on ISSR analysis data. **(A)** 2-dimensional plot and **(B)** 3-dimensional plot.

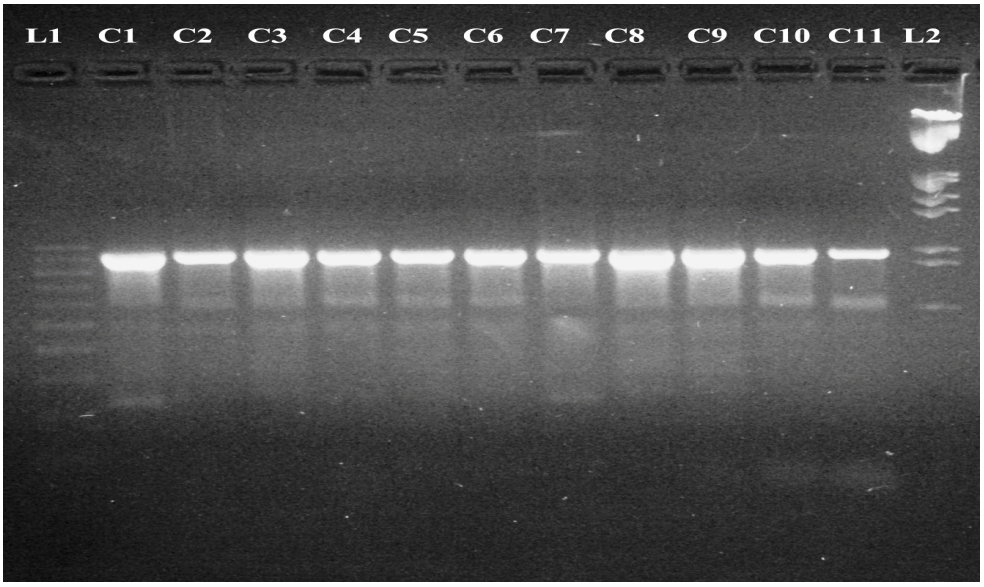

Fig. 4.47. Amplification of 11 species of *Clerodendrum* with matK primer. Lane L1: 100bp DNA ladder; Lane C1-C11: Different species of *Clerodendrum* as listed in Table 3.1 and L2: λ-DNA/EcoRI/HindIII double digest DNA ladder.

4.13.4. PCR-RFLP analysis

PCR-RFLP is a simple and cheap method playing a vital role in accessing the genetic diversity of different plant species. Therefore, it is applied to study the fingerprinting of selected species under the genus *Clerodendrum* found in North Bengal and Assam.

4.13.4.1. PCR amplification of matK

In the present study, 11 species of *Clerodendrum* were employed to PCR amplification using a primer pair consisting of forward and reverse primers to target the matK region of the chloroplast DNA of *Clerodendrum*. The primer pair successfully amplified the matK region of the chloroplast genome. The amplified product is shown in Fig. 4.47.

4.13.4.1.1. PCR product restriction digestion and agarose gel analysis

The PCR product obtained from the primer pair matK were subjected to restriction digestion using 4 different restriction enzymes like HinfI, HaeIII, HpaII and EcoRI to short out the degree of genetic variation among different species of *Clerodendrum*. Amongst 6 enzymes studied, 2 restriction enzymes (MboI and MspI) were found to be unsuccessful to digest the PCR products while the other four restriction enzymes produced a total of 8 polymorphic bands (Table 4.32.). All the restriction enzymes produced two bands each. The total percentage of polymorphism was found to be 100%. The result obtained from restriction

digestion with the enzyme HaeIII and HpaII is depicted in Fig. 4.48.

4.13.4.1.2. PCR-RFLP data analysis

A total of 8 scorable bands were produced using various restriction enzymes. Of the 8 cuts 8 were polymorphic. These clear and distinct bands were scored and used for further analysis (Table 4.32.). A dendrogram was prepared (Fig. 4.49) on the basis of similarity estimates using the unweighted pair group method with arithmetic average (UPGMA) using NTSYSpc version (2.0) (Rohlf, 1998). The dendrogram revealed two major clusters and one outgroup. The first cluster comprises with 3 species (*C. indicum*, *C. splendens* and *C. infortunatum*) while, the second cluster consisted of 7 species (*C. inerme*, *C. japonicum*, *C. chinense*, *C. bracteatum*, *C. speciaosum*, *C. thomsoniae* and *C. colebrookianum*). Interestingly, similar type of closeness among the species of *C. indicum* and *C. splendens* was also observed in the RAPD dendrogram. Henceforth, from the above analysis it could be inferred that in the present study notable polymorphism has been found among the selected species due to their polyphyletic nature of the different species of *Clerodendrum*.

Table 4.32. Total fragments, number of polymorphic bands generated by using different restriction enzymes.

Restriction Enzyme	Optimum temperature	No. of cuts	No. of polymorphic bands	% of polymorphism
matK				
HinfI	37 ºC	2	2	100%
HaeIII	37 ºC	2	2	100%
HpaII	37 ºC	2	2	100%
EcoRI	37 ºC	2	2	100%
		8	**8**	**100%**
Rps16				
HinfI	37 ºC	4	2	50%
HaeIII	37 ºC	2	1	50%
EcoRI	37 ºC	2	1	50%
		8	**4**	**50%**
Taberlet (TrnL-TrnF)				
HinfI	37 ºC	4	2	50%
HaeIII	37 ºC	5	5	100%
HpaII	37 ºC	3	2	66.66%
EcoRI	37 ºC	1	1	100%
TaqI	65 ºC	4	2	50%
		17	**12**	**70.58%**

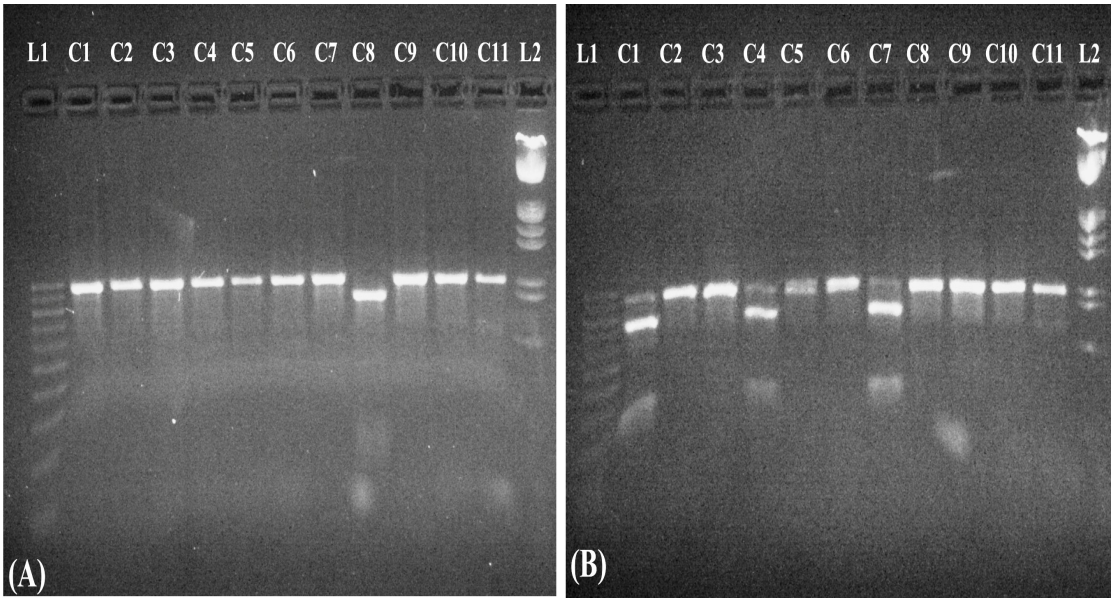

Fig. 4.48. Restriction digestion products of matK region of chloroplast genome by **(A)** HaeIII and **(B)** HpaII. Lane L1: 100 bp molecular marker; Lane C1-C11 different accessions of *Clerodendrum* under study (refer table 3.1); Lane L2: λ-DNA/EcoRI/HindIII double digest DNA ladder.

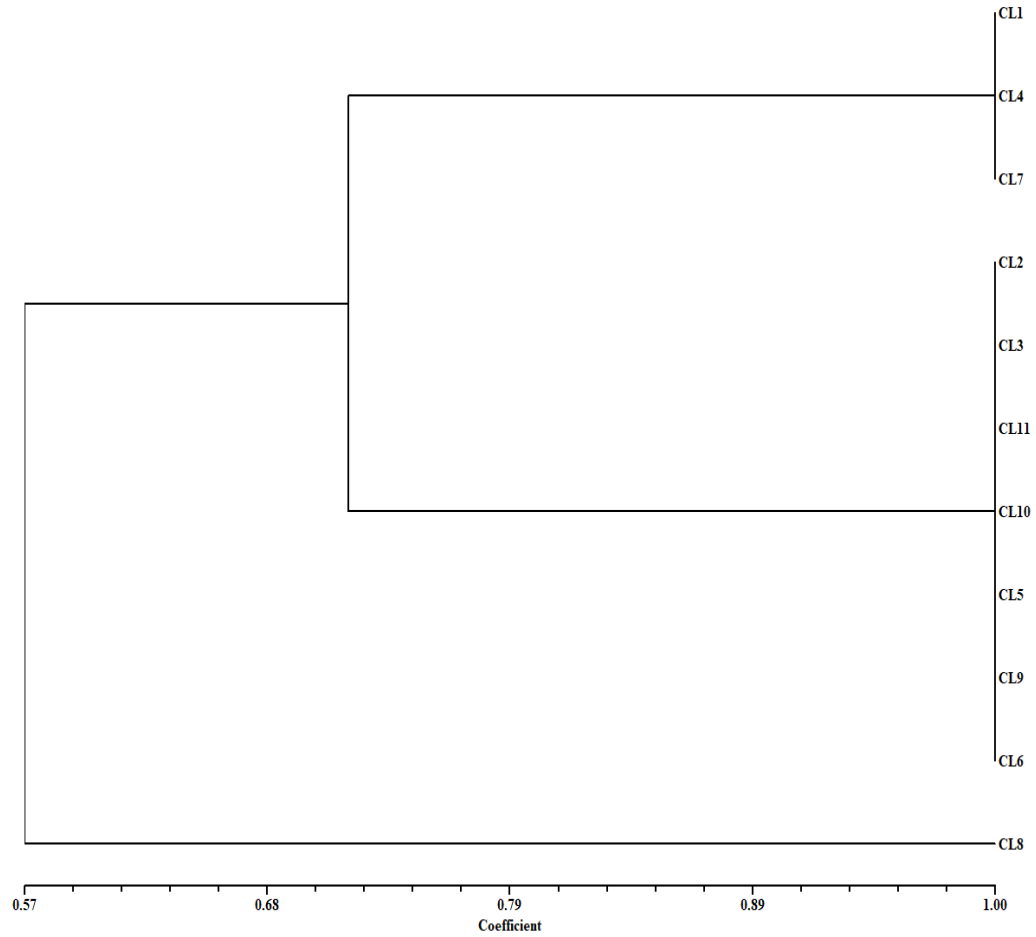

Fig. 4.49. A dendrogram based on the restriction digestion products data of the matK region of 11 species under the genus *Clerodendrum*.

4.13.4.2. PCR amplification of Rps16

In the present study, 11 species of *Clerodendrum* were employed to PCR amplification using a primer pair consisting of forward and reverse primers to target the Rps16 region of the chloroplast DNA of *Clerodendrum*. The primer pair successfully amplified the Rps16 region of the chloroplast genome. The amplified product is shown in Fig. 4.50.

4.13.4.2.1. PCR product restriction digestion and agarose gel analysis

The PCR product obtained from the primer pair Rps16 was subjected to restriction digestion using 3 different restriction enzymes like HinfI, HaeIII and EcoRI to short out the degree of genetic variation among different species of *Clerodendrum*. Amongst 6 enzymes studied, 3 restriction enzymes (AluI, TaqI and MboI) were found to be unsuccessful to digest the PCR products while the other three restriction enzymes produced a total of 4 polymorphic bands (Table 4.32.). Among the three restriction enzymes, HinfI produced two polymorphic bands whereas HaeIII and EcoRI reproduced one band respectively. The total percentage of polymorphism was found to be 50%. The result obtained from restriction digestion with the enzyme EcoRI and HaeIII is depicted in Fig. 4.51.

4.13.4.2.2. PCR-RFLP data analysis

A total of 8 scorable bands were produced by the various restriction digestion enzymes. Of the 8 cuts 4 were polymorphic. These clear and

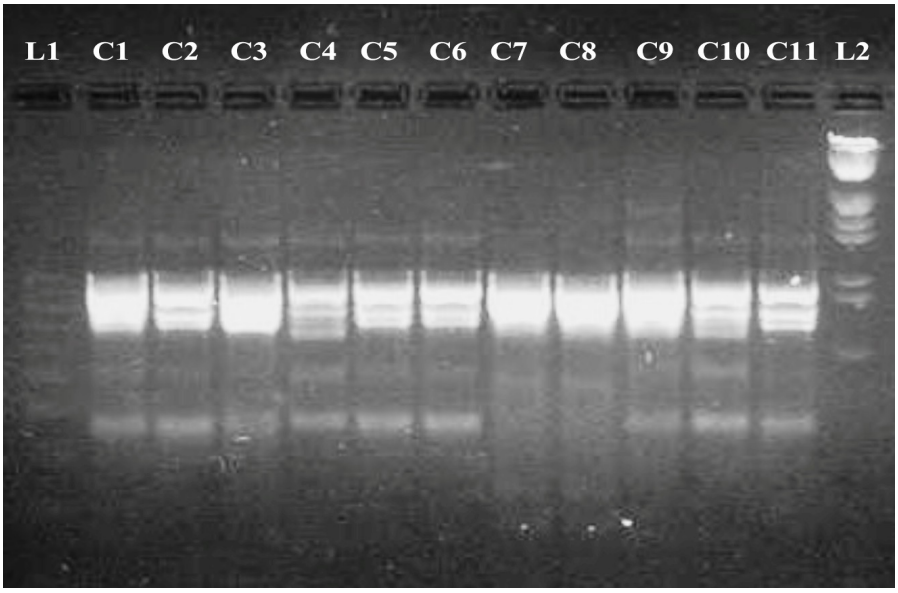

Fig. 4.50. Amplification of 11 species of *Clerodendrum* with Rps 16 primer. Lane L1: 100bp DNA ladder; Lane C1-C11: Different species of *Clerodendrum* as listed in Table 3.1 and L2: λ-DNA/EcoRI/HindIII double digest DNA ladder.

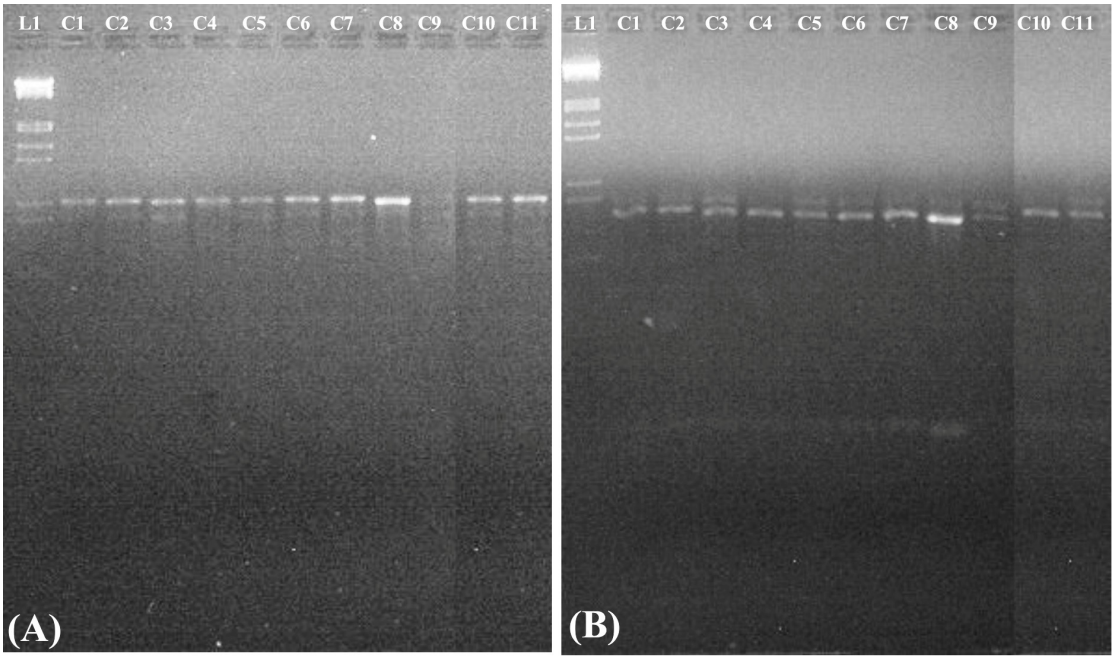

Fig. 4.51. Restriction digestion products of Rps 16 region of chloroplast genome by **(A)** EcoRI and **(B)** HaeIII. Lane L1: λ-DNA/EcoRI/HindIII double digest DNA ladder; Lane C1-C11 different accessions of *Clerodendrum* under study (refer table 3.1).

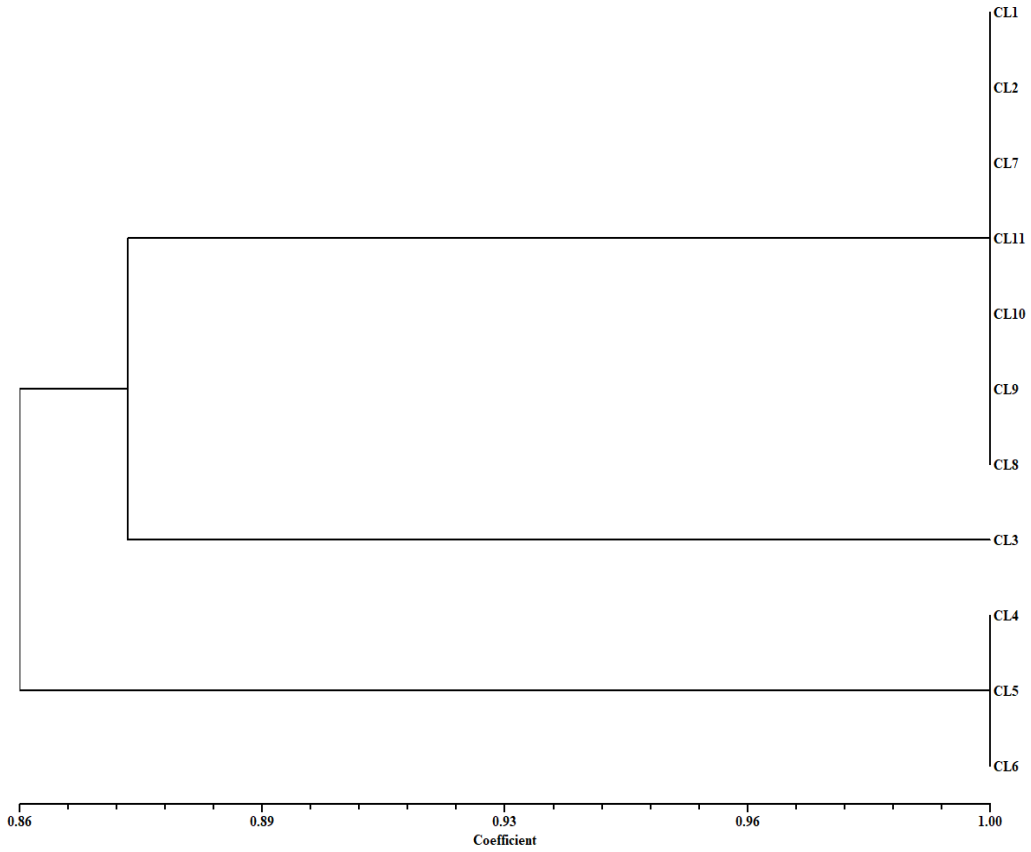

Fig. 4.52. A dendrogram based on the restriction digestion products data of the Rps16 region of 11 species under the genus *Clerodendrum*.

distinct bands were scored and used for further analysis (Table 4.32.). A dendrogram was prepared (Fig. 4.52) on the basis of similarity estimates using the unweighted pair group method with arithmetic average (UPGMA) using NTSYSpc version (2.0) (Rohlf, 1998). The dendrogram revealed two major clusters. The first cluster comprises with 8 species (*C. indicum*, *C. inerme, C. japonicum, C. infortunatum, C. serratum, C. colebrookianum, C. chinense* and *C. bracteatum*) while, the second cluster consisted of 3 species (*C. splendens*, *C. speciaosum* and *C. thomsoniae*). Henceforth, from the above analysis it could be inferred that in the present study notable polymorphism has been found among the selected species due to their polyphyletic nature of the different species of *Clerodendrum*.

4.13.4.3. PCR amplification of trnL-trnF region

In this study the genomic DNA of all the 11 accessions of *Clerodendrum* were subjected to PCR amplification using a primer pair consisting of forward and reverse primers to target the trnL-trnF region of the chloroplast DNA of *Clerodendrum*. The primer pair successfully amplified the trnL-trnF region of the chloroplast genome and the amplified product is shown in Fig. 4.53.

4.13.4.3.1. PCR product restriction digestion and agarose gel analysis

The PCR products were subjected to restriction digestion using different

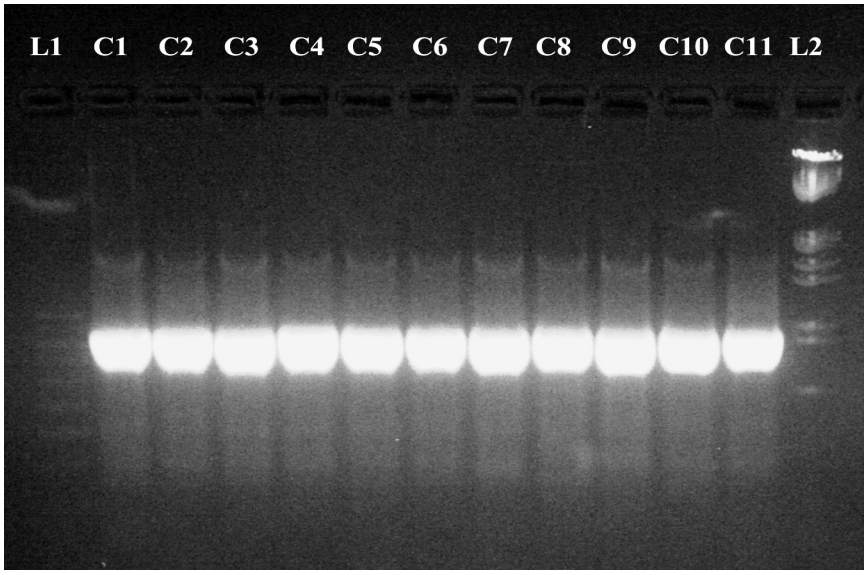

Fig. 4.53. Amplification of 11 species of *Clerodendrum* with Tab c-f (TrnL-TrnF) primer. Lane L1: 100bp DNA ladder; Lane C1-C11: Different species of *Clerodendrum* as listed in Table 3.1 and L2: λ-DNA/EcoRI/HindIII double digest DNA ladder.

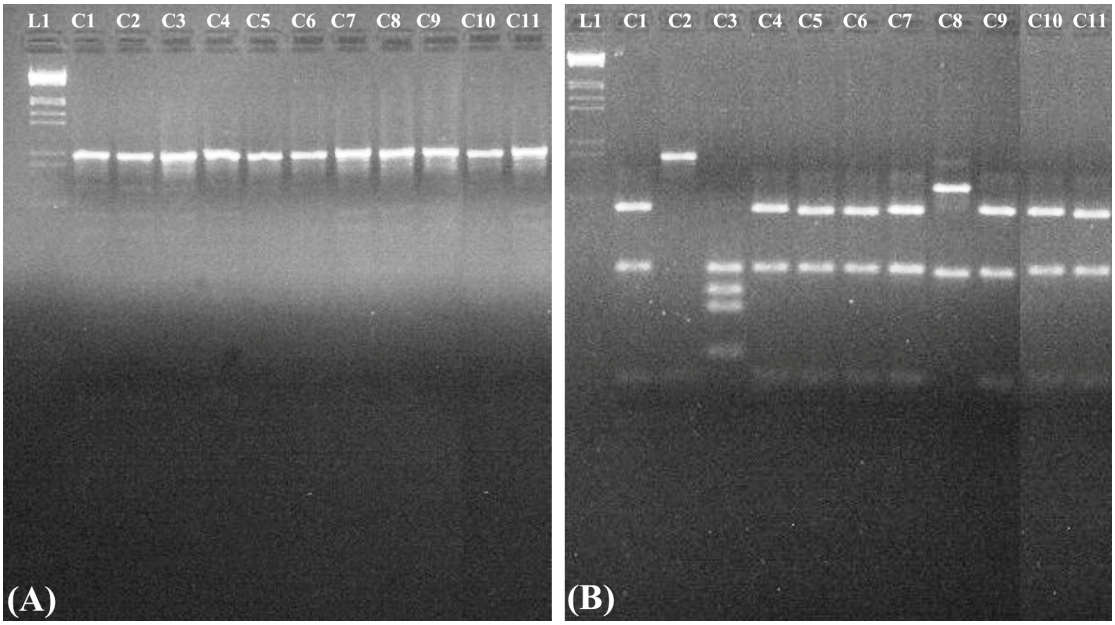

Fig. 4.54. Restriction digestion products of TrnL-TrnF region of chloroplast genome by **(A)** EcoRI and **(B)** HaeIII. Lane L1: λ-DNA/EcoRI/HindIII double digest DNA ladder; Lane C1-C11 different accessions of *Clerodendrum* under study (refer table 3.1).

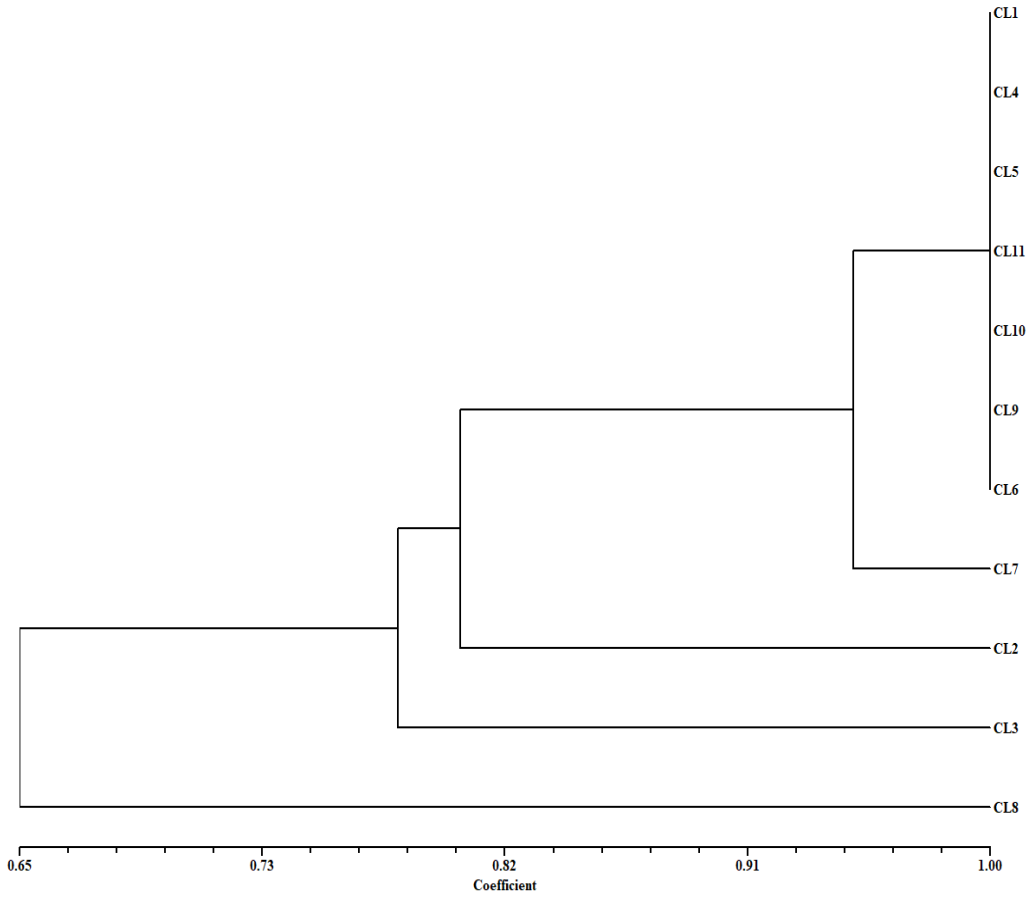

Fig. 4.55. A dendrogram based on the restriction digestion products data of the TrnL-TrnF region of 11 species under the genus *Clerodendrum*.

restriction enzymes like HinfI, HaeIII, HpaII, EcoRI and TaqI to examine the degree of genetic variation among different species of *Clerodendrum*. Different restriction enzyme resulted in different banding pattern and generated bands of different base pairs. The restriction enzyme HaeIII, HinfI and TaqI produced five and four bands respectively. The total percentage of polymorphism was found to be 70.58%. The result obtained from restriction digestion with the enzyme EcoRI and HaeIII is depicted in Fig. 4.54.

4.13.4.3.2. PCR-RFLP data analysis

A total of 17 scorable bands were produced by the various restriction digestion enzymes. Of the 17 cuts 12 were polymorphic. These clear and distinct bands were scored and used for further analysis (Table 4.32.). A dendrogram was prepared (Fig. 4.55) on the basis of similarity estimates using the unweighted pair group method with arithmetic average (UPGMA) using NTSYSpc version (2.0) (Rohlf, 1998). The dendrogram revealed one major clusters and one outgroup. This cluster comprises with 10 species (*C. indicum*, *C. inerme, C. japonicum, C. infortunatum, C. splendens*, *C. speciaosum* and *C. thomsoniae, C. colebrookianum, C. chinense* and *C. bracteatum*). The above analysis showed no major and well supported incongruence in the TrnL-F region of the chloroplast genome of different *Clerodendrum* species. The probable reason for this is that the plastid DNA is generally non-recombining and maternally inherited in most angiosperms.

4.13.5. DNA barcoding analysis

DNA barcoding is a novel and innovative technique which can be used to explore the evolution, identification and genetic relatedness of unknown plants and animal species by using a short stretch of DNA sequence (Hebert *et al.*, 2003). Chloroplast and mitochondrial genes are being recently used to study the sequence variation at generic and species level. The chloroplast genes such as matK, Rps16 and TrnL-F have been utilized by various workers to study the plant evolutionary pattern as well as to resolve various anomalies in the taxonomic levels.

4.13.6. Sequencing of PCR-product and Submission to GenBank

A total of 29 samples (11 matK, 11 Rps16 and 7 TrnL-TrnF) were sequenced from Chromous Biotech

Pvt. Ltd, Bangalore for both the forward and reverse primers individually. The sequencing resulted in an average of 810 bp for each reaction. In the present study, the nucleotide BLAST was performed for each of the sequence obtained to find out the homology with the sequences already present in the GenBank. The nucleotide BLAST showed 95 to 100% identity with the *Clerodendrum* sequence already available in the GenBank. After authentication of the sequences were submitted to the GenBank (Fig. 4.56.A-C). The list of different species of *Clerodendrum* along with their GenBank accession number is given in Table 4.33.

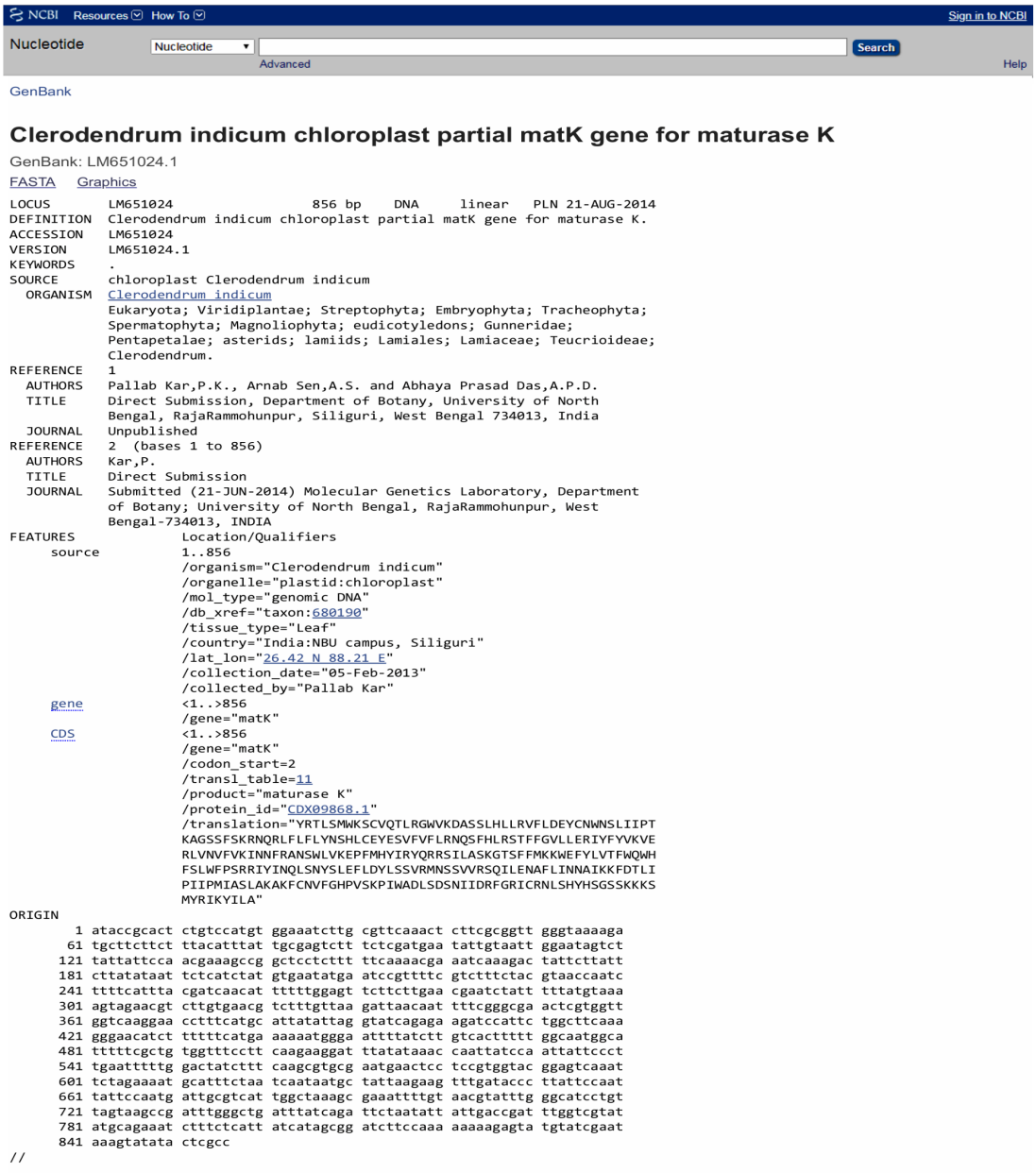

NCBI Resources How To Sign in to NCBI

Nucleotide Nucleotide Search

Advanced Help

GenBank

Clerodendrum indicum chloroplast partial matK gene for maturase K

GenBank: LM651024.1

FASTA Graphics

```
LOCUS       LM651024                856 bp    DNA     linear   PLN 21-AUG-2014
DEFINITION  Clerodendrum indicum chloroplast partial matK gene for maturase K.
ACCESSION   LM651024
VERSION     LM651024.1
KEYWORDS    .
SOURCE      chloroplast Clerodendrum indicum
  ORGANISM  Clerodendrum indicum
            Eukaryota; Viridiplantae; Streptophyta; Embryophyta; Tracheophyta;
            Spermatophyta; Magnoliophyta; eudicotyledons; Gunneridae;
            Pentapetalae; asterids; lamiids; Lamiales; Lamiaceae; Teucrioideae;
            Clerodendrum.
REFERENCE   1
  AUTHORS   Pallab Kar,P.K., Arnab Sen,A.S. and Abhaya Prasad Das,A.P.D.
  TITLE     Direct Submission, Department of Botany, University of North
            Bengal, RajaRammohunpur, Siliguri, West Bengal 734013, India
  JOURNAL   Unpublished
REFERENCE   2  (bases 1 to 856)
  AUTHORS   Kar,P.
  TITLE     Direct Submission
  JOURNAL   Submitted (21-JUN-2014) Molecular Genetics Laboratory, Department
            of Botany; University of North Bengal, RajaRammohunpur, West
            Bengal-734013, INDIA
FEATURES             Location/Qualifiers
     source          1..856
                     /organism="Clerodendrum indicum"
                     /organelle="plastid:chloroplast"
                     /mol_type="genomic DNA"
                     /db_xref="taxon:680190"
                     /tissue_type="Leaf"
                     /country="India:NBU campus, Siliguri"
                     /lat_lon="26.42 N 88.21 E"
                     /collection_date="05-Feb-2013"
                     /collected_by="Pallab Kar"
     gene            <1..>856
                     /gene="matK"
     CDS             <1..>856
                     /gene="matK"
                     /codon_start=2
                     /transl_table=11
                     /product="maturase K"
                     /protein_id="CDX09868.1"
                     /translation="YRTLSMWKSCVQTLRGWVKDASSLHLLRVFLDEYCNWNSLIIPT
                     KAGSSFSKRNQRLFLFLYNSHLCEYESVFVFLRNQSFHLRSTFFGVLLERIYFYVKVE
                     RLVNVFVKINNFRANSWLVKEPFMHYIRYQRRSILASKGTSFFMKKWEFYLVTFWQWH
                     FSLWFPSRRIYINQLSNYSLEFLDYLSSVRMNSSVVRSQILENAFLINNAIKKFDTLI
                     PIIPMIASLAKAKFCNVFGHPVSKPIWADLSDSNIIDRFGRICRNLSHYHSGSSKKKS
                     MYRIKYILA"
ORIGIN
        1 ataccgcact ctgtccatgt ggaaatcttg cgttcaaact cttcgcggtt gggtaaaaga
       61 tgcttcttct ttacatttat tgcgagtctt tctcgatgaa tattgtaatt ggaatagtct
      121 tattattcca acgaaagccg gctcctcttt ttcaaaacga aatcaaagac tattcttatt
      181 cttatataat tctcatctat gtgaatatga atccgttttc gtctttctac gtaaccaatc
      241 ttttcattta cgatcaacat tttttggagt tcttcttgaa cgaatctatt tttatgtaaa
      301 agtagaacgt cttgtgaacg tctttgttaa gattaacaat tttcgggcga actcgtggtt
      361 ggtcaaggaa cctttcatgc attatattag gtatcagaga agatccattc tggcttcaaa
      421 gggaacatct tttttcatga aaaaatggga attttatctt gtcacttttt ggcaatggca
      481 tttttcgctg tggtttcctt caagaaggat ttatataaac caattatcca attattccct
      541 tgaatttttg gactatcttt caagcgtgcg aatgaactcc tccgtggtac ggagtcaaat
      601 tctagaaaat gcatttctaa tcaataatgc tattaagaag tttgataccc ttattccaat
      661 tattccaatg attgcgtcat tggctaaagc gaaattttgt aacgtatttg ggcatcctgt
      721 tagtaagccg atttgggctg atttatcaga ttctaatatt attgaccgat ttggtcgtat
      781 atgcagaaat ctttctcatt atcatagcgg atcttccaaa aaaaagagta tgtatcgaat
      841 aaagtatata ctcgcc
//
```

Fig. 4.56. (A) Snapshot of partial matK gene sequence of *Clerodendrum indicum* submitted to GenBank (NCBI).

NCBI Resources How To Sign in to NCBI

Nucleotide Nucleotide Search

Advanced Help

GenBank

Clerodendrum japonicum chloroplast partial rps16 gene intron, isolate 3

GenBank: LN832027.1

FASTA Graphics

Go to:

```
LOCUS       LN832027               870 bp    DNA     linear   PLN 20-MAY-2015
DEFINITION  Clerodendrum japonicum chloroplast partial rps16 gene intron,
            isolate 3.
ACCESSION   LN832027
VERSION     LN832027.1
KEYWORDS    .
SOURCE      chloroplast Clerodendrum japonicum
  ORGANISM  Clerodendrum japonicum
            Eukaryota; Viridiplantae; Streptophyta; Embryophyta; Tracheophyta;
            Spermatophyta; Magnoliophyta; eudicotyledons; Gunneridae;
            Pentapetalae; asterids; lamiids; Lamiales; Lamiaceae; Teucrioideae;
            Clerodendrum.
REFERENCE   1
  AUTHORS   Kar,P., Mishra,T., Goyal,A.K., Bhattacharya,M., Das,A.P. and Sen,A.
  JOURNAL   Unpublished
REFERENCE   2  (bases 1 to 870)
  AUTHORS   Kar,P.
  TITLE     Direct Submission
  JOURNAL   Submitted (16-MAR-2015) Molecular Genetics Laboratory, Department
            of Botany; University of North Bengal, RajaRammohunpur, West
            Bengal-734013, INDIA
FEATURES             Location/Qualifiers
     source          1..870
                     /organism="Clerodendrum japonicum"
                     /organelle="plastid:chloroplast"
                     /mol_type="genomic DNA"
                     /isolate="3"
                     /db_xref="taxon:167921"
                     /tissue_type="Leaf"
                     /country="India:NBU campus, Siliguri"
                     /lat_lon="26.42 N 88.21 E"
                     /collection_date="05-Feb-2013"
     gene            <1..>854
                     /gene="rps16"
     intron          <1..>854
                     /gene="rps16"
                     /number=1
ORIGIN
        1 ttcatccacc atttttttatt tatctaggaa tgagggtgct cttggctcga cattgtttgt
       61 tctgttacac ctgaaccctt cggttggaat agtccacagt ggagctcgaa tagaaagtat
      121 taattcattt ctcgggggca aggatctagg gttaatacca atcaactgga acaacttcgt
      181 aaatatatgg aacatatata gaaatcaaaa ggatccgatt cgagcaagtt tccaattcaa
      241 aagcaaaact tgttgaaatt gatcaaaaat tttgattcaa agtgtatcac gtgtgaatca
      301 aatgtccata ggattctttg atagaaagaa atcaaaaaaa aaagggtatg ttgctgccat
      361 tttgaaagga ttacgaggca ccgaagtaat gtctaaaccc aatgattaaa aataaggata
      421 aaggatctac gaacaaggaa acaaccttta tatttataat ttaaataatt taattgtctt
      481 gatattctca ataattggat cacactaaag aatccaaata gaatttgaaa tagtttaaat
      541 gagacaaaca acaaacaaaa gggagtaaag gctactcact acatgaaatt gactcaaaat
      601 ttttcctttg aggtatttga gagttattca acttgagtta tgagtatgaa tggtttcttt
      661 ttcattttca ggaagcaaaa aagactgaaa tcatatttat tttctaggcc catttgtcat
      721 ttcatttatt agaattgcat atatatagac aaaactttga atcaaatcat tttttctcga
      781 gccgtacgag gagaaaactt cctatacggt tctgggggggg ggtattgttc atatacatct
      841 atcccaatga gccgtctatc gatcgtgcat
//
```

Fig. 4.56. (B) Snapshot of partial rps16 gene sequence of *Clerodendrum japonicum* submitted to GenBank (NCBI).

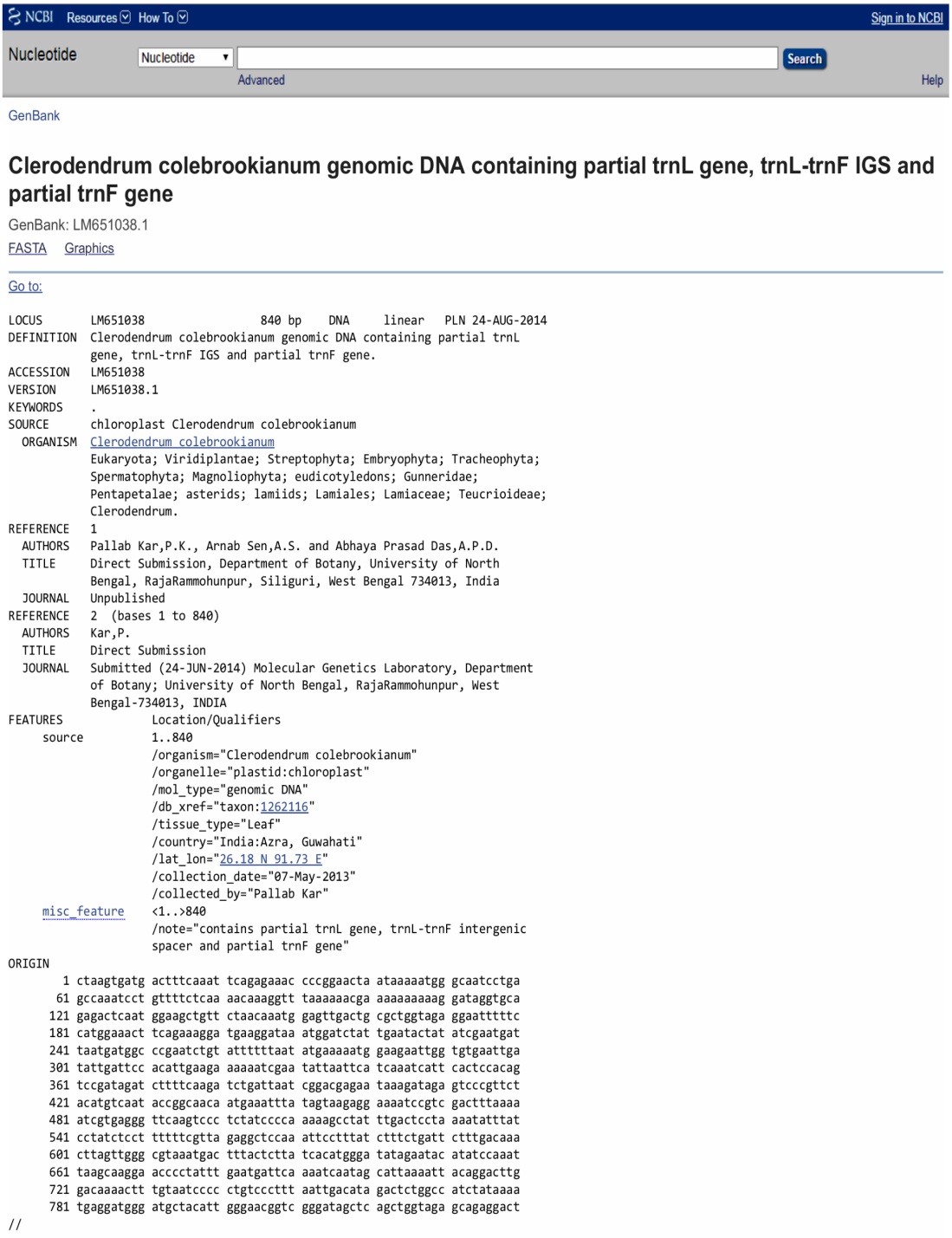

NCBI Resources How To Sign in to NCBI

Nucleotide Nucleotide Search

Advanced Help

GenBank

Clerodendrum colebrookianum genomic DNA containing partial trnL gene, trnL-trnF IGS and partial trnF gene

GenBank: LM651038.1

FASTA Graphics

Go to:

```
LOCUS       LM651038                840 bp    DNA     linear   PLN 24-AUG-2014
DEFINITION  Clerodendrum colebrookianum genomic DNA containing partial trnL
            gene, trnL-trnF IGS and partial trnF gene.
ACCESSION   LM651038
VERSION     LM651038.1
KEYWORDS    .
SOURCE      chloroplast Clerodendrum colebrookianum
  ORGANISM  Clerodendrum colebrookianum
            Eukaryota; Viridiplantae; Streptophyta; Embryophyta; Tracheophyta;
            Spermatophyta; Magnoliophyta; eudicotyledons; Gunneridae;
            Pentapetalae; asterids; lamiids; Lamiales; Lamiaceae; Teucrioideae;
            Clerodendrum.
REFERENCE   1
  AUTHORS   Pallab Kar,P.K., Arnab Sen,A.S. and Abhaya Prasad Das,A.P.D.
  TITLE     Direct Submission, Department of Botany, University of North
            Bengal, RajaRammohunpur, Siliguri, West Bengal 734013, India
  JOURNAL   Unpublished
REFERENCE   2  (bases 1 to 840)
  AUTHORS   Kar,P.
  TITLE     Direct Submission
  JOURNAL   Submitted (24-JUN-2014) Molecular Genetics Laboratory, Department
            of Botany; University of North Bengal, RajaRammohunpur, West
            Bengal-734013, INDIA
FEATURES             Location/Qualifiers
     source          1..840
                     /organism="Clerodendrum colebrookianum"
                     /organelle="plastid:chloroplast"
                     /mol_type="genomic DNA"
                     /db_xref="taxon:1262116"
                     /tissue_type="Leaf"
                     /country="India:Azra, Guwahati"
                     /lat_lon="26.18 N 91.73 E"
                     /collection_date="07-May-2013"
                     /collected_by="Pallab Kar"
     misc_feature    <1..>840
                     /note="contains partial trnL gene, trnL-trnF intergenic
                     spacer and partial trnF gene"
ORIGIN
        1 ctaagtgatg actttcaaat tcagagaaac cccggaacta ataaaaatgg gcaatcctga
       61 gccaaatcct gttttctcaa aacaaaggtt taaaaaacga aaaaaaaaag gataggtgca
      121 gagactcaat ggaagctgtt ctaacaaatg gagttgactg cgctggtaga ggaatttttc
      181 catggaaact tcagaaagga tgaaggataa atggatctat tgaatactat atcgaatgat
      241 taatgatggc ccgaatctgt atttttaat atgaaaaatg gaagaattgg tgtgaattga
      301 tattgattcc acattgaaga aaaaatcgaa tattaattca tcaaatcatt cactccacag
      361 tccgatagat cttttcaaga tctgattaat cggacgagaa taaagataga gtcccgttct
      421 acatgtcaat accggcaaca atgaaattta tagtaagagg aaaatccgtc gactttaaaa
      481 atcgtgaggg ttcaagtccc tctatcccca aaaagcctat ttgactccta aaatatttat
      541 cctatctcct tttttcgtta gaggctccaa attcctttat ctttctgatt ctttgacaaa
      601 cttagttggg cgtaaatgac tttactctta tcacatggga tatagaatac atatccaaat
      661 taagcaagga acccctattt gaatgattca aaatcaatag cattaaaatt acaggacttg
      721 gacaaaactt tgtaatcccc ctgtcccttt aattgacata gactctggcc atctataaaa
      781 tgaggatggg atgctacatt gggaacggtc gggatagctc agctggtaga gcagaggact
//
```

Fig. 4.56. (C) Snapshot of partial trnL-trnF Intergenic Spacer (IGS) sequence of *Clerodendrum colebrookianum* submitted to GenBank (NCBI).

4.13.7. Data analysis

Apart from RAPD and ISSR analysis, DNA barcoding is another kind of taxonomic method that has become a rational approach for identifying million species of plants and animals, based on the analysis of short, standardized and universal DNA

Table 4.33. List of species with the submitted GenBank accession numbers for matK, TrnL-TrnF and rps16.

Taxa	matK accession number	TrnL-F accession number	Rps16 Accession number
Clerodendrum indicum	LM651024	LM651034	LN832025
Clerodendrum inerme (Syn. *Volkameria inermis*)	LM651025	----	LN832026
Clerodendrum japonicum	LM651026	----	LN832027
Clerodendrum splendens	LM651027	----	LN832028
Clerodendrum speciaosum	LM651028	LM651035	LN832029
Clerodendrum thomsoniae	LM651029	----	LN832030
Clerodendrum infortunatum (Syn. *Clerodendrum viscosum*)	LM651030	LM651036	LN832031
Clerodendrum serratum (Syn. *Rotheca serrata*)	LM651031	LM651037	LN832032
Clerodendrum colebrookianum	LM651032	LM651038	LN832033
Clerodendrum chinens (Syn. *Clerodendrum fragrans*)	LN832023	LN823952	LN832034
Clerodendrum bracteatum	LN832024	LN823953	LN832035

regions. Molecular documentation of different taxa and their validated systematic position in the respective family of plant kingdom had always been a challenging task. Chloroplast gene like matK, Rps16 and IGS region like TrnL-F could be essential to resolve this problem. In the present study, a few selected species under the family Lamiaceae (please refer Table 3.8) were employed to explore inter-generic and intra-generic differences using matK, Rps16 and TrnL-F locus. The phylogenetic analysis (Fig. 4.57.A-C) of the matK, Rps16 and TrnL-F region revealed a close relationship among the selected taxa. Interestingly, Fig. 4.57.A revealed all the fourteen genera of the subfamily Ajugoideae were appeared together, whereas, it has been found that the two subfamily Symphorematoideae and Nepetoideae very close to Ajugoideae as found in traditional classification (Cronquist, 1981). Interestingly, Fig. 4.57.B discloses that out of eleven genera from the subfamily Ajugoideae nine genera were clubbed together and two

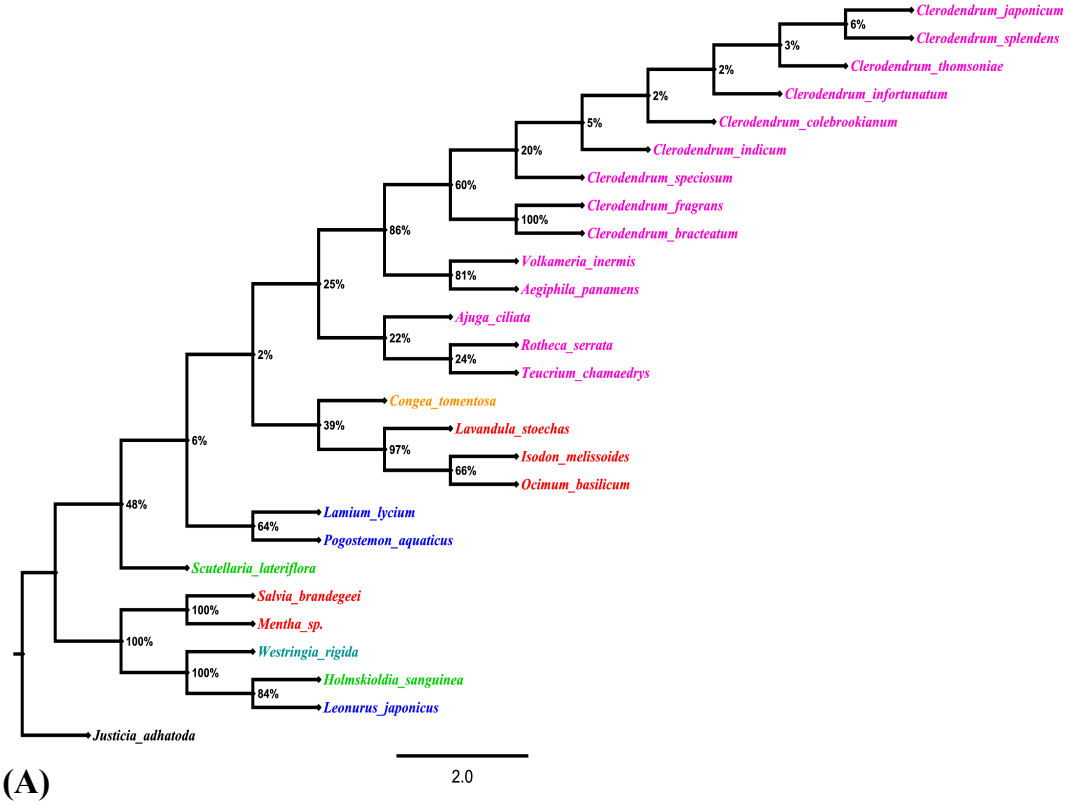

(A)

Fig. 4.57. (A) Most parsimonious tree (neighbour joining method) showing the relationship of matK region of 26 different taxa. Numbers at nodes indicate the bootstrap values.

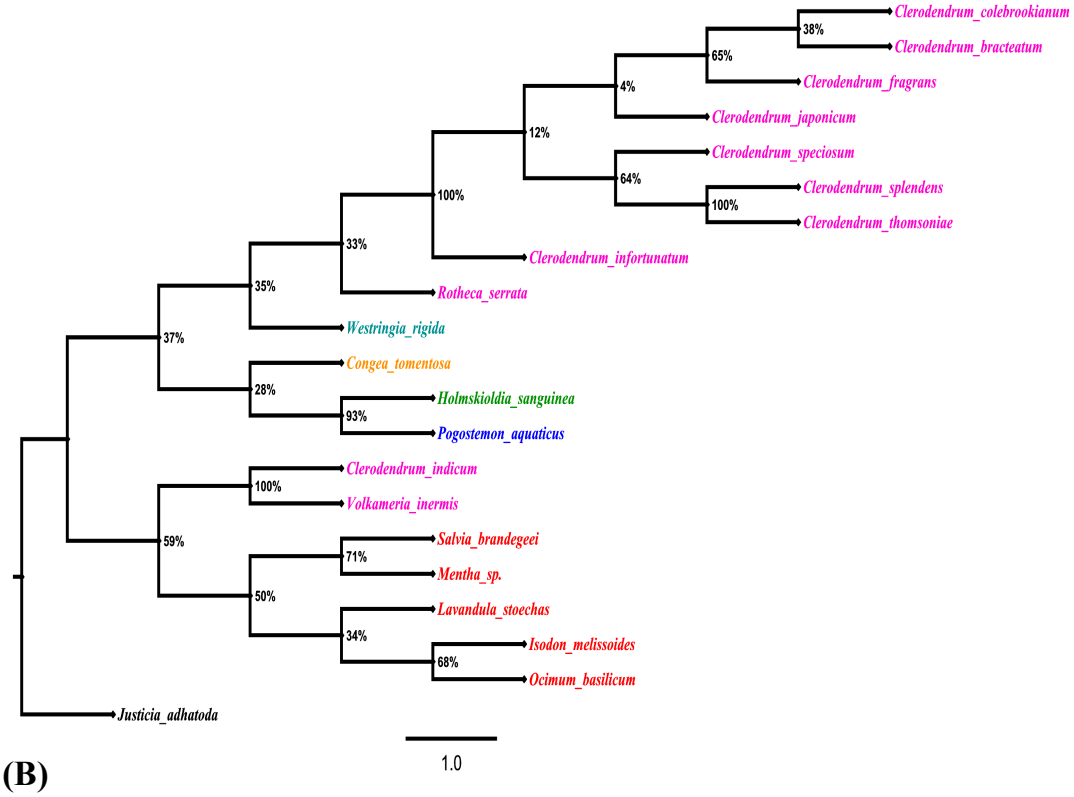

(B)

Fig. 4.57. (B) Most parsimonious tree (neighbour joining method) showing the relationship of Rps16 region of 20 different taxa. Numbers at nodes indicate the bootstrap values.

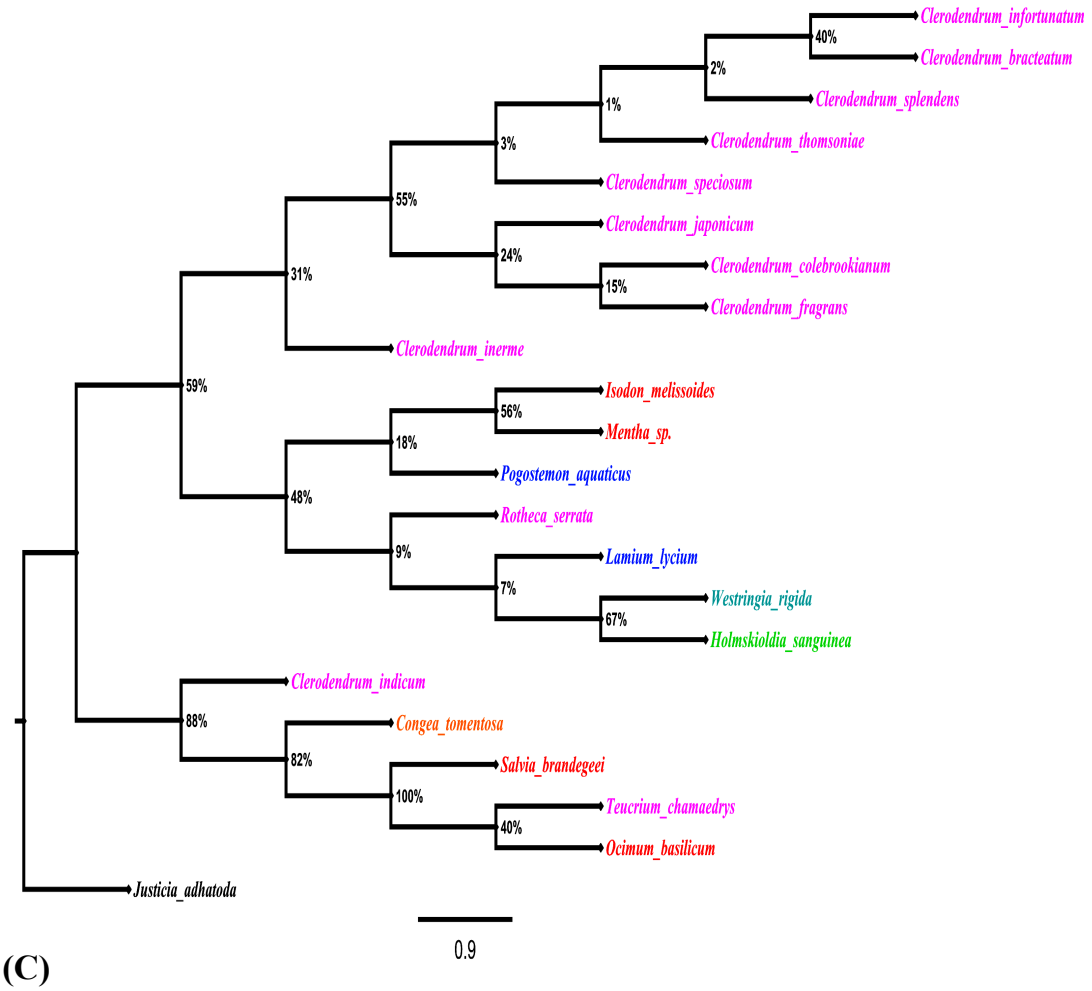

(C)

Fig. 4.57. (C) Most parsimonious tree (neighbour joining method) showing the relationship of TrnL-F region of 21 different taxa. Numbers at nodes indicate the bootstrap values.

genera separated out, whereas, five genera of the subfamily Nepetoideae were appeared together and shared more similarities with each other. A similar trend was also observed in Fig. 4.57.C. Hence, from the above illustration, it may conclude that DNA barcode serve a reliable genetical approach to place the morphologically similar or dissimilar or disputed taxa into its appropriate systematic position (Schäferhoff *et al.*, 2010; Selvaraj *et al.*, 2008).